# Using Azides to Access Nitrogen Heterocycles

A Dissertation

SUBMITTED TO THE FACULTY OF THE

UNIVERSITY OF MINNESOTA

BY

Angela S. Carlson

IN PARTIAL FULFILLMENT OF THE REQUIREMENTS FOR THE DEGREE OF

DOCTOR OF PHILOSOPHY

Professor Joseph Topczewski, Advisor

November 2020

**Table of Contents**

**List of Tables** ..... **ii**

**List of Figures** ..... **iii**

**List of Schemes** ..... **iv**

**List of Abbreviations** ..... **v**

**Chapter 1: Using Azides to Access Nitrogenous Heterocycles** ..... **1**

1.1 Allylic Azides as Precursors to Nitrogen Heterocycles ..... 1

1.2 Azides as Precursors to Bromodomain Inhibitors ..... 3

1.3 Conclusion ..... 4

1.4 References ..... 4

**Chapter 2: Wacker Oxidation of Cinnamyl Azides** ..... **7**

2.1 Wacker Oxidation of Terminal Alkenes ..... 7

2.2 Wacker Oxidation of Internal Alkenes ..... 10

2.3 Azides as Effective and Versatile Directing Groups ..... 12

2.4 References ..... 17

**Chapter 3: Cascade Reaction Between Allylic Azides and Michael Acceptors** ..... **20**

3.1. Background on Tetrahydro-pyrrolo-pyrazole Heterocycles ..... 20

3.2 Optimizing Conditions to Generate Tetrahydro-pyrrolo-pyrazole Heterocycles ..... 22

3.3 Extending the Cascade Reaction with Vinyl Sulfones ..... 30

3.4 Experimental ..... 32

3.5 References ..... 35

**Chapter 4: Mitigating the p38α Activity of Bromodomain Inhibitors** ..... **39**

4.1. Introduction to Bromodomains ..... 39

4.3 Source of BRD4-D1 Selectivity ..... 41

4.3 Mitigating p38α Activity ..... 45

4.4. Improving Potency ..... 53

4.5 References ..... 56

**Bibliography** ..... **73**

**List of Tables**

**Table 2.1.** Optimization of the Wacker Oxidation ..... 14
**Table 2.2.** Robustness Screen..... 15
**Table 2.3.** Substrate Scope of Azide Directed Wacker Oxidation. ..... 16
**Table 3.1.** Synthesis of Triazoline Intermediates. ..... 23
**Table 3.2.** Cascade Optimization with Methyl Acrylate. ..... 25
**Table 3.3.** Scope of the Cascade Reaction with Cinnamyl Azides. ..... 26
**Table 3.4.** Reaction Scope with Substituted Allylic Azides ..... 27
**Table 3.5.** Reaction Scope with Different Michael Acceptors..... 28
**Table 3.6.** Product Functionalization *in Situ* to Expand Cascade ..... 29
**Table 3.7.** Scope of Cascade Reaction with Cinnamyl Azides ..... 32
**Table 4.1.** Stabilization Energy of Structured Waters and Compound **V** Affinity..... 42
**Table 4.2.** ALPHAScreen Analysis of Compound **V** and Compounds **4.2.8a** – **4.2.8c** Against 7 of 8 BET Bromodomains..... 45
**Table 4.3.** Systematically Minimizing Binding to M109 in p38α..... 46
**Table 4.4.** Significance of R Group to BRD4-D1 Binding Affinity. ..... 48
**Table 4.5.** Effect of Nitrogen Atom(s) to BRD4-D1 Affinity..... 49
**Table 4.6.** Demonstrating Selectivity for Compound **5** and **27**..... 50
**Table 4.7.** Viability of MM.1S Cells Treated with Bromodomain Inhibitors..... 52
**Table 4.8.** Affinity and Selectivity for Triazole Analogs..... 54

## List of Figures

**Figure 1.1.** Common Nitrogenous Heterocycles in FDA Approved Pharmaceuticals. ..... 1
**Figure 1.2.** Imidazole and 1,2,3-Triazole Mimicking Acetylated Lysine. ..... 4
**Figure 3.1**. Examples of Tetrahydro-pyrrolo-pyrazoles..... 20
**Figure 3.2.** Select Biologically Active Molecules Containing a Dihydro-pyrrolo-pyrazole. ..... 31
**Figure 4.1.** Native BRD Interaction. ..... 39
**Figure 4.2.** Examples of Dual Kinase-Bromodomain Inhibitors. ..... 40
**Figure 4.3.** State-of-the-art BET Inhibitors..... 41
**Figure 4.4.** Co-crystal Structures of BRD4-D1 with DMSO and Compound **V**. ..... 42
**Figure 4.5.** Hydrogen Bonding in p38α Co-crystal Structures and Proposed Analogues 46
**Figure 4.6.** Comparison of BRD4-D1 Co-crystal Structures with Compounds **4.6a** and **V**. ..... 51
**Figure 4.7.** Functionalizing the piperidine ring..... 55
**Figure 4.8.** Summary of Results..... 56

**List of Schemes**

**Scheme 1.1.** Cyclization of Allylic Azides to form Pyridines and Carboxyquinolines. .... **2**

**Scheme 1.2.** Reductive Cyclization of Allylic Azides. ..... **3**

**Scheme 1.3**. Cascade Reaction Between Allyl Azide and Methyl Acrylate. ..... **3**

**Scheme 2.1.** Original Wacker Oxidation. ..... **7**

**Scheme 2.2.** Catalytic Cycle with Outer Sphere Nucleophilic Attack. ..... **8**

**Scheme 2.3.** Two Mechanisms for Nucleophilic Attack. ..... **9**

**Scheme 2.4.** Ketone Selectivity on Terminal Alkenes. ..... **10**

**Scheme 2.5.** Aldehyde Selective Oxidation of Terminal Alkenes. ..... **10**

**Scheme 2.6.** Poor Selectivity for Wacker Oxidations on Internal Alkenes. ..... **11**

**Scheme 2.7.** Heteroatom-Directed Oxidation of Internal Alkenes. ..... **12**

**Scheme 2.8.** Winstein Rearrangement. ..... **12**

**Scheme 2.9.** Direct Synthesis of Cinnamyl Azides. ..... **13**

**Scheme 2.10.** Gram Scale Reaction and Diversification of Products. ..... **16**

**Scheme 2.11.** Wacker Oxidation on an Equilibrating Allylic Azide. ..... **17**

**Scheme 3.1.** Synthesis of Tetrahydro-pyrrolo-pyrazoles. ..... **22**

**Scheme 3.2.** Mechanism of Cascade Reaction. ..... **24**

**Scheme 3.3.** Stereospecific Cascade Reaction. ..... **28**

**Scheme 3.4.** Selectivity Between Different Alkenes. ..... **29**

**Scheme 3.5.** Gram Scale Reaction and Product Derivatization ..... **30**

**Scheme 3.6.** Extending the Cascade Reaction by Using a Good Leaving Group. ..... **30**

**Scheme 3.7.** Prior Synthesis of Dihydro-pyrrolo-pyrazoles. ..... **31**

**Scheme 4.1.** Convergent Synthesis of Triazole Analogs. ..... **43**

**Scheme 4.2.** First Generation Synthesis of Triazole Analogs. ..... **44**

**Scheme 4.3.** Second Generation Synthesis of Triazole Analogs. ..... **47**

**List of Abbreviations**

| | |
|---|---|
| Ac | acetate |
| Ar | aryl |
| BET | bromodomain and extra terminal |
| Bn | benzyl |
| Boc | tert-butoxycarbonyl |
| BRD | bromodomain |
| BQ | benzoquinone |
| Bz | benzoyl |
| CBz | benzyloxycarbonyl |
| CDK | cyclin-dependent kinase |
| CHO | aldehyde |
| CuAAC | Copper-catalyzed azide-alkyne cycloaddition |
| DBU | 1,8-diazabicyclo(5.4.0)undec-7-ene |
| DCM | dichloromethane |
| DIPEA | diisopropylethylamine |
| DNA | deoxyribonucleic acid |
| DMAP | 4-dimethylaminopyridine |
| DME | dimethoxyethane |
| DMF | dimethylformamide |
| DMSO | dimethyl sulfoxide |
| DPPA | diphenylphosphoryl azide |

| | |
|---|---|
| dr | diastereomeric ratio |
| equiv | equivalents |
| ESI | electrospray ionization |
| $Et_2O$ | ethyl ether |
| EtOAc | ethyl acetate |
| EtOH | ethanol |
| FDA | food and drug administration |
| HFIP | 1,1,1,3,3,3-hexafluoro-2-propanol |
| HPLC | high performance liquid chromatography |
| HRMS | high resolution mass spectrometry |
| Hz | hertz |
| IPA | isopropyl alcohol |
| *J* | coupling constant (NMR) |
| LA | Lewis acid |
| LG | leaving group |
| m | multiplet (NMR) |
| *m*-CPBA | metachloroperoxy benzoic acid |
| MeOH | methanol |
| min | minute |
| mL | milliliter |
| mmol | millimoles |
| MOM | methoxymethyl ether |
| MsCl | methane sulfonyl chloride |

| | |
|---|---|
| NaHMDS | sodium bis(trimethylsilyl)amide |
| *n*-BuLi | normal butyl lithium |
| NMO | *N*-methylmorpholine-*N*-oxide |
| NMR | nuclear magnetic resonance |
| Ph | phenyl |
| PhMe | toluene |
| PLK1 | polo-like kinase 1 |
| $PPh_3$ | triphenyl phosphine |
| *p*-TsOH | *para*-toluenesulfonic acid |
| rt | room temperature |
| s | singlet (NMR) |
| $S_NAr$ | nucleophilic aromatic substitution |
| t | triplet (NMR) |
| TBAF | tetrabutylammonium |
| TBHP | tert-butyl hydroperoxide |
| TBS | tert-butyldimethylsilyl |
| *t*-BuOH | tert-butanol |
| TEA | triethylamine |
| Tf | triflate (or trifluoromethanesulfonate) |
| TFA | trifluoroacetic acid |
| THF | tetrahydrofuran |
| TLC | thin-layer chromatography |
| TMS | trimethylsilyl |

| | |
|---|---|
| Tr | trityl |
| Ts | tosyl (toluenesulfonyl) |

## Chapter 1: Using Azides to Access Nitrogenous Heterocycles

*Parts of this chapter were reproduced from Org. Biomol. Chem.* ***2019****, 17, 4406-4429 with permission from The Royal Society of Chemistry.*

A recent review showed that 59% of FDA approved pharmaceuticals contain a nitrogen heterocycle.[1] The most common nitrogenous heterocycles are 5- and 6-membered rings and include both saturated and aromatic heterocycles (Figure 1.1). Shortening the synthetic route to some of these heterocycles could have a significant impact on the cost and rate of drug discovery.

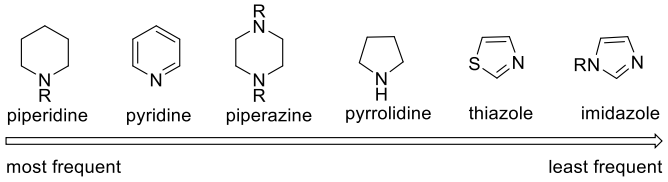


**Figure 1.1.** Common Nitrogenous Heterocycles in FDA Approved Pharmaceuticals.

### 1.1 Allylic Azides as Precursors to Nitrogen Heterocycles

Allylic azides provide a unique scaffold to generate nitrogenous heterocycles. Azides and alkenes are both versatile functional groups and in combination can undergo many cyclization reactions. Azides can easily be converted into amines, imines, nitrenes, and diazo compounds in situ. These reactive intermediates can react with an alkene and/or insert into the substrate to generate a nitrogen heterocycle, which contains the original azide nitrogen(s).

For instance, pyridines and carboxyquinolines have been formed from allylic azides (Scheme 1.1). In 2016, Park and co-workers used diruthenium catalyst **1.1** to convert an allylic azide into a pyridine (Scheme 1.1a).[2] In this reaction, catalyst **1.1** was used to convert the azide into the corresponding imine. Subsequent electrocyclization and oxidation led to the desired pyridine. In 2003, Sá and co-workers reported a Lewis acid catalyzed cyclization to form quinolines (Scheme 1.1b).[3] Unfortunately, the yield was not optimized above 23% due to starting material decomposition. Yu and co-workers

broadened the scope of this reaction by using NBS and visible light to initiate a radical cyclization (Scheme 1.1c).[4]

**Scheme 1.1. Cyclization of Allylic Azides to form Pyridines and Carboxyquinolines.**

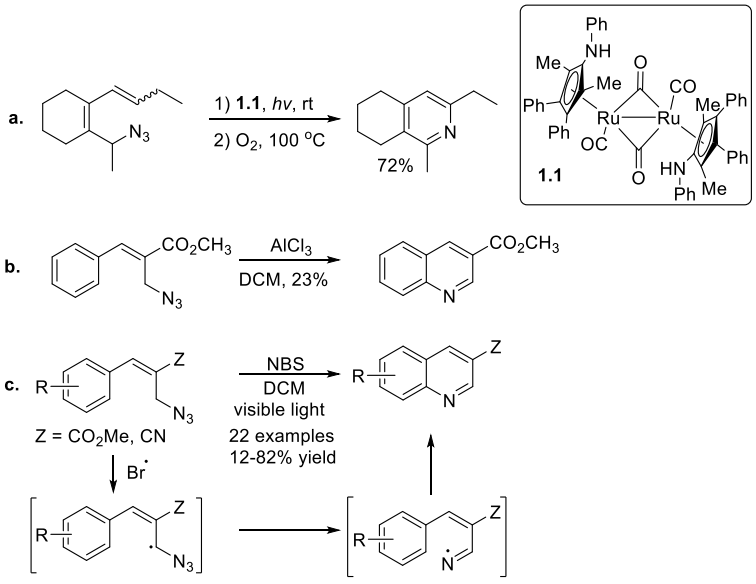


Reductive cyclizations have also been used to generate nitrogenous heterocycles from allylic azides. Zanatta and co-workers used an aza-wittig reaction to form a variety of 2-trifluoromethyl pyrroles (Scheme 1.2a).[5] Simultaneous reduction of both the azide and alkene has been used to synthesize lactams (Scheme 1.2b and 1.2c).[6–8] In 2006, Sudalai and co-workers reported the enantioselective cyclization of an allylic azide conjugated to an ester (Scheme 1.2b).[7,9,10] This work empolyed a cobalt catalyst which can reduce the alkene with good stereoselectivity and reduce the azide to promote lactamization. Sudalai and co-workers demonstrated the utility of this method by performing an enantioselective total synthesis of (*R*)-(-)-rolipram, in which the cyclization proceeded in 92% yield and 92% ee.[7] Tjeng developed a similar global reduction, which resulted in the formation of pyrrolidines.[11] Another lactamization of allylic azides was demonstrated by Murphy and co-workers in 2013 (Scheme 1.2c).[8] Homolytic cleavage of the aryl-iodide bond is thought to initiate a radical cascade to form the desired lactam.

**Scheme 1.2. Reductive Cyclization of Allylic Azides.**

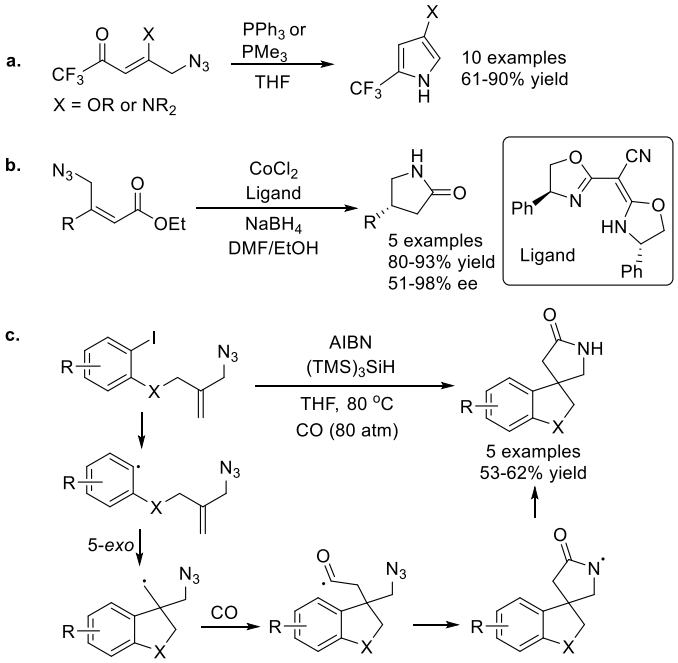


In 1993, Yang demonstrated that allyl azide and methyl acrylate can engage in a cascade reaction to form a bicycle nitrogen heterocycle (Scheme 1.3).[12–14] This cascade reaction is interesting and will be described in more detail later (see Chapter 3).

**Scheme 1.3**. Cascade Reaction Between Allyl Azide and Methyl Acrylate.

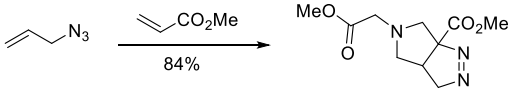


These examples highlight the unique capacity for allylic azides to form nitrogen heterocycles. Many nitrogen heterocycles possess useful biological properties but can be challenging to synthesize. This work focuses on developing new routes to these challenging, but useful, heterocycles by employing allylic azides.

## 1.2 Azides as Precursors to Bromodomain Inhibitors

While azides can react with alkenes, they are more well-known for cyclizing with alkynes. The copper-catalyzed azide-alkyne cycloaddition (CuAAC), which was pioneered by Meldal and Sharpless in 2002,[15,16] enables facile access to a wide variety of 1,2,3-triazoles. These 1,2,3-triazoles, as well as many other *N*-heterocycles, are frequently used

as bioisoteres for amides to improve the potency, selectivity, and pharmacokinetic properties of pharmaceuticals.[17,18]

For instance, several nitrogen heterocycles have been used to mimic acetylated lysines in bromodomain inhibitors.[20] To facilitate DNA transcription, bromodomains bind to acetylated lysine residues on histones (Figure 1.2).[19] To inhibit these protein-protein interactions, many inhibitors have been developed which use nitrogen heterocycles to mimic the acetylated lysine.[20] One promising bromodomain inhibitor (**V**) used an imidazole as the acetylated lysine mimic.[21,22] However, this lead compound required 10 linear steps to synthesize with a 4% overall yield.[22] Optimizing the substituents on this scaffold would be a time-consuming process. This work focused on substituting the imidazole for a 1,2,3-triazole which allows facile access to a variety of analogs. This modification allowed efficient turnover of the designing/synthesizing/testing cycle.

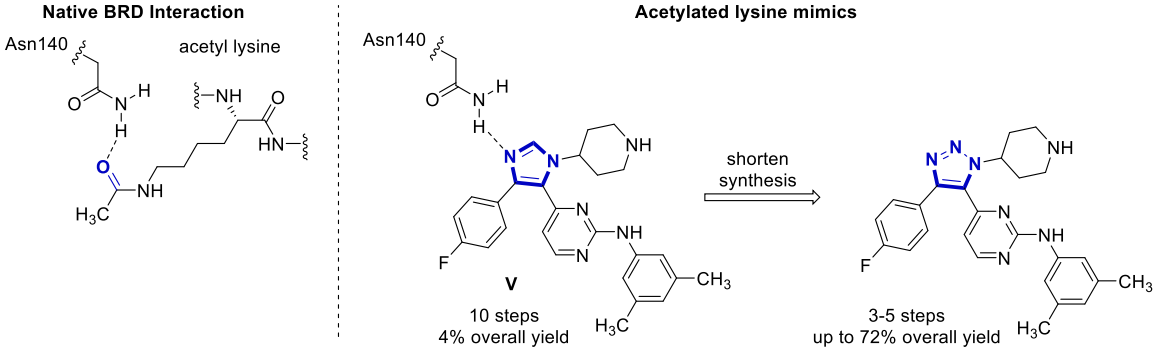


**Figure 1.2.** Imidazole and 1,2,3-Triazole Mimicking Acetylated Lysine.

## 1.3 Conclusion

Overall, this Ph.D. thesis expands azide reactivity to enable efficient synthetic routes to nitrogen heterocycles. Initial efforts focused on developing a one-pot synthesis of allylic azides and performing a Wacker oxidation to form azido-ketones (Chapter 2). These allylic azides could also be used in a cascade reaction with acrylates and vinyl sulfones to form bicyclic nitrogen heterocycles (Chapter 3). Lastly, azides were used to shorten the synthetic route to a bromodomain inhibitor which allowed efficient optimization of the inhibitor's selectivity and potency (Chapter 4).

## 1.4 References

(1) Vitaku, E.; Smith, D. T.; Njardarson, J. T. Analysis of the Structural Diversity,

Substitution Patterns, and Frequency of Nitrogen Heterocycles among U.S. FDA Approved Pharmaceuticals. *J. Med. Chem.* **2014**, *57*, 10257–10274.

(2) Kwon, Y.; Jeon, M.; Park, J. Y.; Rhee, Y. H.; Park, J. Y. Synthesis of 1H-Azadienes and Application to One-Pot Organic Transformations. *RSC Adv.* **2016**, *6*, 661–668.

(3) Sá, M. M. Allylic Azides as Potential Building Blocks for the Synthesis of Nitrogenated Compounds. *J. Braz. Chem. Soc.* **2003**, *14*, 1005–1010.

(4) Wang, W. X.; Zhang, Q. Z.; Zhang, T. Q.; Li, Z. S.; Zhang, W.; Yu, W. N-Bromosuccinimide-Mediated Radical Cyclization of 3-Arylallyl Azides: Synthesis of 3-Substituted Quinolines. *Adv. Synth. Catal.* **2015**, *357*, 221–226.

(5) Zanatta, N.; Schneider, J. M. F. M.; Schneider, P. H.; Wouters, A. D.; Bonacorso, H. G.; Martins, M. A. P.; Wessjohann, L. A. Regiospecific Synthesis of 4-Alkoxy and 4-Amino Substituted 2-Trifluoromethyl Pyrroles. *J. Org. Chem.* **2006**, *71*, 6996–6998.

(6) Chandrasekhar, S.; Narsihmulu, C. Direct Conversion of Azides to Carbamates and Sulfonamides Using Fe/NH4Cl: Effect of Sonication. *Tetrahedron Lett.* **2000**, *41*, 7969–7972.

(7) Paraskar, A. S.; Sudalai, A. Co-Catalyzed Reductive Cyclization of Azido and Cyano Substituted α,β-Unsaturated Esters with NaBH4: Enantioselective Synthesis of (R)-Baclofen and (R)-Rolipram. *Tetrahedron* **2006**, *62*, 4907–4916.

(8) Ueda, M.; Uenoyama, Y.; Terasoma, N.; Doi, S.; Kobayashi, S.; Ryu, I.; Murphy, J. A. A Construction of 4,4-Spirocyclic γ-Lactams by Tandem Radical Cyclization with Carbon Monoxide. *Beilstein J. Org. Chem.* **2013**, *9*, 1340–1345.

(9) Fringuelli, F.; Pizzo, F.; Vaccaro, L. Cobalt(II) Chloride-Catalyzed Chemoselective Sodium Borohydride Reduction of Azides in Water. *Synthesis* **2000**, 646–650.

(10) Satyanarayana, N.; Periasamy, M. Hydroboration or Hydrogenation of Alkenes with CoCl2-NaBH4. *Tetrahedron Lett.* **1984**, *25*, 2501–2504.

(11) Tjeng, A. A. Stereoselective Synthesis of Nitrogen Containing Compounds from Hydroxy Allylic Azides. *Ph.D Diss. Univ. Toronto* **2011**.

(12) Yang, C.; Shen, H. One Pot Multiple-Steps Reactions of Allyl Azide and Alkenes Carrying Electron-Withdrawing Groups. *Tetrahedron Lett.* **1993**, *34*, 4051–4054.

(13) Yang, C. H.; Lee, L. T.; Yang, J. H.; Wang, Y.; Lee, G. H. Spiropyrazolines from Tandem Reaction of Azides and Alkyl Vinyl Ketones. *Tetrahedron* **1994**, *50*,

12133–12142.

(14) Yang, C.-H.; Shen, H.-J.; Wang, R.-H.; Wang, J.-C. 2,3,7-Triazabicyclo[3.3.0]Octenes Prepared by Tandem Cascade Reaction of Allyl Azides and Olefinic Dipolarophiles. *J. Chinese Chem. Soc.* **2002**, *49*, 95–102.

(15) Tornøe, C. W.; Christensen, C.; Meldal, M. Peptidotriazoles on Solid Phase: [1,2,3]-Triazoles by Regiospecific Copper(I)-Catalyzed 1,3-Dipolar Cycloadditions of Terminal Alkynes to Azides. *J. Org. Chem.* **2002**, *67*, 3057–3064.

(16) Rostovtsev, V. V.; Green, L. G.; Fokin, V. V.; Sharpless, K. B. A Stepwise Huisgen Cycloaddition Process: Copper(I)-Catalyzed Regioselective "Ligation" of Azides and Terminal Alkynes. *Angew. Chem. Int. Ed.* **2002**, *41*, 2596–2599.

(17) Bonandi, E.; Christodoulou, M. S.; Fumagalli, G.; Perdicchia, D.; Rastelli, G.; Passarella, D. The 1,2,3-Triazole Ring as a Bioisostere in Medicinal Chemistry. *Drug Discov. Today* **2017**, *22*, 1572–1581.

(18) Sun, S.; Jia, Q.; Zhang, Z. Applications of Amide Isosteres in Medicinal Chemistry. *Bioorganic Med. Chem. Lett.* **2019**, *29*, 2535–2550.

(19) Filippakopoulos, P.; Picaud, S.; Mangos, M.; Keates, T.; Lambert, J. P.; Barsyte-Lovejoy, D.; Felletar, I.; Volkmer, R.; Müller, S.; Pawson, T.; Gingras, A. C.; Arrowsmith, C. H.; Knapp, S. Histone Recognition and Large-Scale Structural Analysis of the Human Bromodomain Family. *Cell* **2012**, *149*, 214–231.

(20) Filippakopoulos, P.; Qi, J.; Picaud, S.; Shen, Y.; Smith, W. B.; Fedorov, O.; Morse, E. M.; Keates, T.; Hickman, T. T.; Felletar, I.; Philpott, M.; Munro, S.; McKeown, M. R.; Wang, Y.; Christie, A. L.; West, N.; Cameron, M. J.; Schwartz, B.; Heightman, T. D.; La Thangue, N.; French, C. a; Wiest, O.; Kung, A. L.; Knapp, S.; Bradner, J. E. Selective Inhibition of BET Bromodomains. *Nature* **2010**, *468*, 1067–1073.

(21) Urick, A. K.; Hawk, L. M. L.; Cassel, M. K.; Mishra, N. K.; Liu, S.; Adhikari, N.; Zhang, W.; Dos Santos, C. O.; Hall, J. L.; Pomerantz, W. C. K. Dual Screening of BPTF and Brd4 Using Protein-Observed Fluorine NMR Uncovers New Bromodomain Probe Molecules. *ACS Chem. Biol.* **2015**, *10*, 2246–2256.

(22) Divakaran, A.; Talluri, S. K.; Ayoub, A. M.; Mishra, N.; Cui, H.; Widen, J. C.; Berndt, N.; Zhu, J.-Y.; Carlson, A. S.; Topczewski, J. J.; Schönbrunn, E.; Harki, D. A.; Pomerantz, W. C. K. Molecular Basis for the N-Terminal Bromodomain and Extra Terminal (BET) Family Selectivity of a Dual Kinase-Bromodomain Inhibitor. *J. Med. Chem.* **2018**, *61*, 9316–9334.

## Chapter 2: Wacker Oxidation of Cinnamyl Azides

*A report on this research project has been published* [*Org. Lett.* **2018**, *20*, 1604-1607] *and is reprinted (adapted) with permission.*

### 2.1 Wacker Oxidation of Terminal Alkenes

The first generation Wacker oxidation was performed in 1894 by Francis Phillips.[1] Phillips observed the conversion of ethylene to acetaldehyde with stochiometric palladium chloride (Scheme 2.1a). Over 60 years later, Smidt and co-workers at Wacker-Chemie revisited this reaction and found that palladium(0) could be re-oxidized to palladium(II) using copper(II) chloride (Scheme 2.1b).[2,3] Additionally, oxygen could be used to oxidize copper(I) chloride to copper(II) chloride. These two discoveries allow ambient oxygen to act as the stochiometric oxidant, which made the Wacker oxidation industrially useful. This method quickly spread throughout the globe and is used to produce over 100,000 tons of acetaldehyde per year.[4]

**Scheme 2.1. Original Wacker Oxidation.**

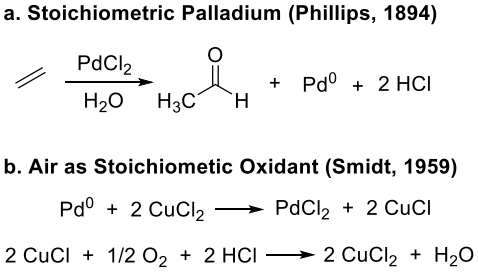


While the mechanism of the Wacker oxidation has been studied extensively, there is still debate over the exact catalytic cycle, the details of which appear condition dependent.[5,6] The overall catalytic cycle is shown in Scheme 2.2 with outer sphere nucleophilic attack. In the presence of chloride ions, palladium dichloride (**2.2.1**) exists in equilibrium with the anionic complex (**2.2.2**). One of the chloride ions is displaced by the alkene (**2.2.3**) and the second is displaced by $H_2O$ (**2.2.4**).

**Scheme 2.2. Catalytic Cycle with Outer Sphere Nucleophilic Attack.**

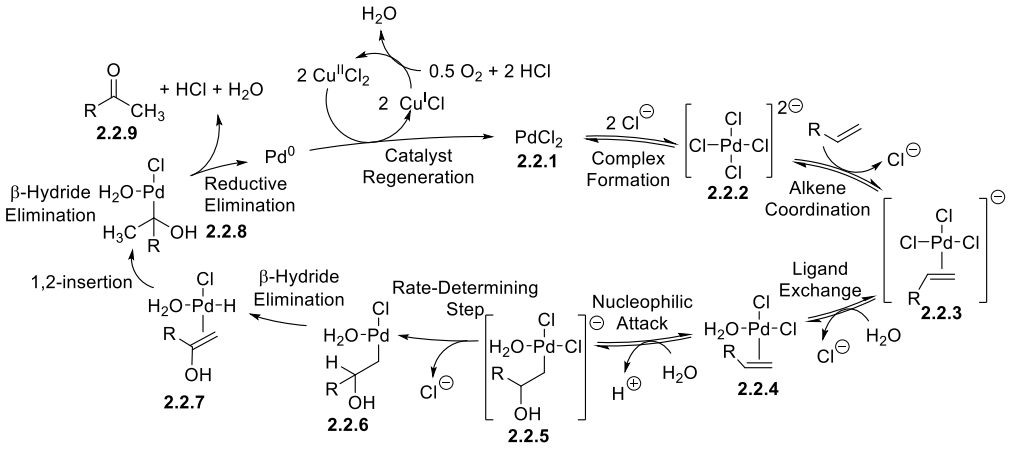


At this point, the reaction is thought to proceed by one of two mechanisms (Scheme 2.3). The palladium-aqua complex (**2.3.1**) exists in equilibrium with the corresponding hydroxo complex (**2.3.2**) and either of the two species can undergo nucleophilic attack. The alkene in the water complex (**2.3.1**) can be attacked via the outer sphere mechanism generating the OH and palladium in a trans relationship (**2.3.3**). Alternatively, the hydroxide complex (**2.3.2**) could undergo a migratory insertion, which would place the OH and palladium on the same side (**2.3.4**). Both mechanisms are possible and the concentrations of chloride ion and copper chloride tend to dictate which mechanism predominates. At low concentrations of chloride ion and copper chloride, the outer sphere mechanism dominates, while at high chloride concentrations the inner sphere mechanism is major. In both mechanisms, nucleophilic attack occurs on the internal end of the olefin to place the sterically bulky palladium complex on the terminal end.

**Scheme 2.3. Two Mechanisms for Nucleophilic Attack.**

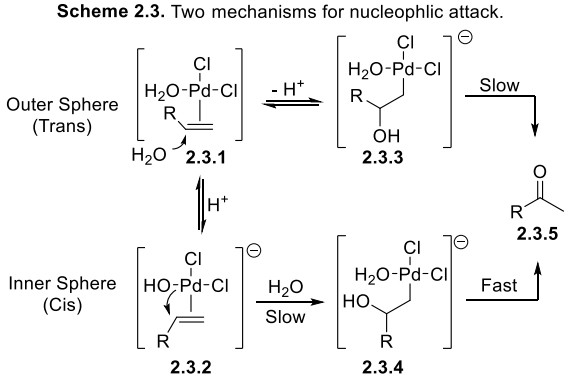


Going back to the catalytic cycle (Scheme 2.2), nucleophilic attack is shown occurring via the outer sphere mechanism (**2.2.5**). This is followed by dissociation of one chloride ion (**2.2.6**), which is thought to be the rate determining step (in the outer sphere mechanism). β-hydride elimination results in the enol (**2.2.7**). Subsequent 1,2-insertion (**2.2.8**) and β-hydride elimination generates the observed ketone (**2.2.9**). The resulting palladium complex undergoes reductive elimination to form palladium (0). In this example, copper is the stoichiometric oxidant which regenerates palladium chloride.

Traditionally, the Wacker oxidation has been performed on terminal alkenes to selectively generate the methyl ketone product (Scheme 2.4a).[5] This selectivity allows the sterically bulky palladium complex to reside on the less hindered terminal carbon. This regioselectivity is also preferred electronically because alkyl groups are electron donating. Attack on the internal end places the greater partial negative charge on the less substituted carbon, which forms the less basic anion. As shown in Makabe's total synthesis of (-)-Cassine, terminal alkenes generally react significantly faster than internal alkenes (Scheme 2.4b).[7] Internal alkenes are sterically congested and thus slow to undergo nucleophilic attack. This allows regioselective oxidation of terminal alkenes in the presence of internal alkenes.

**Scheme 2.4. Ketone Selectivity on Terminal Alkenes.**

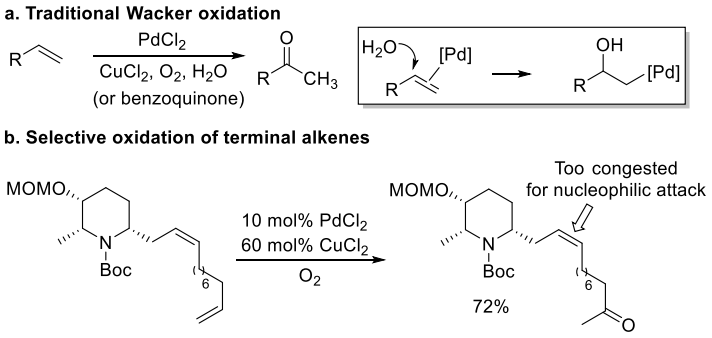


While the Wacker oxidation of terminal alkenes generally exhibits selective ketone formation, a few methods have been developed to obtain the aldehyde. In 2013, Grubbs reported selective aldehyde formation via single electron oxidation (Scheme 2.5a).[8] The nitrite radical attacks the terminal end of the alkene (intermediate **2.5.2**) to form the more stable secondary radical.[9] This is an example of catalyst controlled selectivity. Substrate design can also control selectivity. Allylic heteroatoms can induce aldehyde formation as shown in Brimble's total synthesis of (-)-Herbaric acid (Scheme 2.5b).[10] The allylic heteroatom's electron withdrawing ability causes the terminal end of the alkene to be more electron deficient (intermediate **2.5.5**). This dipole causes nucleophilic attack to occur preferentially at that site. Oxygen coordination to palladium may also contribute to the observed selectivity.

**Scheme 2.5. Aldehyde Selective Oxidation of Terminal Alkenes.**

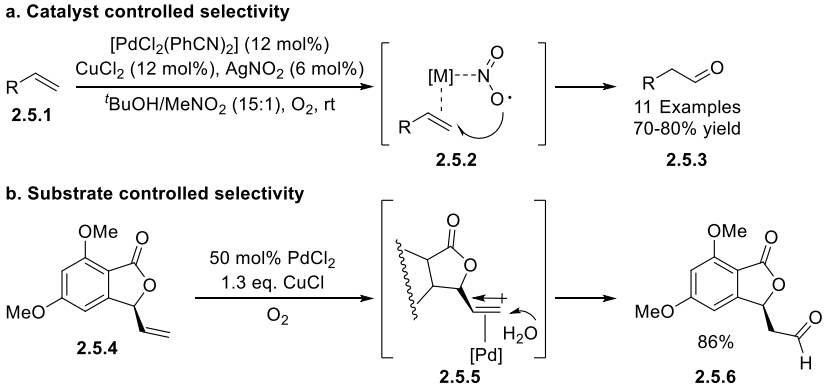


## 2.2 Wacker Oxidation of Internal Alkenes

While Wacker oxidations have traditionally been performed on terminal alkenes, they can also be used to functionalize internal alkenes. Internal alkenes are generally less

reactive and unselective resulting in low yields and mixtures of ketones. In the total synthesis of (+)-Artemisinin, Cook and co-workers performed a Wacker oxidation on an internal alkene (Scheme 2.6). The reaction proceeded in good total yield (92%) but generated a 2:1 mixture of the methyl and ethyl ketones.

**Scheme 2.6. Poor Selectivity for Wacker Oxidations on Internal Alkenes.**

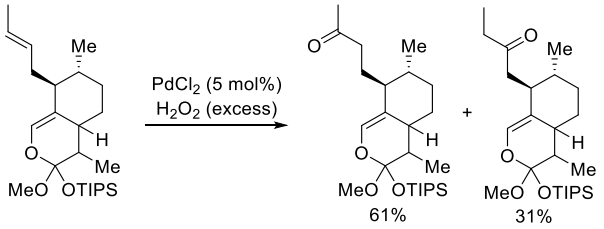


To achieve selectivity on internal alkenes, Sigman and co-workers used allylic heteroatoms to electronically bias the nucleophilic attack (Scheme 2.7a).[11] In the optimized conditions, a bidentate ligand occupies two of palladium's coordination sites and *tert*-butyl hydroperoxide (TBHP) and the alkene occupy the other two (**2.7.1**). Thus, the palladium is coordinatively saturated and the selectivity must be a result of the inductive effect rather than the coordinating effect. Unfortunately, only a few directing groups (e.g. OMOM) afforded high yields and selectivity. The system was particularly ineffective with cis alkenes and alcohol directing groups. Grubbs and co-workers also reported the Wacker oxidation of internal alkenes with allylic heteroatoms employing $Pd(OAc)_2$, benzoquinone, and $HBF_4$ (Scheme 2.7b).[9] This method also produced variable selectivity and was largely substrate and directing group dependent. To increase selectivity, Grubbs switched from allylic heteroatoms to the more electron withdrawing $CF_3$ group (Scheme 2.7c).[12] The $CF_3$ group significantly improved the selectivity and all reported substrates had >20:1 ratios in favor of the distal ketone.

**Scheme 2.7. Heteroatom-Directed Oxidation of Internal Alkenes.**

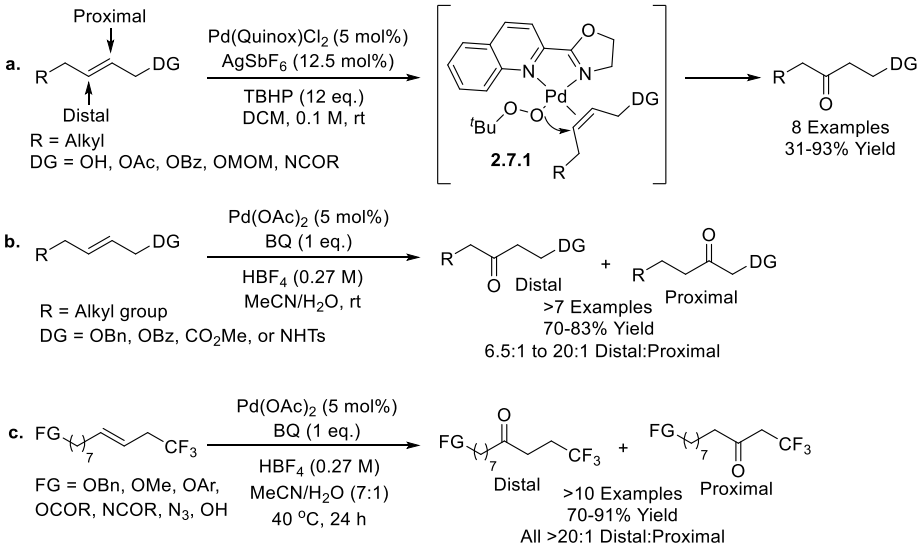


## 2.3 Azides as Effective and Versatile Directing Groups

While the $CF_3$ group provides excellent selectivity, it is not easily diversified. We imagined that azides would be an attractive directing group.[13] Their strong electron withdrawing nature should provide good selectivity and their versatile reactivity will provide a handle for further functionalization.[14] Unlike allylic heteroatoms and $CF_3$ groups, allylic azides can undergo a [3,3]-sigmatropic rearrangement, known as the Winstein rearrangement (Scheme 2.8).[15,16] This causes many allylic azides to exist as a mixture of isomers (Scheme 2.8a). One way to bias the equilibrium is through conjugation. When one isomer is conjugated, the other unconjugated isomer is generally not observed (Scheme 2.8b). I decided to optimize the Wacker oxidation on cinnamyl azides to minimize complicating factors caused by an equilibrating mixture.

**Scheme 2.8. Winstein Rearrangement.**

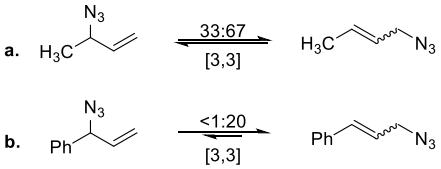


Cinnamyl azides are a convenient starting material because we previously developed a route to synthesize them in one step from benzaldehydes and vinyl Grignard.[17] Vinyl Grignard addition into benzaldehydes afforded the corresponding alkoxide (not shown).

Subsequent addition of diphenylphosphoryl azide (DPPA) generated intermediate **2.9.2** and azide anion. $S_N2$ attack by azide anion generates the unconjugated isomer (**2.9.3**), which quickly rearranges to the more stable conjugated isomer (**2.9.4**). Alternatively, $S_N2$' attack by azide anion on intermediate **2.9.2** could generate the conjugated isomer (**2.9.4**) directly. Regardless of the mechanism, only the conjugated isomer **2.9.4** is observed after the reaction.

**Scheme 2.9. Direct Synthesis of Cinnamyl Azides.**

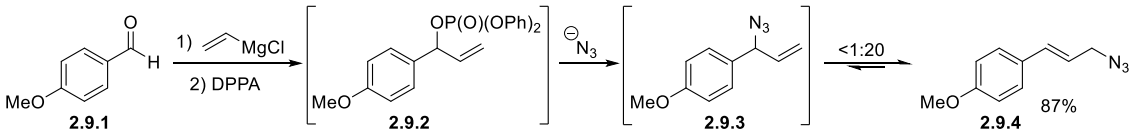


With convenient access to cinnamyl azides, I focused on identifying a highly reactive catalyst (Table 2.1). Given the low reactivity associated with internal alkenes, I examined cationic palladium complexes to achieve the desired oxidation.[9] Preliminarily, $Pd(PhCN)_2Cl_2$ was used as a convenient pre-catalyst and a variety of silver salts were added (entries 1-5). Chloride ions exhibit strong coordination and no Wacker oxidation was observed with the pre-catalyst alone (entry 1). Oxidation of the azide to the corresponding cinnamaldehyde was observed as a background reaction.[18,19] However, in the presence of silver (I) salts, the desired Wacker oxidation was observed (entries 2-5). Presumably, halogen abstraction generates a more reactive cationic palladium species *in situ*. The conversion and yield increased with all of the examined non-coordinating counter ions. This suggests the formation of solvated $Pd^{2+}(MeCN)_4$ and a presumed leveling effect under the aqueous conditions. The addition of catalytic quantities of benzoquinone was advantageous (entry 5 vs 6). When benzoquinone was used as the stoichiometric oxidant, the yield was diminished (entry 7). Furthermore, control experiments revealed that silver is not necessary (entry 8), and that the nitrate ion is beneficial (entry 8 vs 9). Lastly, the procedure could be further optimized by reducing the amount of water used as a co-solvent and by adding the Oxone portion-wise to slow the background azide oxidation (entry 10 vs 11). The final procedure is operationally simple, was conducted on the benchtop, and uses readily available materials.

**Table 2.1.** Optimization of the Wacker Oxidation

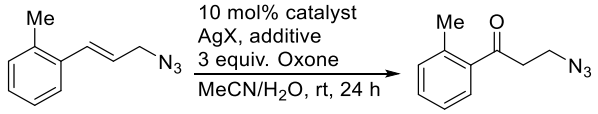


| entry | [Pd] | AgX | Additive(s) | Yield (%)[b] |
|---|---|---|---|---|
| 1 | $Pd(PhCN)_2Cl_2$ | - | - | 0 |
| 2 | $Pd(PhCN)_2Cl_2$ | AgOTf | - | 33 |
| 3 | $Pd(PhCN)_2Cl_2$ | $AgSbF_6$ | - | 39 |
| 4 | $Pd(PhCN)_2Cl_2$ | $AgBF_4$ | - | 18 |
| 5 | $Pd(PhCN)_2Cl_2$ | $AgNO_3$ | - | 40 |
| 6 | $Pd(PhCN)_2Cl_2$ | $AgNO_3$ | BQ | 73 |
| 7[c] | $Pd(MeCN)_4(BF_4)_2$ | - | 1.2 equiv. BQ, $KNO_3$ | 51 |
| 8 | $Pd(MeCN)_4(BF_4)_2$ | - | BQ | 59 |
| 9 | $Pd(MeCN)_4(BF_4)_2$ | - | BQ, $KNO_3$ | 71 |
| 10[d] | $Pd(PhCN)_2Cl_2$ | $AgNO_3$ | BQ | 67 |
| 11[e] | $Pd(PhCN)_2Cl_2$ | $AgNO_3$ | BQ | 80 |

[a]Reaction conditions: substrate (60 μmol), naphthalene standard (12 μmol), [Pd] (6 μmol, 10 mol%), AgX (15 μmol, 25 mol%), benzoquinone (15 μmol, 25 mol%), Oxone (180 μmol, 3 equiv.), water (50 μL), MeCN (400 μL), under air, room temperature. [b]Conversion and yield were determined by calibrated GC-FID analysis. Reactions were run in duplicate and the average value is reported. [c]Reaction was conducted with 1.2 equivalents of benzoquinone and no Oxone. [d]Reaction was run using double the volume of water (100 μL). [e]Oxone was added portion-wise.

To determine the functional group tolerance of this Wacker oxidation, the robustness screen advocated by Glorius was performed.[20,21] The full test set, plus a few additional additives, is shown in Table 2.2. Several of the functional groups were well tolerated including a free alcohol (**2.2a**), nitrile (**2.2b**), ketone (**2.2c**), heterocycle (**2.2d**), alkyl halide (**2.2e**), and aryl halide (**2.2f**). Readily oxidized functional groups such as aniline (**2.2g**), furan (**2.2h**), pyrrole (**2.2i**), and benzaldehyde (**2.2j**), were degraded. Acetal **2.2l** hydrolyzed to benzaldehyde. Terminal alkenes (**2.2m**) underwent Wacker oxidation faster than the cinnamyl azide and alkynes inhibited the reaction (**2.2n** and **2.2o**). Additionally, as would be expected for an electrophilic metal center, good ligands inhibited the catalyst (**2.2p**-**2.2q**). In some cases, these limitations could be overcome. For instance, 2,6-lutidine

(**2.2r**) was not as strong of an inhibitor and acetanilide (**2.2s**) was tolerated even though aniline was not.

**Table 2.2.** Robustness Screen

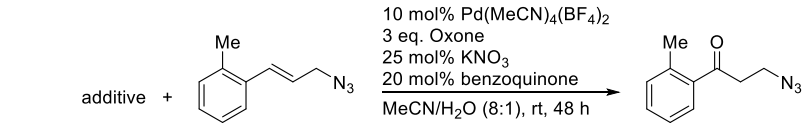


| | | | | | | | |
|---|---|---|---|---|---|---|---|
| none | A: n/a<br>S: 1%<br>P: 83% | **2.2e** 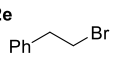 | A: >95%<br>S: 3%<br>P: 84% | **2.2j** 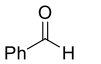 | A: 47%<br>S: 7%<br>P: 52% | **2.2o** 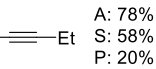 | A: 78%<br>S: 58%<br>P: 20% |
| **2.2a** 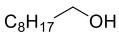 | A: 75%<br>S: 3%<br>P: 66% | **2.2f**  | A: >95%<br>S: 4%<br>P: 78% | **2.2k**  | A: 67%<br>S: 48%<br>P: 25% | **2.2p**  | A: 45<br>S: 76%<br>P: nd |
| **2.2b** 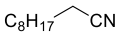 | A: >95%<br>S: 5%<br>P: 82% | **2.2g** 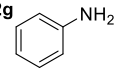 | A: 1%<br>S: 81%<br>P: nd | **2.2l** 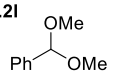 | A: nd[b]<br>S: 5%<br>P: 62% | **2.2q** 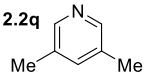 | A: 58%<br>S: 69%<br>P: nd |
| **2.2c** 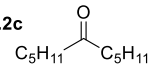 | A: >95%<br>S: 5%<br>P: 80% | **2.2h** 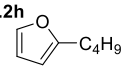 | A: 2%<br>S: 52%<br>P: nd | **2.2m** 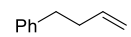 | A: nd[c]<br>S: 32%<br>P: 46% | **2.2r** 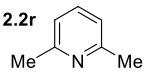 | A: 56%<br>S: 16%<br>P: 46% |
| **2.2d** 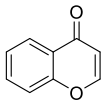 | A: 78%<br>S: 6%<br>P: 80% | **2.2i**  | A: nd<br>S: 75%<br>P: nd | **2.2n** 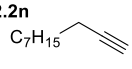 | A: nd<br>S: 46%<br>P: 33% | **2.2s** 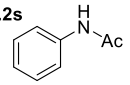 | A: 89%<br>S: 9%<br>P: 85% |

A = additive % remaining; S = starting material % remaining; P = product % formed. Reported values determined by GC-FID analysis. A and S were determined based on a single point calibration. P was calibrated by linear regression. Values reported are the average of duplicate trials. [b]Benzaldehyde was observed as the major product. [c]4-Phenyl-2-butanone was observed as the major product.

A variety of substrates were examined (Table 2.3). Cinnamyl azide was oxidized in comparable yield to the model substrate (**2.3b**). Other electronically neutral or methylated aryl rings provided acceptable yields (**2.3c** – **2.3f**). Double *ortho*-substitution was tolerated and ketone **2.3g** was isolated in moderate yield. More electron rich aryl rings were the preferred substrates (**2.3h** – **2.3n**). Even though benzyl acetal **2.3l** was hydrolyzed, the BOM acetal present in **2.3n** was compatible with the reaction. Lastly, the reaction was qualitatively slowed with electron withdrawing groups. This resulted in diminished but acceptable yields (**2.3o** and **2.3p**).

**Table 2.3.** Substrate Scope of Azide Directed Wacker Oxidation.

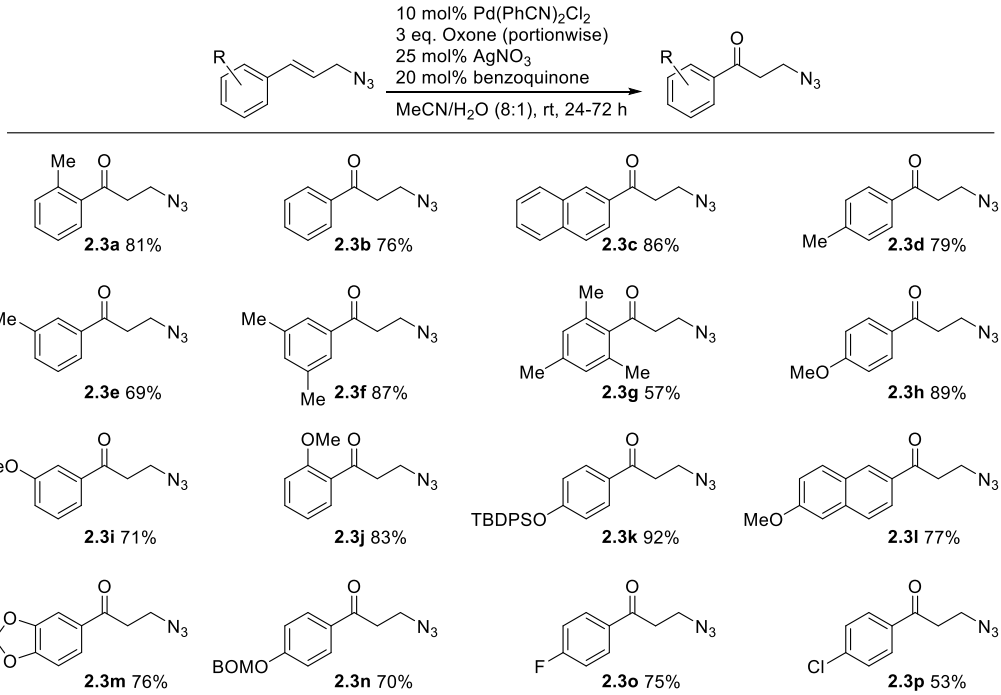


Yields are of isolated and purified material. Values reported are the average of duplicate trials.

This procedure was easily conducted on a gram scale (Scheme 2.10). The β-azido-ketone was readily diversified. The ketone was selectively reduced to provide alcohol **2.10.1**. Allylation of the ketone was successful without azide elimination and afforded alcohol **2.10.2**. A copper-catalyzed azide-alkyne cycloaddition afforded triazole **2.10.3**.

**Scheme 2.10. Gram Scale Reaction and Diversification of Products.**

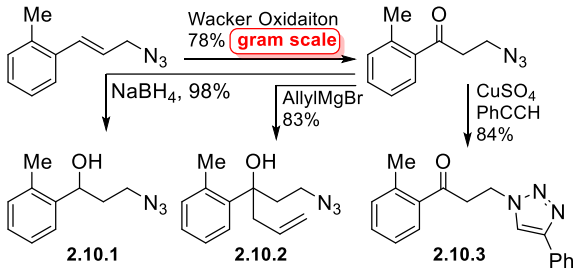


I also performed this Wacker oxidation on an aliphatic azide (Scheme 2.11). This was complicated by the Winstein rearrangement, which causes most aliphatic azides to exist as a mixture of isomers.[15,16,22] The equilibrium mixture of azides **2.11.1** and **2.11.2** was subjected to the reaction conditions. This reaction afforded an acceptable yield of ketone **2.11.3**, which was contaminated with small quantities of the regioisomer **2.11.4**. Azide

**2.11.2** provided aldehyde **2.11.5**. Aldehyde **2.11.5** is not stable under the reaction conditions, and a number of over oxidized products were observed.

**Scheme 2.11. Wacker Oxidation on an Equilibrating Allylic Azide.**

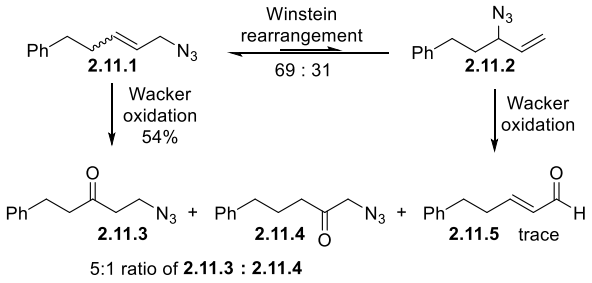


In conclusion, we developed a Wacker oxidation for cinnamyl azides that provides the aryl ketone with excellent selectivity. The procedure is operationally simple, conducted under air, and uses Oxone as the stoichiometric oxidant. A robustness screen was conducted that defines the limitations of this method. Many substrates provide a high yield of the ketone product and this procedure can be conducted on a gram scale.

## 2.4 Experimental

All the experimental details and characterization data from this chapter can be found in the supplemental information for *Org. Lett.* **2018**, *20*, 1604-1607.

## 2.5 References


(1) Phillips, F. C. Researches upon the Phenomena of Oxidation and Chemical Properties of Gases. *Am. Chem. J.* **1894**, *16*, 255–277.

(2) Jira, R. Acetaldehyde from Ethylene - A Retrospective on the Discovery of the Wacker Process. *Angew. Chem. Int. Ed.* **2009**, *48*, 9034–9037.

(3) Smidt, J.; Hafner, W.; Jira, R.; Sedlmeier, F.; Sieber, R.; Kojer, H.; Juttinger, R. Catalytic Reactions of Olefins on Compounds of the Platinum Group. *Angew. Chem.* **1959**, *71*, 176.

(4) Eckert, M.; Fleischmann, G.; Jira, R.; Bolt, H.; Golka, K. Acetaldehyde. *Ullman's Encycl. Ind. Chem.* **2012**, *1*, 191–205.

(5) Keith, J. A.; Henry, P. M. The Mechanism of the Wacker Reaction: A Tale of Two Hydroxypalladations. *Angew. Chem. Int. Ed.* **2009**, *48*, 9038–9049.

(6) Kurti, L.; Czako, B. *Strategic Applications of Named Reactions in Organic Synthesis*; 2005.

(7) Makabe, H.; Kong, L. K.; Hirota, M. Total Synthesis of (-)-Cassine. *Org. Lett.* **2003**, *5*, 27–29.

(8) Wickens, Z. K.; Morandi, B.; Grubbs, R. H. Aldehyde-Selective Wacker-Type Oxidation of Unbiased Alkenes Enabled by a Nitrite Co-Catalyst. *Angew. Chem. Int. Ed.* **2013**, *52*, 11257–11260.

(9) Morandi, B.; Wickens, Z. K.; Grubbs, R. H. Regioselective Wacker Oxidation of Internal Alkenes: Rapid Access to Functionalized Ketones Facilitated by Cross-Metathesis. *Angew. Chem. Int. Ed.* **2013**, *52*, 9751–9754.

(10) Choi, P. J.; Sperry, J.; Brimble, M. A. Heteroatom-Directed Reverse Wacker Oxidations. Synthesis of the Reported Structure of (-)-Herbaric Acid. *J. Org. Chem.* **2010**, *75*, 7388–7392.

(11) Deluca, R. J.; Edwards, J. L.; Steffens, L. D.; Michel, B. W.; Qiao, X.; Zhu, C.; Cook, S. P.; Sigman, M. S. Wacker-Type Oxidation of Internal Alkenes Using Pd(Quinox) and TBHP. *J. Org. Chem.* **2013**, *78*, 1682–1686.

(12) Lerch, M. M.; Morandi, B.; Wickens, Z. K.; Grubbs, R. H. Rapid Access to β-Trifluoromethyl-Substituted Ketones: Harnessing Inductive Effects in Wacker-Type Oxidations of Internal Alkenes. *Angew. Chem. Int. Ed.* **2014**, *53*, 8654–8658.

(13) Carlson, A. S.; Calcanas, C.; Brunner, R. M.; Topczewski, J. J. Regiocontrolled Wacker Oxidation of Cinnamyl Azides. *Org. Lett.* **2018**, *20*, 1604–1607.

(14) Bräse, S.; Gil, C.; Knepper, K.; Zimmermann, V. Organic Azides: An Exploding Diversity of a Unique Class of Compounds. *Angew. Chem. Int. Ed.* **2005**, *44*, 5188–5240.

(15) Gagneux, A.; Winstein, S.; Young, W. G. Rearrangement of Allyl Azides. *J. Am. Chem. Soc.* **1960**, *82*, 5956–5957.

(16) Carlson, A. S.; Topczewski, J. J. Allylic Azides: Synthesis, Reactivity, and the Winstein Rearrangement. *Org. Biomol. Chem.* **2019**, *17*, 4406–4429.

(17) Goswami, P. P.; Suding, V. P.; Carlson, A. S.; Topczewski, J. J. Direct Conversion of Aldehydes and Ketones into Azides by Sequential Nucleophilic Addition and Substitution. *Eur. J. Org. Chem.* **2016**, 4805–4809.

(18) Giovani, S.; Singh, R.; Fasan, R. Efficient Conversion of Primary Azides to Aldehydes Catalyzed by Active Site Variants of Myoglobin. *Chem. Sci.* **2016**, *7*, 234–239.

(19) Barragan, E.; Bugarin, A. π-Conjugated Triazenes: Intermediates That Undergo Oxidation and Substitution Reactions. *J. Org. Chem.* **2017**, *82*, 1499–1506.

(20) Collins, K. D.; Glorius, F. A Robustness Screen for the Rapid Assessment of Chemical Reactions. *Nat. Chem.* **2013**, *5*, 597–601.

(21) Gensch, T.; Teders, M.; Glorius, F. Approach to Comparing the Functional Group Tolerance of Reactions. *J. Org. Chem.* **2017**, *82*, 9154–9159.

(22) Packard, M. H.; Cox, J. H.; Suding, V. P.; Topczewski, J. J. The Effect of Proximal Functionality on the Allylic Azide Equilibrium. *Eur. J. Org. Chem.*

**2017**, *2017*, 6365–6368.

## Chapter 3: Cascade Reaction Between Allylic Azides and Michael Acceptors

*This chapter describes the outcome of a collaborative research project carried out with En-chih Liu. A report on this research project has been published* [*J. Org. Chem.* **2020**, *85*, 6044-6059*] which has been reprinted (adapted) with permission. I started this project and performed the initial optimization and substrate scope. ECL helped complete the optimization of problematic substrates and expanded the substrate scope.*

### 3.1. Background on Tetrahydro-pyrrolo-pyrazole Heterocycles

Nitrogenous heterocycles are ubiquitous in pharmaceuticals, agrochemicals, and natural products. A 2014 analysis of FDA approved pharmaceuticals concluded that 59% of small-molecule active pharmaceutical ingredients contain a nitrogenous heterocycle.[1] A recent analysis indicates, that in the last 3 years, over half of the newly FDA approved drugs contain a *saturated N*-heterocycle.[2] Saturated heterocycles confer a number of adventitious properties relative to heteroarenes[3–5] such as offering stereochemical complexity, increased aqueous solubility,[6] and enhanced metabolic stability.[6,7] Shortening the route to some of these heterocycles could have a significant impact on the cost and rate of drug discovery. One subset of nitrogen heterocycles that are particularly challenging to synthesize are bicyclic nitrogen heterocycles. This problem was emphasized by scientists at Merck in a recent review which stated that one "key unsolved problem in synthetic chemistry [is the] concise synthesis of highly functionalized constrained bicyclic amines."[8] One such example that highlights this issue are substituted tetrahydro-pyrrolo-pyrazole heterocycles (Figure 3.1). These heterocycles are known to be biologically active with a variety of potential applications but can be challenging to synthesize.[9–13]

**Figure 3.1**. Examples of Tetrahydro-pyrrolo-pyrazoles.

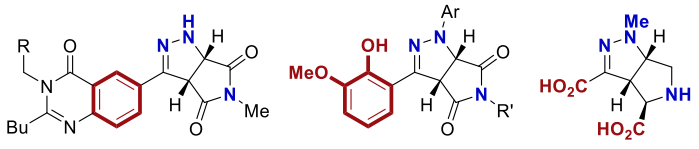


When the pyrrolidine moiety contains two carbonyls (e.g. compounds **3a** and **3b**), the heterocycles can easily be generated through cycloaddition of a diazo species to activated maleimide derivatives[9] or via conjugate addition/cyclization with a hydrazone (Scheme 3.1a).[11] In this case, neither regioselectivity nor stereoselectivity are an issue. However,

when the pyrrolidine is not symmetrical (e.g. compound **3c**), the synthesis becomes much more challenging. Compound **3c** was formed through an alkene-hydrazone cycloaddition which generated two regioisomer, each as a pair of diastereomers. Preparatory HPLC was required to isolate the desired isomer.

One method to enforce the desired regio- and diasteroselectivity is through intramolecularity. Zard demonstrated that hydrazones with pendant alkenes can be oxidized to the diazo species (Scheme 3.1b, **3.1.5**).[14] Intermediate **3.1.5** can undergo an intramolecular diazo-alkene cycloaddition to form heterocycle (**3.1.6**) with excellent regio- and diastereoselectivity. However, this approach requires pre-installation of all the necessary functionality into one molecule. Jahn demonstrated a more modular approach to access the diazo-alkene intermediate (**3.1.9**, Scheme 3.1c).[15,16] Treatment of amine **3.1.7** with *n*-BuLi and an acrylate triggered an *aza*-Michael reaction to generate enolate **3.1.8**. Subsequent addition of $NfN_3$ initiated a diazo transfer reaction to afford diazo-alkene intermediate (**3.1.9**). This intermediate cyclized to form compound **3.1.10** albeit with variable diastereoselectivity. This sequence provides a more modular approach, but it requires an alkyl group on the amine, which can be hard to remove and may make the products less versatile. Additionally, the use of *n*-BuLi and $NfN_3$ make it less attractive on a large scale and more complicated to perform. Yang and co-workers reported a different approach to accessing the diazo-alkene intermediate (**3.1.13**, Scheme 3.1d).[17,18] Simply by mixing allyl azide with methyl acrylate, triazoline **3.1.12** is formed. Triazolines can exist in equilibrium with the corresponding diazo compound (**3.1.13**).[19,20] Subsequent cycloaddition of diazo **3.1.13** generates tetrahydro-pyrrolo-pyrazole (**3.1.14**).

**Scheme 3.1. Synthesis of Tetrahydro-pyrrolo-pyrazoles.**

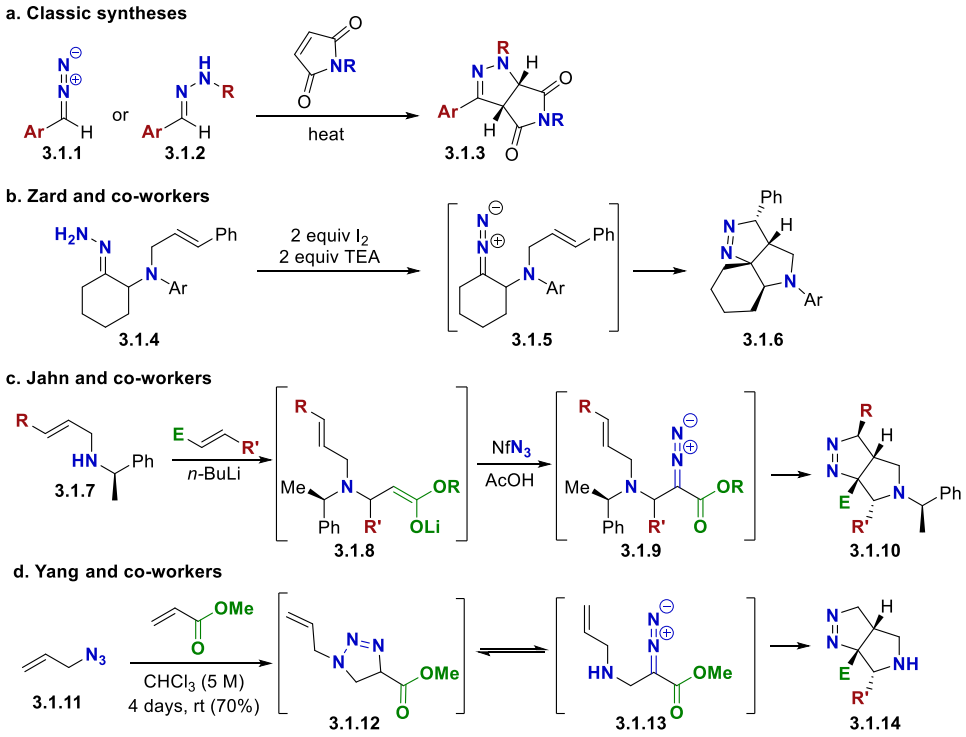


## 3.2 Optimizing Conditions to Generate Tetrahydro-pyrrolo-pyrazole Heterocycles

While Yang's report is exciting, the reported conditions were mostly restricted to allyl azide and our attempts to perform this reaction on cinnamyl azide proceeded in very low yields (~15%). We recognized that this could be a powerful reaction if the conditions were reoptimized to make it more widely applicable. When trying a slight variation of Yang's conditions, large quantities of the triazoline intermediates were observed (Table 3.1). This prompted me to examine conditions that would promote triazoline conversion into the desired heterocycle. When mixed with TEA, triazoline **3.1a** cleanly converted to the tetrahydro-pyrrolo-pyrazole (Scheme 3.2, **3.2.6**) product in ~30 min at rt. Unfortunately, when TEA is added to the reaction, the TEA also promotes a subsequent conjugate addition. The mechanism of this cascade reaction involves several reactive intermediates that can undergo other side reactions.

**Table 3.1.** Synthesis of Triazoline Intermediates.

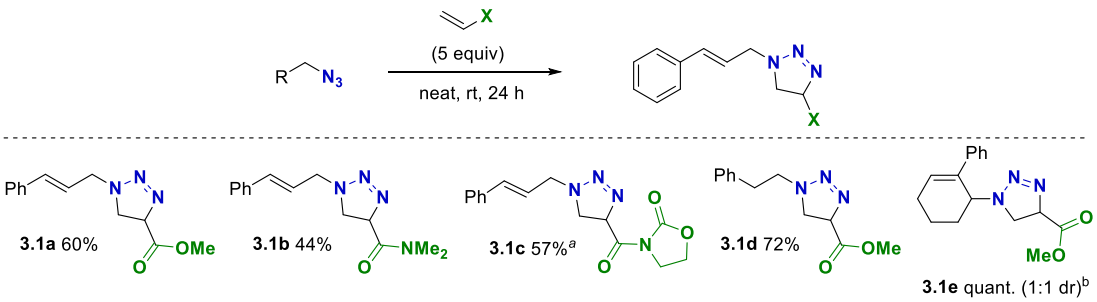


Yields are reported for isolated and purified products. [a]Reaction was run in DCM (3 M). [b]Reaction was run in toluene (0.2 M) at 80 °C.

A plausible mechanism for this cascade reaction and side product formation are shown in Scheme 3.2. This proposal is based on the work of L'abbe[20,21] and Yang.[18,22] The cascade is thought to proceed via an initial Huisgen cycloaddition to afford triazoline **3.2.3**.[20,21,23–27] This cycloaddition generally proceeds with good selectivity, but the regioisomeric triazoline **3.2.2** was frequently observed (~5%).[20] Triazoline **3.2.3** can equilibrate to achiral diazo species **3.2.4**.[19,20] Amine bases facilitate this equilibrium, which likely explains the observation that TEA facilities conversion from the triazoline to the fused ring product.[20,21] Intermediate **3.2.4** can undergo an intramolecular diazo-alkene cycloaddition to afford compound **3.2.5**.[18,22] Alternatively, in the presence of excess acrylate, diazo **3.2.4** can intercept a second equivalent of acrylate to form product **3.2.8**.[18,22,28,29] When compound **3.2.5** contains a hydrogen atom at the benzylic position, it can tautomerize to generate conjugated product **3.2.6**.[18,22] Cyclopropane **3.2.9** can arise from intermediate **3.2.5** via the loss of nitrogen.[18,30] Lastly, products **3.2.5** and **3.2.6** are sufficiently nucleophilic to engage excess acrylate in a conjugate addition, affording compound **4.**[18,22] While TEA promotes product formation, it also facilitates this conjugate addition.

**Scheme 3.2. Mechanism of Cascade Reaction.**

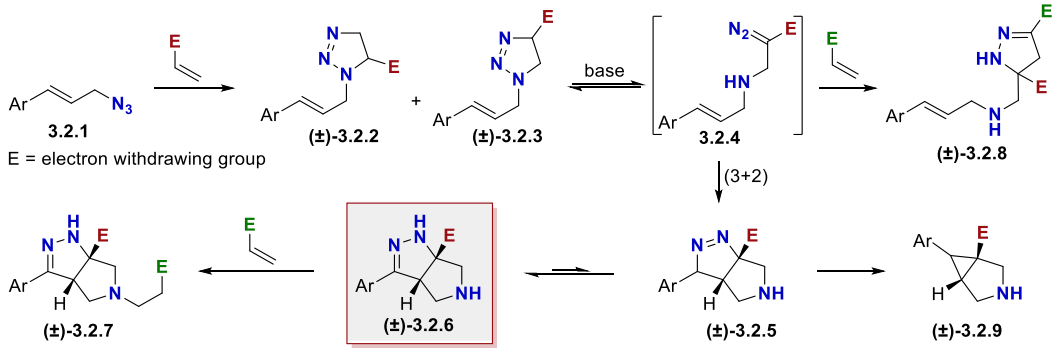


En-chih Liu and I jointly completed the reaction optimization and substrate scope. Qualitatively, the cascade reaction appeared to proceed more efficiently with a cinnamyl azide featuring a polarizing aryl substituent. This was true regardless of if the substituent is commonly thought of as electron donating (e.g. OMe) or withdrawing (e.g. $NO_2$) group (*vide infra*). The substrate 2-nitrocinnamyl azide (**3.2a**) was selected for optimization along with methyl acrylate due to the availability of 2-nitrocinnamaldehyde (Table 3.2). Solvents with a range of polarities were examined (entries 1-5). Polar solvents promoted the conjugate addition that formed product **3.2d** (entries 1-2), while non-polar solvents suppressed the conjugate addition (entries 4-5). The observation that formation of product **3.2d** could be suppressed in non-polar media is consistent with the need to form ionic intermediates during conjugate addition. When hexane was used, a significant amount of the conjugate addition was observed because the product was insoluble in hexane, resulting in a reaction that was pseudo-neat in methyl acrylate (entry 3).

Having identified THF and benzene as the optimal solvents, TEA and several other additives were examined. The addition of acetic acid or HFIP promoted the conjugate addition likely because the acidic reagents active methyl acrylate for nucleophilic attack (entries 6-7). Consistent with our previous observations, TEA and other amine bases were the most effective at converting triazoline intermediate **3.2b** to the desired product (entries 8-11). DIPEA was chosen as the optimal base because it efficiently converted the triazoline into the product without further promoting the conjugate addition. Given the complications associated with conjugate addition (e.g. polymerization of acrylate), it is perhaps unsurprising that DMAP and pyridine provided poor results and that less nucleophilic amine bases were preferred. Ultimately, conditions utilizing DIPEA in benzene (entry 11)

were chosen as the optimal conditions. Toluene and THF were suitable alternative solvents (entries 12-14).

**Table 3.2.** Cascade Optimization with Methyl Acrylate.

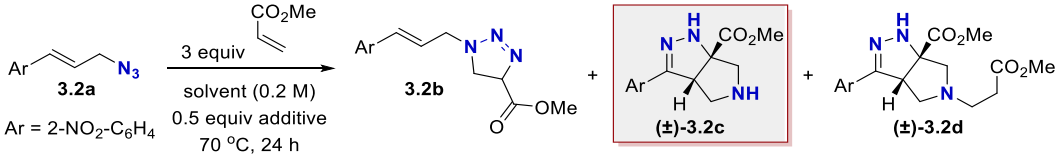


| entry | solvent | additive | **3.2b** (%)[a] | **3.2c** (%)[a] | **3.2d** (%)[a] |
|---|---|---|---|---|---|
| 1 | DMSO | - | n.d. | 77 | 14 |
| 2 | MeOH | - | n.d. | n.d. | 95 |
| 3 | Hexane | - | n.d. | 35 | 54 |
| 4 | THF | - | 34 | 46 | n.d. |
| 5 | $C_6H_6$ | - | 37 | 11 | n.d. |
| 6 | $C_6H_6$ | AcOH | n.d. | n.d. | 67 |
| 7 | $C_6H_6$ | HFIP | n.d. | 17 | 55 |
| 8 | $C_6H_6$ | DMAP | n.d. | 80 | 8 |
| 9 | $C_6H_6$ | pyridine | 5 | 41 | n.d. |
| 10 | $C_6H_6$ | TEA | n.d. | 85 | n.d. |
| **11** | **$C_6H_6$** | **DIPEA** | **n.d.** | **91** | **n.d.** |
| 12 | PhMe | DIPEA | n.d. | 83 | n.d. |
| 13 | THF | TEA | n.d. | 72 | n.d. |
| 14 | THF | DIPEA | n.d. | 78 | n.d. |

[a]Reactions were conducted with azide **1b** (70 µmol), methyl acrylate (210 µmol), and additive (35 µmol) in solvent (0.2 M) at 70 °C. Conversion and yield were determined by calibrated GC-FID analysis. Reactions were run in duplicate and the average value is reported. Not detected = n.d.

The optimized reaction conditions work well with a variety of cinnamyl azides (Table 1). Compound **3.3a** was isolated in 94% yield. The product from cinnamyl azide (**3.3b**) was crystalline and diffraction analysis confirmed the structure (crystal structure was solved by Ryan Daley). Other cinnamyl azides containing electron donating groups (**3.3c**, **3.3d**, and **3.3h**) and electron withdrawing groups (**3.3f**, **3.3g**, and **3.3i**) were tolerated. *Ortho* substitution was tolerated (**3.3a**, **3.3h**, and **3.3i**). Lastly, products with an electron

rich heteroarene (**3.3j** and **3.3k**) or an electron deficient heteroarene (**3.3l** – **3.3n**) were isolated in good yield. It is worth noting that at the end of these reactions, the desired product frequently existed as a mixture of the two tautomers **3.2.5** and **3.2.6** (see Scheme 3.2). TFA was added during the workup to convert the mixture into the more stable conjugated tautomer **3.2.6**. In some instances, silica gel and DBU were also able to promote tautomerization.

**Table 3.3.** Scope of the Cascade Reaction with Cinnamyl Azides.

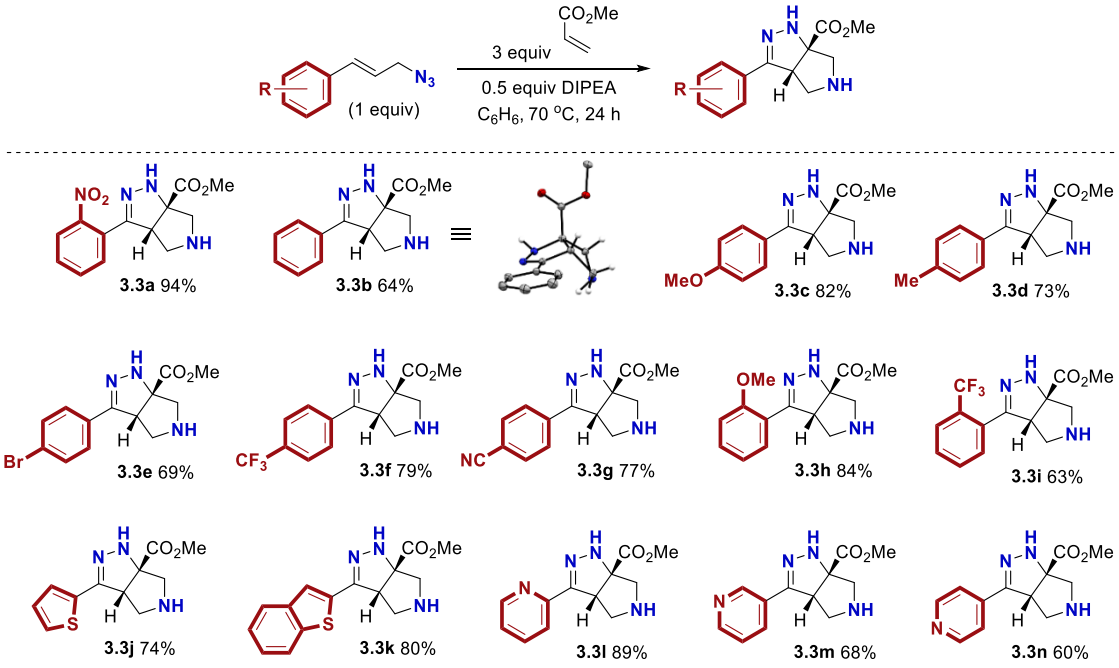


Yields are reported for isolated and purified products. Yield values reflect the average of duplicate trials. ORTEP structure of **3.3b** shown with select hydrogen atoms displayed.

When the optimized conditions were used with more highly substituted allylic azides, diazo cycloaddition with a second equivalent of methyl acrylate was a major side reaction (product **3.2.8**, Scheme 3.2). To mitigate this side product, a second procedure was developed for products where the intramolecular cyclization was slow (Table 3.4). The triazoline was pre-formed by mixing the azide and acrylate neat at room temperature. Excess acrylate was removed in *vacuo.* Then the triazoline was heated in the presence of DIPEA in $C_6H_6$, which triggered the remainder of the cascade. A methyl or a phenyl group could be incorporated adjacent to the azide (**3.4a** and **3.4b**). A minor diastereomer was not detected for compound **3.4b** and the relative configuration was assigned based on a crystal

structure (not shown). The relative stereochemistry of product **3.4a** was assigned by analogy. For product **3.4a**, a minor diastereomer was observed.[31,32] A tertiary azide afforded product **3.4c**. A methyl group could be incorporated in the α or β position relative to the arene, affording compounds **3.4d** and **3.4e**. A branched allylic azide was suitable and afforded product **3.4f**. This product is noteworthy because significant eclipsing interactions likely exist between the bridgehead substituents. Furthermore, a cyclic azide afforded caged systems (**3.4g**-**3.4h**). A proximal arene was not required (**3.4i**).

**Table 3.4.** Reaction Scope with Substituted Allylic Azides

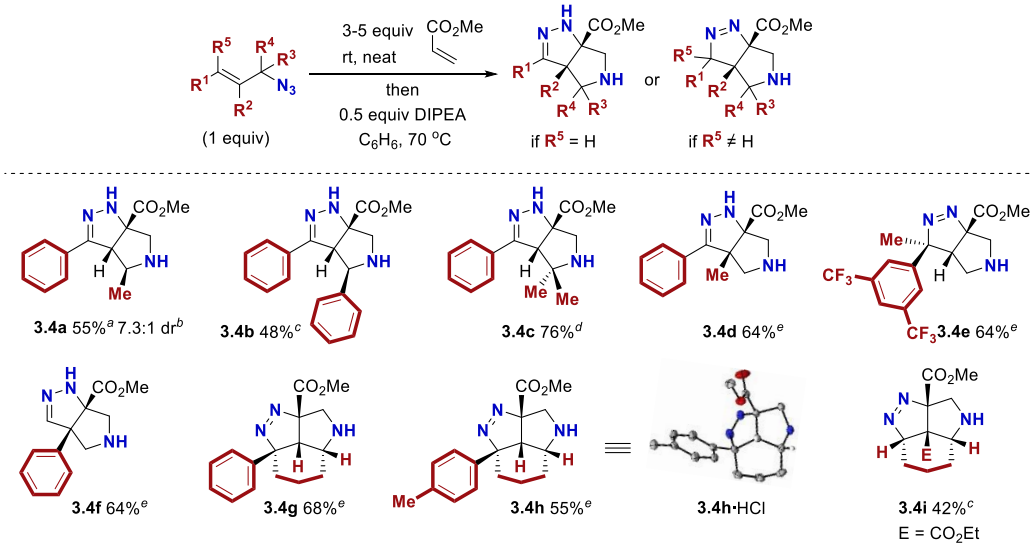


Yields are reported for isolated and purified products. Yield values reflect the average of duplicate trials. [a]Initial 72 h incubation at rt with an additional 24 h at 70 °C. [b]Diastereomeric ratio determined by crude $^1$H NMR spectroscopy. [c]Reaction for 48 h at 70 °C. [d]Reaction for 72 h at 70 °C. [e]Initial 48 h incubation at rt with an additional 24 h at 70 °C.

A single enantiomer of azide **3.3.1** (>99:1 er) was utilized (Scheme 3.3).[33] Product **3.4h** could be isolated with no loss in enantiomeric purity (>99:1 er). This represents a tremendous amplification of stereochemical complexity. Azide **3.3.1** contains only a single stereocenter. Product **3.4h** contains four contiguous stereocenters, three of which are generated from this cascade reaction. Two stereocenters are formed at tetrasubstituted carbon atoms that bear a nitrogen substituent, which are known to be particularly challenging stereocenters to establish.[8,34]

**Scheme 3.3. Stereospecific Cascade Reaction.**

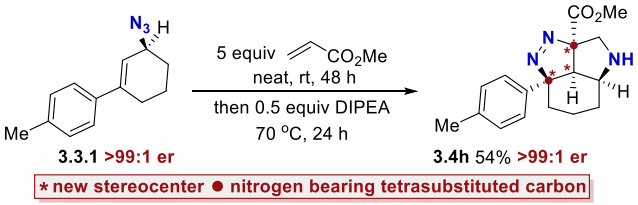


The reaction was investigated with other Michael acceptors (Table 3.5). Simple acrylates provided high yields (**3.5a-3.5c**). The use of methyl or benzyl crotonate afforded products **3.5d** and **3.5e** in high yield and modest dr. The relative configuration of compound **3.5d** was determined by X-ray diffraction analysis (En-chih Liu solved the crystal structure) and the configuration of product **3.5e** was assigned by analogy. The use of methyl vinyl ketone afforded product **3.5f** exclusively. The Michael addition could be suppressed by trapping the initial adduct with TsCl (**3.5g**). Other Michael acceptors including acrylamide (**3.5h**), acrylonitrile (**3.5i**), and diethyl vinyl phosphonate (**3.5j**) were effective. When diethyl vinyl phosphonate was used as the Michael acceptor, the regioisomeric triazoline (**3.2.2**, from Scheme 3.2) was a significant byproduct (ca. 1:1).

**Table 3.5.** Reaction Scope with Different Michael Acceptors

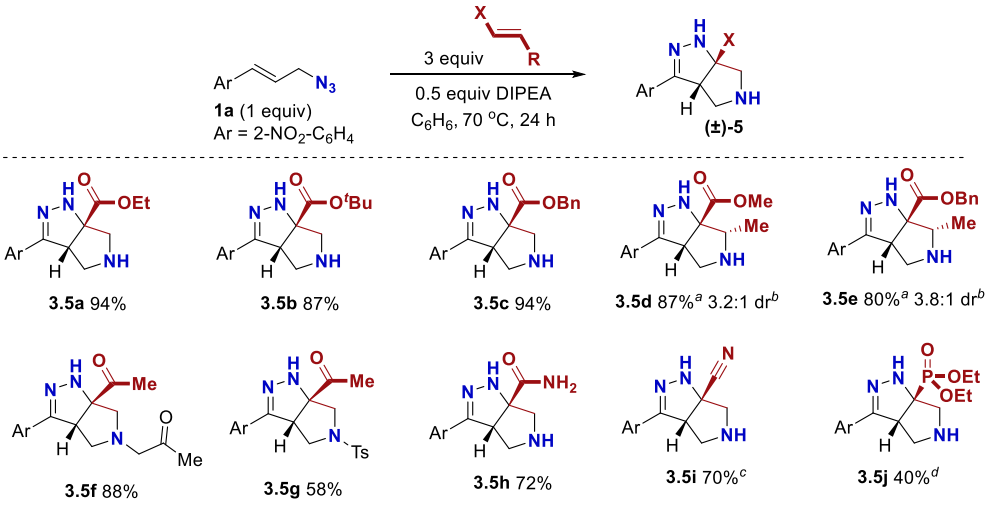


Yields are reported for isolated and purified products. Yield values reflect the average of duplicate trials. [a]Reaction for 5 days at 70 °C. [b]Diastereomeric ratio determined by crude $^1$H NMR spectroscopy. [c]Initial 24 h incubation neat at 40 °C. Then $C_6H_6$ and DIPEA were added for an additional 24 h at 40 °C. [d]Reaction was heated to 90 °C.

To investigate the chemoselectivity of the final diazo-alkene cycloaddition, the reaction was run with acrylate **3.4.1**. Azide **3.2a** will form the triazoline and subsequently

equilibrate to diazo intermediate **3.4.2**. At this point, the diazo can potentially cyclize with either pendant alkene to form two different [5,5]-fused ring systems (product **3.4.3** or **3.4.4**). In this reaction, only product **3.4.3** was observed. This may result from the most stable ester geometry placing the alkene away from the diazo.

**Scheme 3.4. Selectivity Between Different Alkenes.**

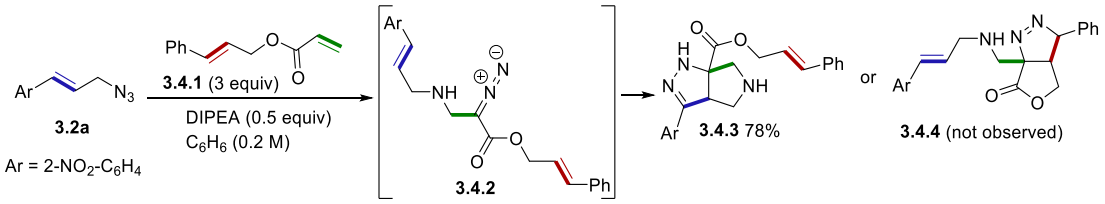


Conducting the cascade reaction in the presence of various electrophiles was a productive means to extend the cascade process (Table 3.6). The addition of $Boc_2O$ (**3.6a**), TsCl (**3.6b**), TrCl (**3.6c**), and CbzCl (**3.6d**) all afforded derivatized products directly in good yield.

**Table 3.6.** Product Functionalization *in Situ* to Expand Cascade

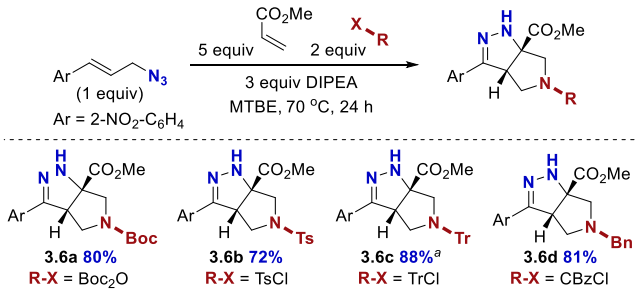


Yields are reported for isolated and purified products. [a]Yield reflects the sum of both tautomers.

The cascade cyclization could be conducted on a gram scale without any decrease in efficiency (Scheme 3.5). Each of the functional groups present in product **3.3a** could be selectively derivatized. The nitro group could be selectively reduced to afford aniline **3.5.1**. The ester present in product **3.3a** could be reduced to afford alcohol **3.5.2** or hydrolyzed to acid **3.5.3**. The pyrrolidine nitrogen could be alkylated, arylated, or acylated to afford products **3.6d**, **3.5.4**, and **3.5.5**. Lastly, the hydrazine motif could be acylated, yielding compound **3.5.6**. These results clearly highlight how the dense functionality present on the pyrrolidine-dihydropyrazole core can be selectively elaborated and diversified.

**Scheme 3.5. Gram Scale Reaction and Product Derivatization**

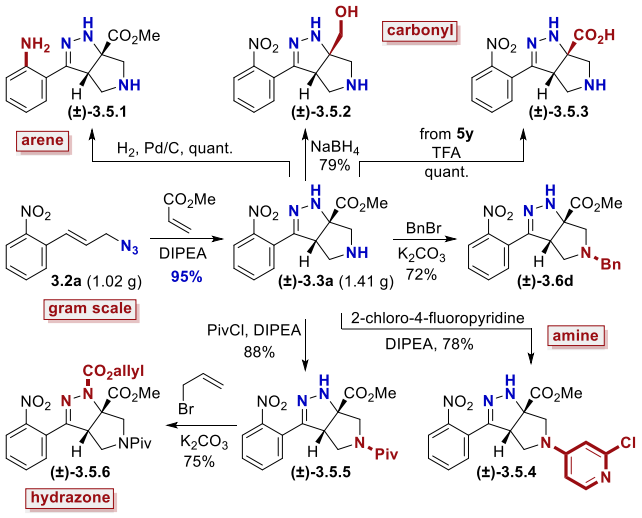


In conclusion, cinnamyl azides and Michael accepters can engage in a modular cascade cyclization to directly generate fused tetrahydro-pyrrolo-pyrazole heterocycles. The reaction proceeds on an array of coupling partners. Furthermore, the products can be derivatized *in situ*. This reaction rapidly amplifies the complexity of two trivial coupling partners and directly affords functionally dense bicyclic amine building blocks. This cascade is modular and amenable to diversification.

### 3.3 Extending the Cascade Reaction with Vinyl Sulfones

The cascade reaction between allylic azides and electron deficient alkenes can be extended by using a good leaving group as the electron withdrawing substituent (Scheme 3.6). After the initial adduct (**3.6.1**) is formed, the leaving group can eliminate to generate the aromatic version of the heterocycle (**3.6.2**).

**Scheme 3.6. Extending the Cascade Reaction by Using a Good Leaving Group.**

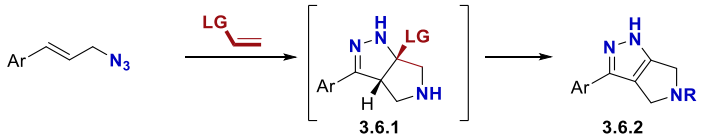


The dihydro-pyrrolo-pyrazole ring system in compound **3.6.2** is found in a variety of biologically important molecules (Figure 3.2). This fused ring system is a key substructure in omarigliptin, which Merck developed to treat type 2 diabetes.[5] Danusertib, which

entered clinical trials to treat chronic myelogenous leukemia (Figure 3.2),[3,4] also contains this ring system. The dihydro-pyrrolo-pyrazole substructure also appears in a glycine transporter-1 inhibitor, a P21-activated kinase inhibitor, and elsewhere.[6,7]

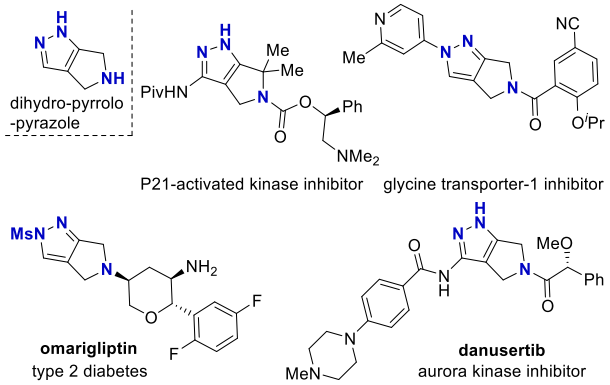


**Figure 3.2.** Select Biologically Active Molecules Containing a Dihydro-pyrrolo-pyrazole.

Versatile synthetic routes to dihydro-pyrrolo-pyrazole heterocycles are lacking, which is surprising in light of the stated utility. Current methods to synthesize dihydro-pyrrolo-pyrazoles are primarily based on carbonyl condensation with hydrazine (Scheme 3.7). Exposing 1,3-diketones or β-keto-nitriles to hydrazine can generate the pyrazole (Scheme 3.7a).[8] Other prefunctionalized ketones can condense with hydrazine (Scheme 3.7b).[5,8,9] Alternatively, an intramolecular dipolar cycloaddition is operative (Scheme 3.7c).[10,11] While effective, these approaches require preformation of the substrate. Ideally, there would be a divergent method to generate a wide variety of these heterocycles directly from simple starting materials.

**Scheme 3.7. Prior Synthesis of Dihydro-pyrrolo-pyrazoles.**

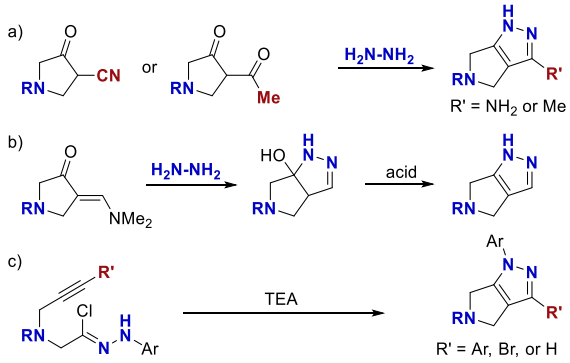

Synthesizing these heterocycles from simple allylic azides and commercially available alkenes would provide a simple, modular approach. Sulfones were identified as a group that would both be electron withdrawing to lower the pka of the intermediate triazoline and a good leaving group that could readily eliminate. Using similar reaction conditions, the desired cascade reaction was performed on a variety of cinnamyl azides (Table 3.7). The yields for these reactions are modest, but acceptable given the complexity of the cascade reaction. The reaction can tolerate electron withdrawing (**3.7a** – **3.7b**) and electron donating substituents (**3.7c - 3.7d**) on the arene. Also, the benzene ring could be replaced by a furan (**3.7f**), thiophene (**3.7g**), or benzothiophene (**3.7h**). More highly substituted azides also worked well in the reaction (**3.7i** – **3.7j**).

**Table 3.7.** Scope of Cascade Reaction with Cinnamyl Azides

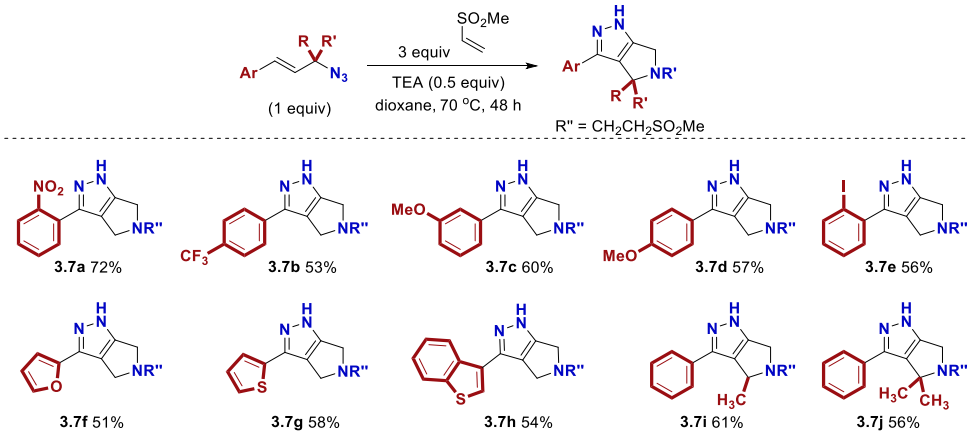


In conclusion, two cascade reactions were developed to generate tetrahydro-pyrrolo-pyrazoles and dihydro-pyrrolo-pyrazoles. These cascade reactions allow simple allylic azides and commodity alkenes to be converted into fused nitrogen heterocycles which can be challenging to access via previously reported methods.

### 3.4 Experimental

Most of the experimental details and characterization data from this chapter have been published.[35,36] The unpublished experimental details are included below.

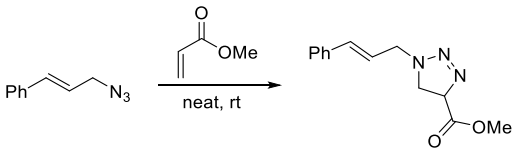


**Compound 3.1a**

Cinnamyl azide (520 mg, 3.27 mmol) was added neat to methyl acrylate (1.5 mL, 16 mmol). The reaction was sealed under air at rt. After 24 h, the product was concentrated under reduced pressure. Purification by column chromatography (0-80% EtOAc in hexanes) afforded triazoline **3.1a** (484 mg, 60%) as a yellow oil.

**$^1$H NMR (500 MHz,CDCl$_3$)** δ 7.40 (d, *J* = 7.5 Hz, 2H), 7.35 (t, *J* = 7.5 Hz, 2H), 7.31 – 7.26 (m, 1H), 6.63 (d, *J* = 15.8 Hz, 1H), 6.24 (dt, *J* = 15.9, 6.7 Hz, 1H), 5.01 (t, *J* = 11.9 Hz, 1H), 4.52 (dd, *J* = 15.0, 6.5 Hz, 1H), 4.36 (dd, *J* = 15.0, 6.8 Hz, 1H), 3.85 (s, 3H), 3.40 (d, *J* = 11.8 Hz, 2H).

**$^{13}$C NMR (126 MHz, CDCl$_3$)** δ 169.0, 136.1, 134.4, 128.7, 128.1, 126.6, 123.3, 78.3, 53.0, 52.7, 46.9.

**IR (NaCl, thin film, cm$^{-1}$):** 3027, 2953, 1741, 1359, 1214, 1177, 1086, 970, 928, 750, 697.

**HRMS (ESI-TOF)** *m/z* [M + Na]$^+$ calcd for $C_{13}H_{15}N_3NaO_2^+$ 268.1056, found 268.1046.

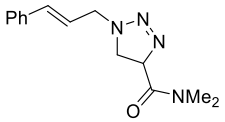


**Compound 3.1b**

Cinnamyl azide (987 mg, 6.21 mmol) was added neat to *N*,*N*-dimethylacrylamide (1.9 mL, 19 mmol). The reaction was sealed under air at rt. After 24 h, the product was concentrated under reduced pressure. Purification by column chromatography (0-30% IPA in hexanes) afforded **3.1b** (702 mg, 44%) as a yellow oil.

**$^1$H NMR (500 MHz, CDCl$_3$)** δ 7.37 (d, *J* = 7.5 Hz, 2H), 7.30 (t, *J* = 7.5 Hz, 2H), 7.26 – 7.21 (m, 1H), 6.60 (d, *J* = 15.8 Hz, 1H), 6.23 (dt, *J* = 15.9, 6.6 Hz, 1H), 5.17 (t, *J* = 11.9 Hz, 1H), 4.53 (dd, *J* = 15.1, 6.2 Hz, 1H), 4.25 (dd, *J* = 15.1, 7.0 Hz, 1H), 3.67 (dd, *J* = 11.7, 9.8 Hz, 1H), 3.36 (s, 3H), 3.27 (dd, *J* = 12.0, 9.7 Hz, 1H), 3.01 (s, 3H).

**$^{13}$C{$^1$H} NMR (126 MHz, CDCl$_3$)** δ 166.2, 136.3, 134.1, 128.7, 128.0, 126.6, 123.8, 77.7, 52.9, 46.5, 37.6, 36.2.

**IR (NaCl, thin film, cm$^{-1}$):** 3027, 2931, 1651, 1494, 1449, 1399, 1261, 1071.

**HRMS (ESI-TOF)** *m/z* [M + Na]$^+$ calcd for $C_{14}H_{18}N_4NaO^+$ 281.1373, found 281.1374.

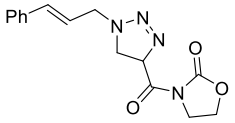


**Compound 3.1c**

To a solution of cinnamyl azide (300 mg, 1.88 mmol) in DCM (0.70 mL) was added 1-acryloyl-2-pyrrolidinone (305 mg, 2.16 mmol). The reaction was sealed under air at rt. After 24 h, the reaction was concentrated under reduced pressure. Purification by column

chromatography (0-100% EtOAc in hexanes) afforded triazoline **3.1c** (321 mg, 57%) as a white solid.
**$^1$H NMR (500 MHz, $CDCl_3$)** δ 7.41 (d, *J* = 7.7 Hz, 2H), 7.35 (t, *J* = 7.5 Hz, 2H), 7.31 – 7.26 (m, 1H), 6.63 (d, *J* = 15.8 Hz, 1H), 6.29 – 6.18 (m, 2H), 4.56 – 4.53 (m, 1H), 4.50 (t, *J* = 7.7 Hz, 2H), 4.39 (dd, *J* = 15.1, 6.8 Hz, 1H), 4.14 – 4.07 (m, 2H), 3.54 – 3.38 (m, 2H).
**$^{13}$C{$^1$H} NMR (126 MHz, $CDCl_3$)** δ 167.6, 153.2, 136.1, 134.3, 128.7, 128.1, 126.6, 123.4, 77.2, 62.5, 52.7, 46.5, 42.8.
**IR (NaCl, thin film, cm$^{-1}$):** 3367, 2923, 2103 (diazo), 1780, 1724, 1702, 1476, 1448, 1391, 1364, 1272, 1224, 1120, 1043.
**HRMS (ESI-TOF)** *m/z* $[M + Na]^+$ calcd for $C_{15}H_{16}N_4NaO_3^+$ 323.1115, found 323.1118.

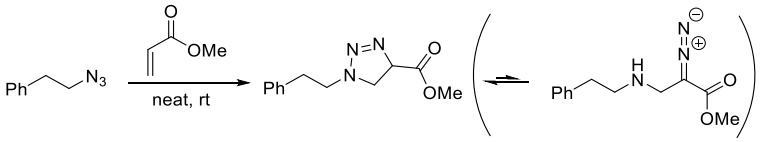


**Compound 3.1d**
Phenethyl azide (505 mg, 3.44 mmol) was added neat to methyl acrylate (1.5 mL, 17 mmol). The reaction was sealed under air at rt. After 18 h, the product was concentrated under reduced pressure. Final purification by column chromatography (0-80% EtOAc in hexanes) afforded triazoline **3.1d** (580 mg, 72%) as a yellow oil.
**$^1$H NMR (500 MHz, $CDCl_3$)** δ 7.35 – 7.31 (m, 2H), 7.27 – 7.22 (m, 3H), 4.95 (t, *J* = 12.1 Hz, 1H), 3.97 (dt, *J* = 14.6, 7.4 Hz, 1H), 3.84 (s, 3H), 3.82 – 3.74 (m, 1H), 3.33 (dd, *J* = 12.1, 4.5 Hz, 2H), 3.03 (t, *J* = 7.3 Hz, 2H).
**$^{13}$C{$^1$H} NMR (126 MHz, $CDCl_3$)** δ 169.0, 138.4, 128.8, 128.7, 126.7, 78.1, 52.9, 51.8, 47.7, 34.7. **IR (NaCl, thin film, cm$^{-1}$):** 3028, 2952, 2860, 2089 (diazo), 1742, 1691, 1454, 1362, 1207, 1104. **HRMS (ESI-TOF)** *m/z* $[M + Na]^+$ calcd for $C_{12}H_{15}N_3NaO_2^+$ 256.1056, found 256.1047.

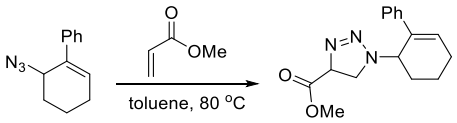


**Compound 3.1e**
To a solution of azide (46.8 mg, 0.235 mmol) in toluene (1.0 mL) was added methyl acrylate (0.10 mL, 1.2 mmol). The reaction was sealed under air and heated to 80 °C. After 18 h, the reaction was concentrated under reduced pressure to afford triazoline **3.1e** in quantitative yield as a 1:1 mixture of diastereomers. The diastereomers were separated by column chromatography (0-50% EtOAc in hexanes).

**Diastereomer 1**:
**$^1$H NMR (500 MHz, $CDCl_3$)** δ 7.37 – 7.34 (m, 2H), 7.33 – 7.28 (m, 2H), 7.27 – 7.22 (m, 1H), 6.30 (td, *J* = 4.0, 1.5 Hz, 1H), 5.50 – 5.37 (m, 1H), 4.65 (dd, *J* = 13.2, 11.2 Hz, 1H), 3.80 (s, 3H), 3.46 (dd, *J* = 11.2, 10.0 Hz, 1H), 2.93 (dd, *J* = 13.2, 10.0 Hz, 1H), 2.32 – 2.25 (m, 2H), 2.08 – 2.00 (m, 2H), 1.86 – 1.77 (m, 2H).

**$^{13}C\{^{1}H\}$ NMR (126 MHz, $CDCl_3$)** δ 169.4, 139.9, 135.6, 131.5, 128.4, 127.2, 126.1, 76.9, 54.8, 52.8, 43.7, 28.3, 25.7, 19.7.
**IR (NaCl, thin film, $cm^{-1}$):** 2938, 1741, 1461, 1444, 1224, 1118, 1080.
**HRMS (ESI-TOF)** *m/z* $[M + Na]^+$ calcd for $C_{16}H_{19}N_3NaO_2^+$ 308.1369, found 308.1365.

**Diastereomer 2**:
**$^{1}H$ NMR (500 MHz, $CDCl_3$)** δ 7.34 – 7.27 (m, 4H), 7.25 – 7.20 (m, 1H), 6.28 (dt, *J* = 4.0, 2.0 Hz, 1H), 5.31 – 5.26 (m, 1H), 4.81 (dd, *J* = 13.2, 11.3 Hz, 1H), 3.65 (s, 3H), 3.32 (dd, *J* = 13.2, 9.9 Hz, 1H), 3.18 (dd, *J* = 11.3, 9.9 Hz, 1H), 2.34 – 2.24 (m, 2H), 2.14 – 2.02 (m, 2H), 1.83 – 1.77 (m, 2H).
**$^{13}C\{^{1}H\}$ NMR (126 MHz, $CDCl_3$)** δ 169.0, 140.0, 135.8, 131.4, 128.3, 127.1, 126.3, 76.8, 54.8, 52.7, 44.6, 28.5, 25.7, 19.3.
**IR (NaCl, thin film, $cm^{-1}$):** 2938, 1742, 1444, 1365, 1202, 1116, 1042.
**HRMS (ESI-TOF)** *m/z* $[M + Na]^+$ calcd for $C_{16}H_{19}N_3NaO_2^+$ 308.1369, found 308.1370.

### 3.5 References


(1) Vitaku, E.; Smith, D. T.; Njardarson, J. T. Analysis of the Structural Diversity, Substitution Patterns, and Frequency of Nitrogen Heterocycles among U.S. FDA Approved Pharmaceuticals. *J. Med. Chem.* **2014**, *57*, 10257–10274.

(2) Wang, Y.-Y.; Bode, J. W. Olefin Amine (OLA) Reagents for the Synthesis of Bridged Bicyclic and Spirocyclic Saturated N-Heterocycles by Catalytic Hydrogen Atom Transfer (HAT) Reactions. *J. Am. Chem. Soc.* **2019**, *141*, 9739–9745.

(3) Lovering, F.; Bikker, J.; Humblet, C. Escape from Flatland: Increasing Saturation as an Approach to Improving Clinical Success. *J. Med. Chem.* **2009**, *52*, 6752–6756.

(4) Lovering, F. Escape from Flatland 2: Complexity and Promiscuity. *Med. Chem. Commun.* **2013**, *4*, 515–519.

(5) Meanwell, N. A. Improving Drug Design: An Update on Recent Applications of Efficiency Metrics, Strategies for Replacing Problematic Elements, and Compounds in Nontraditional Drug Space. *Chem. Res. Toxicol.* **2016**, *29*, 564–616.

(6) Ritchie, T. J.; MacDonald, S. J. F.; Young, R. J.; Pickett, S. D. The Impact of Aromatic Ring Count on Compound Developability: Further Insights by Examining Carbo- and Hetero-Aromatic and -Aliphatic Ring Types. *Drug Discov. Today* **2011**, *16*, 164–171.

(7) Orr, S. T. M.; Ripp, S. L.; Ballard, T. E.; Henderson, J. L.; Scott, D. O.; Obach, R. S.; Sun, H.; Kalgutkar, A. S. Mechanism-Based Inactivation (MBI) of Cytochrome P450 Enzymes: Structure–Activity Relationships and Discovery Strategies To Mitigate Drug–Drug Interaction Risks. *J. Med. Chem.* **2012**, *55*, 4896–4933.

(8) Campos, K. R.; Coleman, P. J.; Alvarez, J. C.; Dreher, S. D.; Garbaccio, R. M.; Terrett, N. K.; Tillyer, R. D.; Truppo, M. D.; Parmee, E. R. The Importance of Synthetic Chemistry in the Pharmaceutical Industry. *Science* **2019**, *363*, 244–252.

(9) Levin, J. I.; Venkatesan, A. M.; Chan, P. S.; Bailey, T. K.; Vice, G.; Coupet, J. 6-Substituted Quinazolinone Angiotensin II Receptor Antagonists. *Bioorg. Med. Chem. Lett.* **1994**, *4*, 1819–1824.

(10) Møllerud, S.; Pinto, A.; Marconi, L.; Frydenvang, K.; Thorsen, T. S.; Laulumaa, S.; Venskutonyte, R.; Winther, S.; Moral, A. M. C.; Tamborini, L.; Conti, P.; Pickering, D. S.; Kastrup, J. S. Structure and Affinity of Two Bicyclic Glutamate Analogues at AMPA and Kainate Receptors. *ACS Chem. Neurosci.* **2017**, *8*, 2056–2064.

(11) Liu, G.-N.; Luo, R.-H.; Zhou, Y.; Zhang, X.-J.; Li, J.; Yang, L.-M.; Zheng, Y.-T.; Liu, H. Synthesis and Anti-HIV-1 Activity Evaluation for Novel 3a,6a-Dihydro-1H-Pyrrolo[3,4-c]Pyrazole-4,6-Dione Derivatives. *Molecules* **2016**, *21*, 1198-1210.

(12) Chen, P.; Feng, D.; Qian, X.; Apgar, J.; Wilkening, R.; Kuethe, J. T.; Gao, Y. D.; Scapin, G.; Cox, J.; Doss, G.; Eiermann, G.; He, H.; Li, X.; Lyons, K. A.; Metzger, J.; Petrov, A.; Wu, J. K.; Xu, S.; Weber, A. E.; Yan, Y.; Roy, R. S.; Biftu, T. Structure-Activity-Relationship of Amide and Sulfonamide Analogs of Omarigliptin. *Bioorganic Med. Chem. Lett.* **2015**, *25*, 5767–5771.

(13) Deaton, D. N.; Haffner, C. D.; Henke, B. R.; Jeune, M. R.; Shearer, B. G.; Stewart, E. L.; Stuart, J. D.; Ulrich, J. C. 2,4-Diamino-8-Quinazoline Carboxamides as Novel, Potent Inhibitors of the NAD Hydrolyzing Enzyme CD38: Exploration of the 2-Position Structure-Activity Relationships. *Bioorganic Med. Chem.* **2018**, *26*, 2107–2150.

(14) Quiclet-Sire, B.; Zard, S. Z. Observations on the Reaction of Hydrazones with Iodine: Interception of the Diazo Intermediates. *Chem. Commun.* **2006**, 1831–1832.

(15) Kapras, V.; Pohl, R.; Císařová, I.; Jahn, U. Asymmetric Domino Aza-Michael Addition/[3+2] Cycloaddition Reactions as a Versatile Approach to α,β,γ-Triamino Acid Derivatives. *Org. Lett.* **2014**, *16*, 1088–1091.

(16) Just, D.; Hernandez-Guerra, D.; Kritsch, S.; Pohl, R.; Císařová, I.; Jones, P. G.; Mackman, R.; Bahador, G.; Jahn, U. Lithium Chloride Catalyzed Asymmetric Domino Aza-Michael Addition/[3+2] Cycloaddition Reactions for the Synthesis of Spiro- and Bicyclic α,β,γ-Triamino Acid Derivatives. *Eur. J. Org. Chem.* **2018**, 5213–5221.

(17) Yang, C.-H.; Sherf, H.-J.; Wang, R.-H.; Wang, J.-C. 2,3,7-Triazabicyclo[3.3.0]Octenes Prepared by Tandem Cascade Reaction of Allyl Azides and Olefinic Dipolarophiles. *J. Chin. Chem. Soc.* **2002**, *49*, 95–102.

(18) Yang, C.; Shen, H. One Pot Multiple-Steps Reactions of Allyl Azide and Alkenes Carrying Electron-Withdrawing Groups. *Tetrahedron Lett.* **1993**, *34*, 4051–4054.

(19) Herdeis, C.; Schiffer, T. Synthesis of Nonracemic 2,3,6-Trisubstituted Piperidine Derivatives from Sugar Lactones via Tandem Wittig [2+3] Cycloaddition Reaction. A Novel Entry to Prosopis and Cassia Alkaloids. *Tetrahedron* **1999**, *55*, 1043–1056.

(20) Broeckx, W.; Overbergh, N.; Samyn, C.; Smets, G.; L'abbé, G. Cycloaddition Reactions of Azides with Electron-Poor Olefins. *Tetrahedron* **1971**, *27*, 3527–3534.

(21) L'abbé, G. Decomposition and Addition Reactions of Organic Azides. *Chem. Rev.* **1969**, *69*, 345–363.

(22) Yang, C.-H.; Shen, H.-J.; Wang, R.-H.; Wang, J.-C. 2,3,7-Triazabicyclo[3.3.0]Octenes Prepared by Tandem Cascade Reaction of Allyl Azides and Olefinic Dipolarophiles. *J. Chinese Chem. Soc.* **2002**, *49*, 95–102.

(23) Huisgen, R. Proceedings of the Chemical Society. October 1961. *Proc. Chem. Soc.* **1961**, 357–396.

(24) Huisgen, R.; Szeimies, G.; Möbius, L. 1.3-Dipolar Cycloadditions. XXXII. Kinetics of the Addition of Organic Azides to Carbon-Carbon Multiple Bonds. *Chem. Ber.* **1967**, *100*, 2494–2507.

(25) Liddon, J. T. R.; Lindsay-Scott, P. J.; Robertson, J. Secondary Products from Intramolecular Cycloadditions of Azidoalkyl Enol Ethers and Azidoalkyl Vinyl Bromides: 1-Azadienes, Their Reactions with Diphenylketene, and Radical Cyclizations To Form Bi- and Tricyclic Lactams. *J. Org. Chem.* **2019**, *84*, 13780–13793.

(26) Xie, S.; Lopez, S. A.; Ramström, O.; Yan, M.; Houk, K. N. 1,3-Dipolar Cycloaddition Reactivities of Perfluorinated Aryl Azides with Enamines and Strained Dipolarophiles. *J. Am. Chem. Soc.* **2015**, *137*, 2958–2966.

(27) Krivopalov, V. P.; Shkurko, O. P. 1,2,3-Triazole and Its Derivatives. Development of Methods for the Formation of the Triazole Ring. *Russ. Chem. Rev.* **2005**, *74*, 339–379.

(28) Yang, C. H.; Lee, L. T.; Yang, J. H.; Wang, Y.; Lee, G. H. Spiropyrazolines from Tandem Reaction of Azides and Alkyl Vinyl Ketones. *Tetrahedron* **1994**, *50*, 12133–12142.

(29) Teng, J.-T.; Yang, C.-H. A Stereoselective Preparation of 1,2,7-Triazabicyclo[3.3.0]Oct-2-Enes. *J. Chinese Chem. Soc.* **1998**, *45*, 375–380.

(30) Hamadi, N. Ben; Louhichi, N.; Msaddek, M. Synthesis and Photolysis of Hexahydropyrrolo [3,4-c] Pyrazole Derivatives. *J. Chem. Res.* **2007**, *10*, 569–571.

(31) Gagneux, A.; Winstein, S.; Young, W. G. Rearrangement of Allyl Azides. *J. Am. Chem. Soc.* **1960**, *82*, 5956–5957.

(32) Carlson, A. S.; Topczewski, J. J. Allylic Azides: Synthesis, Reactivity, and the Winstein Rearrangement. *Org. Biomol. Chem.* **2019**, *17*, 4406–4429.

(33) Ott, A. A.; Packard, M. H.; Ortuño, M. A.; Johnson, A.; Suding, V. P.; Cramer, C. J.; Topczewski, J. J. Evidence for a Sigmatropic and an Ionic Pathway in the Winstein Rearrangement. *J. Org. Chem.* **2018**, *83*, 8214–8224.

(34) Nugent, T. C. *Chiral Amine Synthesis: Methods, Developments and Applications*, 1st ed.; Wiley, 2010.

(35) Carlson, A. S.; Liu, E.-C.; Topczewski, J. J. A Cascade Reaction of Cinnamyl Azides with Acrylates Directly Generates Tetrahydro-Pyrrolo-Pyrazole Heterocycles. *J. Org. Chem.* **2020**, 85, 6044-6059.

(36) Carlson, A. S.; Petre, A. M.; Topczewski, J. J. A Cascade Reaction of Cinnamyl Azides with Vinyl Sulfones Directly Generates Dihydro-Pyrrolo-Pyrazole Heterocycles. *Submitted*.

## Chapter 4: Mitigating the p38α Activity of Bromodomain Inhibitors

*This chapter describes the outcome of a collaborative research project carried out with Huarui Cui and Anand Divakaran (advised by William Pomerantz). Two reports on this research project have been published* [*J. Med. Chem.* **2018**, *61*, 9316-9334 and *ACS Med. Chem. Lett.* **2019**, *10*, 1296-1301] *and these reports have been reprinted (adapted) here with permission. I synthesized the triazole analogs and Huarui Cui and Anand Divakaran performed the bioassays.*

### 4.1. Introduction to Bromodomains

Bromodomains are an important part of DNA transcription. Specifically, they bind *N*-ε-acetylated lysine residues on histones and transcription factors to regulate cellular processes including the cell cycle, proliferation, and cellular differentiation.[1] The 61 human bromodomains (BRD) have been subdivided into eight classes based on structural or sequence similarities.[2] The Bromodomain and Extra Terminal (BET) family includes BRD2, BRD3, BRD4 and BRDT. These four proteins each contain two tandem bromodomains (D1 and D2) and an extra-terminal domain.

Inhibiting BET bromodomains from binding to *N*-ε-acetylated lysine residues is a key target for potential treatment of BET related diseases, including cancer, inflammation and heart diseases.[2–5] For example, the BRD4 and BRDT bromodomains can recognize *N*-ε-acetylated lysine residues on histones and recruit transcription factors to super-enhancer regions. Inhibition of BRD4 at super-enhancer regions can reduce *c-Myc* expression, which could be a therapeutic strategy for treating cancer.[6] Given the significant roles that BET bromodomains play in oncogene expression and in inflammation, several clinical trials are underway to assess the therapeutic effects of BET inhibition.[2,7]

Bromodomain's native ligands are acetylated lysines, which hydrogen bond to an asparagine in the binding site (Figure 4.1). To mimic this native interaction, bromodomain inhibitors generally contain a hydrogen bond acceptor that can engage this hydrogen bond.

**Figure 4.1.** Native BRD Interaction.

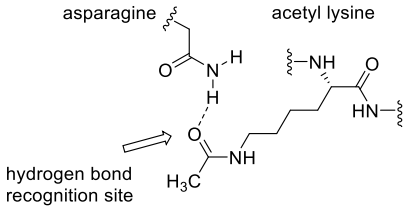

One method for identifying bromodomain inhibitors has been screening kinase libraries against the bromodomain of interest (Figure 4.2).[8–13] The first dual kinase-bromodomain inhibitor reported was Dinacicilib.[12] This cyclin-dependent kinase (CDK) inhibitor was found to have modest affinity for BRDT. The pyridine oxide serves as the *N*-ε-acetylated lysine mimic and is recognized by Asn109 on BRDT. In 2014, both Ciceri et al. and Ember et al. identified several dual kinase-bromodomain inhibitors including BI-2536, which is a polo-like kinase 1 (PLK1) inhibitor with high affinity for BRD4-D1.[8,11] The dihydropteridinone carbonyl and the methylamino group function as the *N*-ε-acetylated lysine mimic. Since these reports, developing bromodomain inhibitors by kinase library screening has attracted more attention.[8,11,13,14]

Urick *et al.* from William Pomerantz's lab screened a library of 229 small molecules by protein-observed fluorine NMR and subsequently developed the dual p38α-BRD4-D1 inhibitor compound **V**.[13,15] While BI-2536 and Dinaciclib are pan-BET inhibitors, compound **V** was shown to selectively inhibit the N-terminal BET bromodomains with the highest affinity for BRD4-D1. The amino acid sequences of proteins within the BET family are highly conserved which makes this selectivity notable. I began collaborating with Huarui Cui and Anand Divakaran from the Pomerantz lab to investigate the source of this selectivity. Additionally, we endeavored to mitigate the p38a activity to create a selective bromodomain inhibitor. Although, dual kinase-bromodomain inhibitors may produce synergistic effects in some cases,[9,11,14,16] selective inhibition is ideal for understanding the physiological and pharmacological effect of BET inhibition as well as minimizing potential side effects.[17]

**Figure 4.2.** Examples of Dual Kinase-Bromodomain Inhibitors.

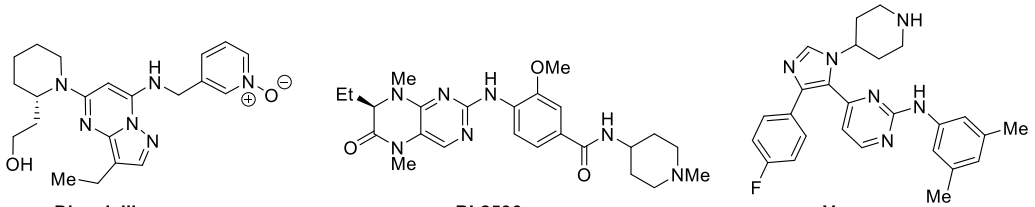

### 4.3 Source of BRD4-D1 Selectivity

As previously mentioned, the sequence identity is highly conserved among BET proteins. Because of this, most reported inhibitors are pan-BET inhibitors, such as (+)-JQ1 (Figure 4.3), and do not discriminate among individual bromodomains.[18,19] Ouyang *et al.* reported FL-411, which is selective for BRD4 over other BET proteins.[20] Nevertheless, the potential off-target effects and dose-limiting thrombocytopenia associated with pan-BET inhibitors in clinical trials highlight the need for novel scaffolds with improved selectivity and/or potency.[4,21,22] Compound **V** selectively inhibits the N-terminal BET bromodomains with the highest affinity for BRD4-D1.[15] This level of selectivity within the BET family is unusual and warranted further investigation.

**Figure 4.3.** State-of-the-art BET Inhibitors.

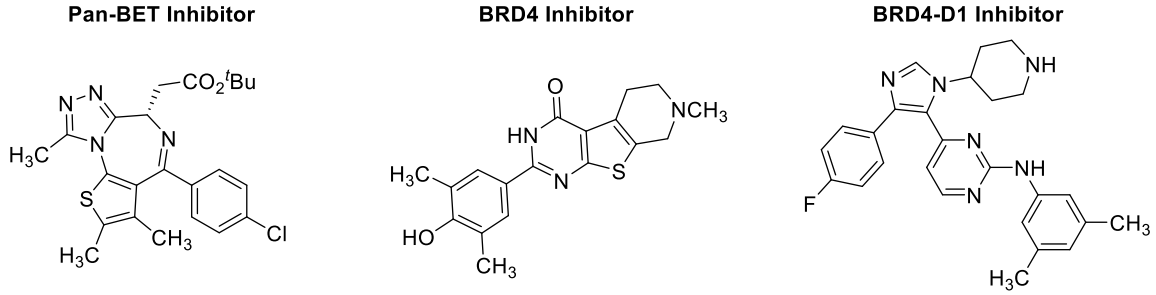

| Pan-BET Inhibitor | BRD4 Inhibitor | BRD4-D1 Inhibitor |
|---|---|---|
| **(+)-JQ1** | **FL-411** | **V** |
| BRD2-D1 $K_d$ = 0.13 μM | BRD2-D1 $IC_{50}$ = 24.6 μM | BRD2-D1 $IC_{50}$ = 29 μM |
| BRD2-D2 $K_d$ = ND | BRD2-D2 $IC_{50}$ = >100 μM | BRD2-D2 $IC_{50}$ = 67 μM |
| BRD3-D1 $K_d$ = 0.059 μM | BRD3-D1 $IC_{50}$ = >100 μM | BRD3-D1 $IC_{50}$ = 11 μM |
| BRD3-D2 $K_d$ = 0.082 μM | BRD3-D2 $IC_{50}$ = >100 μM | BRD3-D2 $IC_{50}$ = >100 μM |
| BRD4-D1 $K_d$ = 0.049 μM | BRD4-D1 $IC_{50}$ = 0.47 μM | BRD4-D1 $IC_{50}$ = 1.8 μM |
| BRD4-D2 $K_d$ = 0.090 μM | BRD4-D2 $IC_{50}$ = 0.93 μM | BRD4-D2 $IC_{50}$ = >100 μM |
| BRDT-D1 $K_d$ = 0.190 μM | BRDT-D1 $IC_{50}$ = >100 μM | BRDT-D1 $IC_{50}$ = 5.3 μM |

Recent computational studies suggest a possible explanation compound **V**'s unusual selectivity within the bromodomain family (Table 4.1).[23,24] The BET bromodomains each contain a network of structured waters in the binding site, but the affinity of these networks varies between the bromodomains. BRD4-D1 and BRDT-D1 contain the weakest structured water networks, which implies that these waters are the easiest to displace. These two bromodomains also exhibit the highest affinity for compound **V**. It appears that when inhibitor **V** enters the binding site, it displaces the structured waters. Since the weakest water networks are the easiest to displace, compound **V** binds preferentially to the bromodomains with weak water networks. Such an effect would at least partly explain the

observed selectivity of compound **V** for BRD4-D1 and BRDT-D1 over the other BET bromodomains.

**Table 4.1.** Stabilization Energy of Structured Waters and Compound **V** Affinity.[15,23,24]

| Bromodomain | $\Delta G_{network}$ (kcal/mol) | Compound **V** (μM) |
|---|---|---|
| BRD2-D1 | -2.5 ± 1.4 | 29 |
| BRD2-D2 | -2.4 ± 0.9 | 67 |
| BRD3-D1 | -3.2 ± 0.4 | 11 |
| BRD3-D2 | -3.5 ± 0.9 | >100 |
| BRD4-D1 | -0.4 ± 1.0 | 1.8 |
| BRD4-D2 | -4.2 ± 0.1 | >100 |
| BRDT-D1 | +0.2 ± 1.6 | 5.3 |

This hypothesis is further supported by co-crystal structures of DMSO and Compound **V** in BRD4-D1 (Figure 4.4). With only DMSO in the binding site, six waters are present including the four conserved structured waters. Three of the four structured waters are displaced when compound **V** is present, and the water network is reorganized by the fluorophenyl group. Based on these observations, it appears that changing the 4-fluorophenyl group to a small methyl group would leave the structured waters intact. This should eliminate the BRD4-D1 selectivity. Additionally, a hydroxymethyl group might strengthen inhibition via hydrogen bonding to these waters.

**Figure 4.4.** Co-crystal Structures of BRD4-D1 with DMSO and Compound **V**.

**a. DMSO in BRD4-D1** **b. Compound V in BRD4-D1**

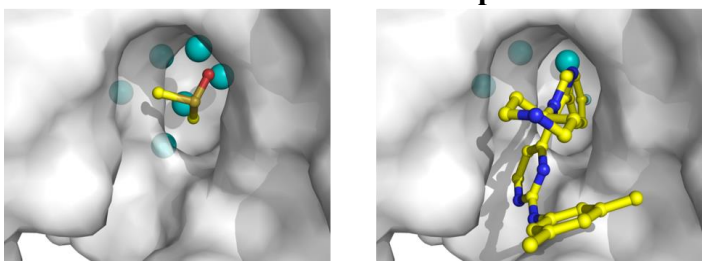

Before testing these hypotheses, a shorter synthesis was developed. The synthesis of compound **V** is 10 linear steps with a 4% overall yield. Synthesizing dozens of analogs via this route would be tedious. Switching the imidazole in compound **V** to a triazole (Scheme

4.1, compound **4.1.1**) could significantly accelerate analog synthesis. In compound **V**, the unsubstituted imidazole nitrogen hydrogen bonds to Asn140 in BRD4-D1 and acts as the *N*-ε-acetylated lysine mimic. Ideally, the analogous triazole could also fulfill this role.

A three linear step synthesis was designed to assemble the desired triazole analogs (Scheme 4.1). Triazole **4.1.1** could be generated from compound **4.1.2** via double Boc-deprotection. A cross-coupling between triazole **4.1.3** and pyrimidine **4.1.4** was envisioned to construct compound **4.1.2**. Triazole **4.1.3** and pyrimidine **4.1.4** could be formed via a copper-catalyzed azide-alkyne cycloaddition (CuAAC) and SNAr reaction, respectively. Thus, these triazole analogs should be accessible in 3 linear steps.

**Scheme 4.1. Convergent Synthesis of Triazole Analogs.**

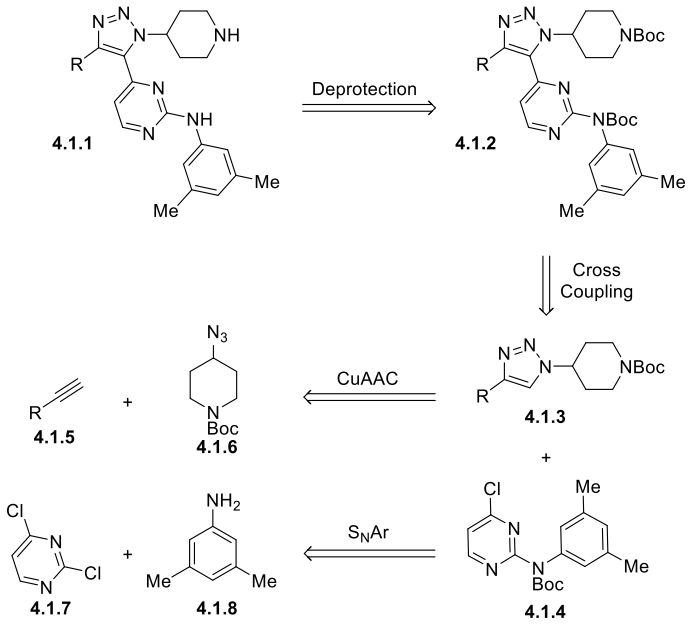


The first few analogs were synthesized in a six-step route (Scheme 4.2). Commercially available mesylate **4.2.1** was converted into azide **4.2.2** with $NaN_3$ in DMF. A CuAAC with azide **4.2.2** and a variety of alkynes generated triazoles (**4.2.3a** - **4.2.3c**). These triazole can be converted into the organozinc complex by deprotonating the triazole with *n*-BuLi followed by addition of $ZnCl_2$. Subsequent addition of pyrimidine **4.2.4** and SPhosPdG3 initiated a Negishi coupling to generate compound **4.2.5**. Subsequent oxidation with Oxone® followed by an $S_NAr$ reaction with 3,5-dimethylaniline afforded compounds **4.2.7a** – **4.2.7c**. Treatment with TFA afforded the desired products (**4.2.8a** - **4.2.8c**).

**Scheme 4.2. First Generation Synthesis of Triazole Analogs.**

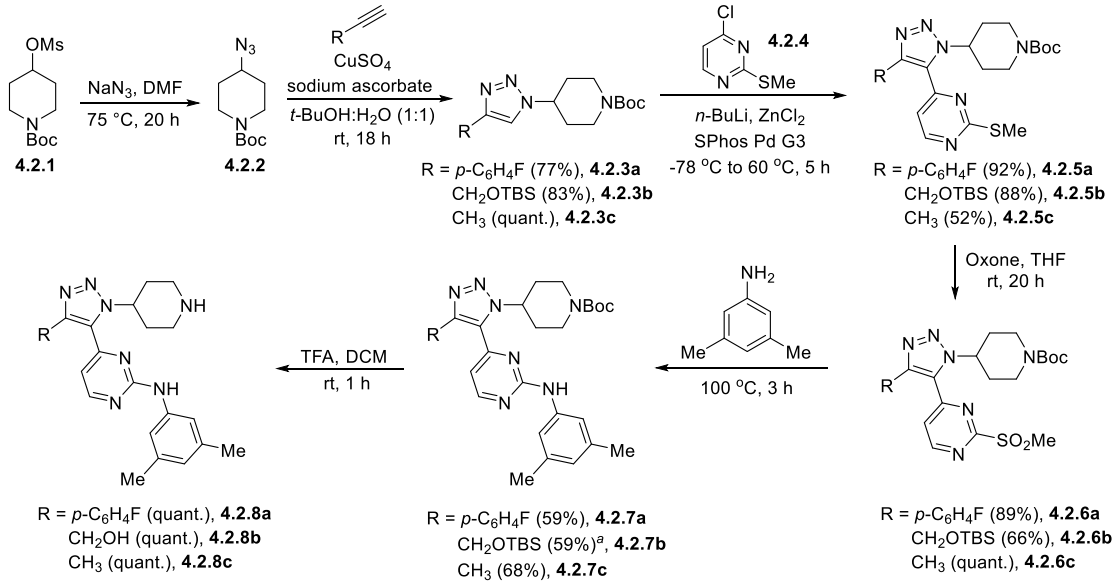


[a]This reaction was run with NaHMDS at -78 °C.

These three compounds were analyzed by ALPHAScreen (a commercial assay performed by Reaction Biology) against 7 of the 8 BET bromodomains (Table 4.2). Substituting the imidazole ring in compound **V** with a triazole (compound **4.2.8a)** resulted in a moderate loss of BRD4-D1 potency ($IC_{50}$ = 1.8 μM for compound **V** vs. 27 μM for **4.2.8a**). Triazoles are less basic than imidazoles and likely form a weaker hydrogen bond to Asn140.[25–27] Replacement of the fluorophenyl group with a hydroxymethyl (**4.2.8b**) group resulted in further reduced binding with $IC_{50}$'s > 100 μM. Rather than providing an additional hydrogen bond, this polar side chain is possibly incompatible with the hydrophobic nature of the binding pocket. In contrast, truncation of the fluorophenyl group to a methyl in compound **4.2.8c** enhanced binding 20-fold relative to **4.2.8a** ($IC_{50}$ = 1.3 μM for **4.2.8c** vs 155 μM for **4.2.8a**). The large gain in potency is consistent with the energetic penalty associated with displacing the structured waters. Additionally, the selectivity was lost, which is consistent with the hypothesis that displacing the structured waters imparts selectivity. A co-crystal structure of a similar methyl triazole and BRD4-D1 (see Figure 4.6 below) showed that the structured waters are still in place and that the triazole binds in the same orientation as the imidazole. While the structured waters are likely an important factor in compound **V**'s selectivity, the fact that compound **4.2.8a** does not exhibit the same level of selectivity indicates that other factors are also involved.

**Table 4.2.** ALPHA Screen Analysis of Compound **V** and Compounds **4.2.8a** – **4.2.8c** Against 7 of 8 BET Bromodomains.

| Protein | $IC_{50}$ by ALPHA Screen (μM)[a] | | | |
|---|---|---|---|---|
| | 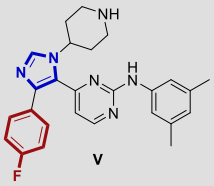 V | 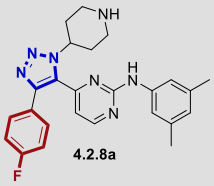 4.2.8a | 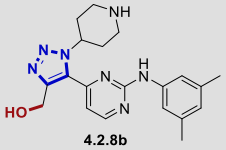 4.2.8b | 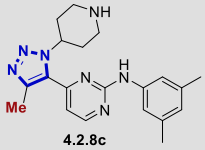 4.2.8c |
| BRD2-D1 | 29 | 43 | >250 | 1.8 |
| BRD2-D2 | 67 | 30 | 260 | 12 |
| BRD3-D1 | 11 | 51 | 200 | 0.77 |
| BRD3-D2 | >100 | 110 | 310 | 2.4 |
| BRD4-D1 | 1.8 | 27 | 160 | 1.3 |
| BRD4-D2 | >100 | 75 | 102 | 0.56 |
| BRDT-D1 | 5.3 | 36 | 110 | 1.6 |

[a]$IC_{50}$ values were determined by ALPHA Screen which is a commercial assay performed by Reaction Biology.

### 4.3 Mitigating p38α Activity

The second goal was to mitigate the p38a activity and make these compounds selective bromodomain inhibitors. This study began by studying how compounds like **V** bind kinases. Co-crystal structures of p38α and similarly structured hinge-binding kinase inhibitors provided hypotheses for a systematic SAR study aimed at mitigating p38α activity. These co-crystal structures indicate that one of the inhibitor's pyrimidine nitrogen atoms serves as a hydrogen bond acceptor and the exocyclic N-H is a hydrogen bond donor (Figure 4.5); both interactions are made to the M109 peptide backbone in p38α.[28–30] If the exocyclic N-H were replaced by an ether linkage, there would no longer be a hydrogen bond donor, which would weaken binding to p38α.[30] Hypothetically, binding to M109 could be further minimized by replacing the pyrimidine nitrogen with a C-H unit (pyridine), which would not be a suitable hydrogen bond acceptor.

**Figure 4.5.** Hydrogen Bonding in p38α Co-crystal Structures and Proposed Analogs

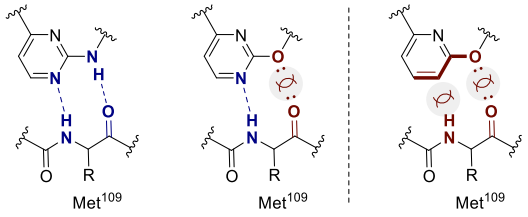


Given the significance of these two interactions, four inhibitors were synthesized, each with one of the four possible X/Y substitution combinations (Table 4.3). Switching from an exocyclic amine (**4.2.8a**) to an ether (**4.3a**) led to a ~50-fold reduction in p38α binding. A ~1000-fold reduction in kinase binding was observed with analogs of another dual kinase-bromodomain inhibitor, based on compound **BI-2536**.[17] When the pyrimidine was replaced with a pyridine (**4.2.8a** vs. **4.3b**), the p38α affinity was reduced by a factor of ~3,000. Thus, in this scaffold, removing the pyrimidine nitrogen appears to be more important to mitigating the p38α activity than installing an ether linkage. This was supported by examining a compound with both an ether linkage and a pyridine ring (**4.3c**). This compound displayed significantly diminished p38α binding relative to the pyrimidine (**4.3a**), but it was on a par with the analog with the corresponding exocyclic nitrogen (**4.3b**).

**Table 4.3.** Systematically Minimizing Binding to M109 in p38α

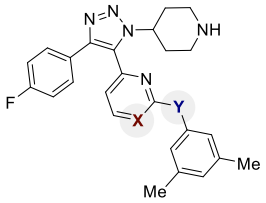

| Compound | X | Y | p38α *Kd* (nM)[a] |
|---|---|---|---|
| **4.2.8a** | N | NH | 2.2 ± 0.63 |
| **4.3a** | N | O | 120 ± 51 |
| **4.3b** | CH | NH | 6500 ± 6300 |
| **4.3c** | CH | O | 5000 ± 6100 |

[a] $K_d$ values were determined by KINOMEscanTM. Data represents the mean and standard error from two independent trials.

In addition to hydrogen bonding to M109, the p38α binding affinity is likely enhanced by van der Waals interactions to the 4-fluorophenyl group in compounds **4.2.8a**, **4.3a - 4.3c**. An analogous p38α inhibitor, SB220025, demonstrates this interaction where the 4-

fluorophenyl ring sits in a hydrophobic pocket between L104 and T106.[29–31] Reductions in p38α activity have been observed when the 4-fluorophenyl group is replaced with an ethyl group.[32] Minimizing this van der Waals interaction would likely further mitigate the p38α activity and produce a selective BET inhibitor if bromodomain binding could be maintained.

Inhibitors containing a variety of alkyl chains were synthesized to investigate this hypothesis (Scheme 4.3). The sequence began with a CuAAC reaction,[33] which afforded the respective triazole. The triazole could be directly coupled to an aryl halide through a metalation/Negishi cross-coupling reaction. The direct C-H arylation provided facile access to fully substituted triazoles in a regiocontrolled manner. The resulting product **4.3.3** could be deprotected to yield amine **4.3.4**. Subsequent guanidinylation (**4.3.5**) and deprotection afforded inhibitors **4.3.6a – 4.3.6d**. The guanidine motif was added to increase solubility at the highest concentrations assayed. The key piperidyl amine (**4.3.4**) can synthesized in 3 linear steps. This allows much quicker access to a wide variety of analogs relative to the 10-step route required for compound **V**.[15]

**Scheme 4.3. Second Generation Synthesis of Triazole Analogs.**

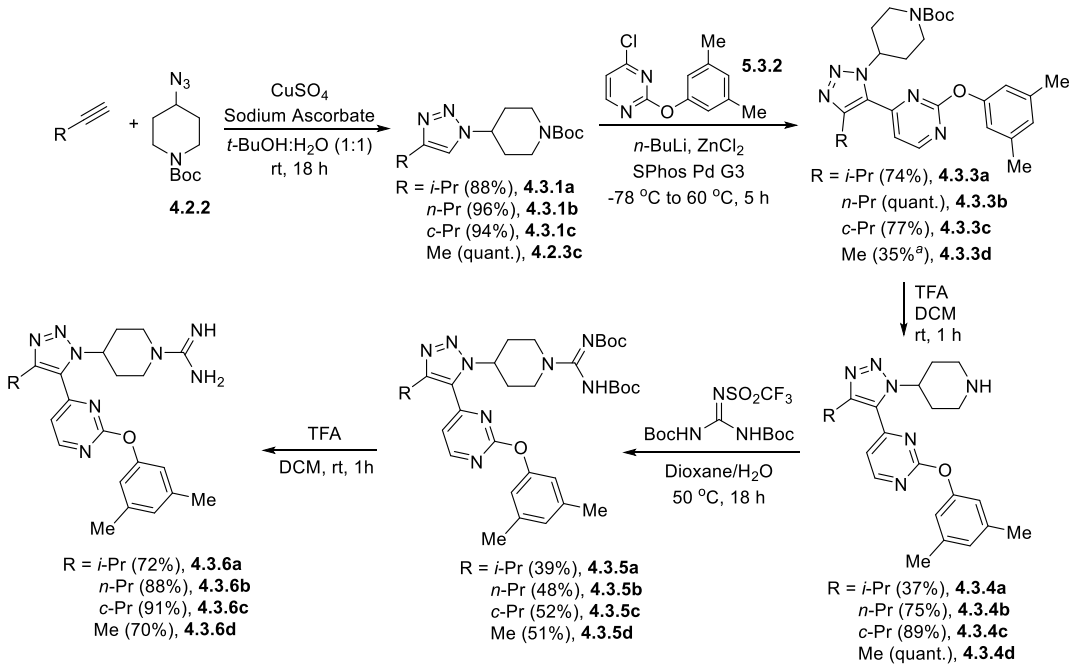


[a]Compound **13d** was synthesized through an alternate three-step route with an overall yield of 35%.

Huarui Cui determined the activity of these compounds by fluorescence anisotropy against BRD4-D1 (Table 4.4). The 4-fluorophenyl containing compound (**4.3a**) was a weak BRD4-D1 ligand in this assay (>100 μM). The low solubility of **4.3a**, **4.4a**, **4.4b** and **4.4c** was an issue in the fluorescence anisotropy assay. Herein, the guanidine group was added to increase the solubility. Most of the alkyl groups yielded little activity except for the methyl group. The methyl triazole (**4.3.6d**) was much more potent. This is similar to the results in a SAR study with compound **BI-2536** that demonstrated methyl was the optimal *N*-substituent in the *N*-ε-acetylated lysine mimic.[17]

**Table 4.4.** Significance of R Group to BRD4-D1 Binding Affinity.

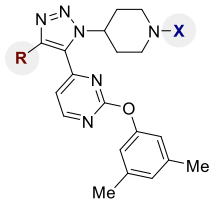


| Compound | R | X | BRD4-D1 $IC_{50}$ (μM)[a] |
|---|---|---|---|
| **4.3a** | 4-F-$C_6H_4$ | H | >100[b] |
| **4.4a** | *c*-hexyl | H | >100 |
| **4.4b** | *c*-pentyl | H | >100 |
| **4.4c** | *t*-Bu | H | >100 |
| **4.3.6a** | *i*-Pr | C(NH)$NH_2$ | >100 |
| **4.3.6b** | *n*-Pr | C(NH)$NH_2$ | >100 |
| **4.3.6c** | *c*-Pr | C(NH)$NH_2$ | 61 ± 8.1 |
| **4.3.6d** | Me | C(NH)$NH_2$ | 9.7 ± 1.8 |

[a]$IC_{50}$ values were determined by fluorescence anisotropy. Data represents the mean and standard deviation of three independent trials. [b]The $IC_{50}$ value could not be determined by fluorescence anisotropy. The $IC_{50}$ value was determined to be 27 μM by AlphaScreen by Reaction Biology.

Having identified that a methyl substituent significantly enhanced BRD4-D1 binding, attention was turned towards determining the pyrimidine ring's significance with regard to BRD4-D1 binding. This seemed prudent given the findings on p38α activity in Table 4.3. Based on a co-crystal structure of BRD4-D1 and compound **V**, the 3,5-dimethylaniline ring appears to provide an edge-to-face π-π interaction with W81 and the pyrimidine ring occupies the WPF shelf through a non-specific van der Waals interaction (Table 4.5 shows

analogous interaction with compound **4.5b**).[15] This analysis indicated that, unlike binding to p38α, neither nitrogen atom in the pyrimidine ring provided a key binding interaction. Replacing the pyrimidine ring (**4.3.6d**) with a benzene ring (**4.5a**) had minimal impact on binding (Table 4.5), which is consistent with this analysis. Converting the pyrimidine to a pyridine ring resulted in mixed results. Improved binding was observed when the nitrogen atom was at the 1 position (**4.5b**). Placing a nitrogen atom at the 2 position was tolerated (**4.5c**), while placing the nitrogen atom at either the 3 (**4.5d**) or 4 (**4.5e**) position resulted in complete loss of affinity. By comparison to compound **4.3.6d**, the loss in affinity of compounds **4.5d** and **4.5e** may indicate an unfavorable interaction of the nitrogen lone pair. The enhanced binding observed with compound **4.5b** was exciting in light of the diminished p38α binding observed with the 2,6-disubstituted pyridine (**4.3b** - **4.3c**, Table 4.3).

**Table 4.5.** Effect of Nitrogen Atom(s) to BRD4-D1 Affinity

Co-crystal structure of compound **4.5b** and BRD4-D1

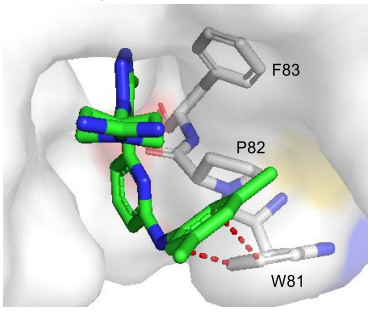


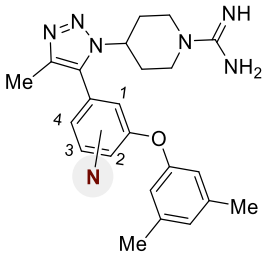


| Compound | N Atom | BRD4-D1 IC50 (μM)*a* |
|---|---|---|
| **4.3.6d** | 1,2 | 9.7 ± 1.8 |
| **4.5a** | none | 12 ± 1.1 |
| **4.5b** | 1 | 3.6 ± 0.05 |
| **4.5c** | 2 | 97 ± 2.6 |
| **4.5d** | 3 | >100 |
| **4.5e** | 4 | >100 |

[a]$IC_{50}$ values were determined by fluorescence anisotropy. Data represents the mean and standard deviation of three independent trials.

The selectivity of compounds **4.5b** and **4.6a** was further characterized (Table 4.6). The BRD4-D1 $K_d$ of these two compounds was determined by BROMOscanTM and was

consistent with the fluorescence anisotropy assay.[34,35] The methyl triazole demonstrated minimal selectivity for the two domains in BRD4, which is consistent with other Pan-BET inhibitors. Minimal binding to SMARCA2 and CBP was observed (Table 4.6). SMARCA2 and CBP were selected as representative non-BET family bromodomains. Prior work with compound **V** demonstrated modest binding to SMARCA2 and CBP.15 Most significantly, compound **4.5b** did not demonstrate any detectible activity towards p38α (*Kd* >200 μM). This indicates that this SAR study was able to systematically reduce p38α affinity by >200,000 fold (relative to compound **4.2.8a**, $K_d$ = 2.2 nM).

**Table 4.6.** Demonstrating Selectivity for Compound **4.5b** and **4.6a**.

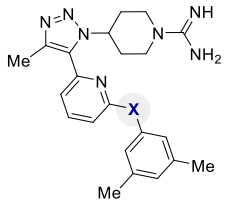


| Protein Target | X = O (**4.5b**) | X = NH (**4.6a**) |
|---|---|---|
| BRD4-D1 $IC_{50}$ (μM)*a* | 3.6 ± 0.05 | 4.5 ± 0.35 |
| BRD4-D1 $K_d$ (μM)*b* | 1.1 ± 0.63 | 1.2 ± 0.62 |
| BRD4-D2 $K_d$ (μM)*b* | 0.94 ± 0.48 | 2.1 ± 1.1 |
| SMARCA2 $K_d$ (μM)*b* | >100 | >100 |
| CBP $K_d$ (μM) | >100 | 78 ± 48 |
| p38α $K_d$ (μM)*c* | >200 | >25 |

[a]$IC_{50}$ values were determined by fluorescence anisotropy. Data represents the mean and standard deviation of three independent trials. [b]$K_d$ values were determined by BROMOscanTM. Data represents the mean and standard error from two independent trials. [c]$K_d$ values were determined by KINOMEscanTM. Data represents the mean and standard error from two independent trials.

To gain a structural understanding, a BRD4-D1 co-crystal structure was obtained with compound **4.6a** (crystal structure was solved by Jorden Johnson). This information could be compared to a co-crystal structure of **V** (PDB ID 6MH1).[13] The central triazole nitrogen (N2) in compound **4.6a** serves as the *N*-ε-acetylated lysine mimic by forming a direct hydrogen bond to N140 (Figure 4.6a). This was somewhat surprising because the terminal nitrogen (N3) has been calculated to be more basic than the central nitrogen (N2).[36] One explanation for this binding mode is that the terminal nitrogen (N3) in compound **4.6a** is forming a hydrogen bond to Y97 via a bridging structured water molecule in the co-crystal

structure. Similar interactions are observed for methyl isoxazoles and pyrazoles.[35,37,38] In the BRD4-D1 co-crystal structure with compound **V**, the 4-fluorophenyl group displaces three of four structured water molecules in this binding pocket relative to a DMSO co-crystal structure (PDB ID 4IOR), including the water bridging to Y97.[15] This mode of interaction was used to support the BRD4-D1 selectivity observed with compound **V**. The analogous structured waters in the co-crystal structure with compound **4.6a** are still present. Overlaying the BRD4-D1 co-crystal structures containing compounds **4.6a** vs **V** demonstrates that the pyrimidine ring and pyridine ring occupy similar binding poses relative to the WPF shelf (Figure 4.6b). This supports the notion that while the pyrimidine nitrogen atom in compound **V** is essential for p38α binding (Table 4.3), replacing the nitrogen with a C-H unit only minimally effects the BRD4-D1 binding.

**Figure 4.6.** Comparison of BRD4-D1 Co-crystal Structures with Compounds **4.6a** and **V**.

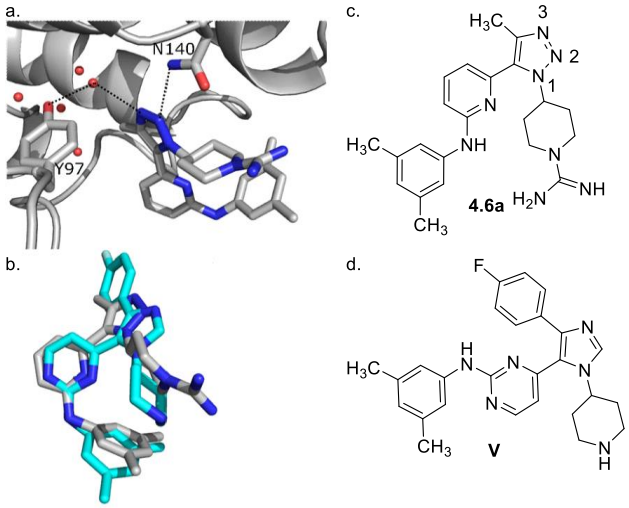


[a]Co-crystal structure of compound **4.6a** with BRD4-D1 (PDB ID 6MH1). Key interactions include a hydrogen bond of N2 to the amine of N140 (3.1 Å) and a water mediated hydrogen bond of N3 to the hydroxyl of Y97 (2.9 Å, 2.6Å). [b]Overlay of compounds **4.6a** (green) and **V** (gray). [c]Structure of compound **4.6a**. [d]Structure of compound **V**.

Anand Divakaran assayed these inhibitors in MM.1S cells. Multiple Myeloma cell strains from hematological cancers have a strong dependence on *c-Myc*.[6] The survival of MM.1S cells are highly BRD4-dependent because of an IgH and MYC rearrangement.[6] Reports have shown that BET inhibitors effectively decrease *c-Myc* transcription, which results in decreased cell viability.[15,39] In MM.1S cells, guanidinylated compounds **4.3.6d**, **4.5b**, and **4.6a** displayed weak activity (Table 4.7, $EC_{50}$ > 50 μM). This weak activity may

be due to decreased cell permeability. To test this hypothesis, several analogs with a free piperidine NH were assayed. Compounds **4.7a** - **4.7c** demonstrated clear anti-proliferative effects in MM.1S cells (EC50 = 6.6 μM, 2.9 μM, and 6.3 μM, respectively). The observed $EC_{50}$ values loosely correlate to the BRD4-D1 in vitro fluorescence anisotropy assay $IC_{50}$ values.

**Table 4.7.** Viability of MM.1S Cells Treated with Bromodomain Inhibitors.

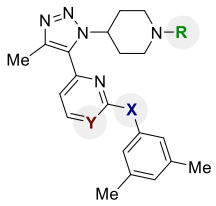


| Compound | R | X | Y | BRD4-D1 $IC_{50}$ (μM)[a] | MM.1S $EC_{50}$ (μM)[b] |
|---|---|---|---|---|---|
| **4.3.6d** | $C(NH)NH_2$ | O | N | 9.7 ± 1.8 | >50 |
| **4.5b** | $C(NH)NH_2$ | O | CH | 3.6 ± 0.05 | >50 |
| **4.6a** | $C(NH)NH_2$ | N | CH | 4.5 ± 0.35 | >50 |
| **4.7a** | H | O | N | 11 ± 2.5 | 6.6 ± 1.9 |
| **4.7b** | H | O | CH | 2.9 ± 0.07 | 2.9 ± 0.6 |
| **4.7c** | H | N | CH | 3.9 ± 0.35 | 6.3 ± 1.1 |

[a]$IC_{50}$ values were determined by fluorescence anisotropy. Data represents the mean and standard deviation of three independent trials. [b]Data reported are mean ± SEM of 3 biological replicates, with 3 technical replicates each. $EC_{50}$ values were determined using the Non-linear fit algorithm on GraphPad Prism.

In conclusion, we have both identified a likely source of the BRD4-D1 selectivity that compound **V** exhibits and have significantly mitigated the p38α activity. It appears that the 4-fluorophenyl group present in compound **V** promotes selectivity by displacing structured waters from the BRD4-D1 binding site. Since, the analogous water networks in other BET bromodomains are stronger, they are more difficult to displace. Originally, compound **4.2.8a** demonstrated a >10,000-fold selectivity for p38α over BRD4-D1. By modifying the hinge binding motif and removing a hydrophobic 4-fluorophenyl group, compound **4.5b** demonstrated a selectivity for BRD4-D1 and BRD4-D2 over p38α by >200-fold. This represents a >1,400,000 relative difference in binding. A co-crystal structure and cellular assays further support the binding mode of the triazole inhibitor and

the BET activity. In the future, this molecular design approach may be applied to other previously reported dual p38-BET inhibitors including **V**, SB-202190, and SB-203580.

### 4.4. Improving Potency

The last goal was to improve the potency of these compounds. The phenol ring was identified an optimal site for late stage modifications. To synthesize the desired analogs, two divergent steps were employed (Scheme **4.4**). The ether linkage can be constructed via nucleophilic aromatic substitution with the desired phenol and fluoropyridine (**4.4.1**, approach 1). This method is convenient when the necessary phenols are commercially available. However, a thorough study of the size and position of phenol substituents requires many phenols which are not commercial and would likely be three steps to synthesize. To circumvent this issue, bromines were installed at the desired positions (approach 2). A subsequent Kumada or Negishi cross-coupling reaction allowed incorporation of many alkyl and aryl groups. Thus, each new analog only requires two steps (cross-coupling and deprotection) after the common bromine intermediate.

**Scheme 4.4. Divergent Synthesis.**

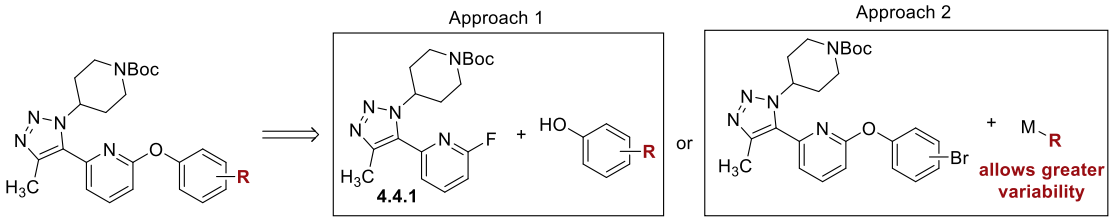


Synthesizing the desired analogs proceeded smoothly (Scheme 4.5). Initial cross-coupling between triazole **4.2.2** and 2-chloro-6-fluoropyridine produced fluoropyridine **4.4.1** in 87% yield. It is worth noting that attempts to perform this same coupling with 2,6-dichloropyridine resulted in only trace amounts of the desired product due to overwhelming double coupling of two triazoles to one pyridine. Treatment of fluoropyridine **4.4.1** with 3,5-dibromophenol and $K_2CO_3$ afforded the desired divergent intermediate **4.5.1**. The necessary Grignard or organo-zinc reagent and Pd(dppf)$Cl_2$ were used to install various alkyl substituents (**4.5.2a** – **4.5.2f**). Deprotection with TFA generated the desired analogs (**4.5.3a** – **4.5.3f**).

**Scheme 4.5. Synthesis of alkyl substituted phenols.**

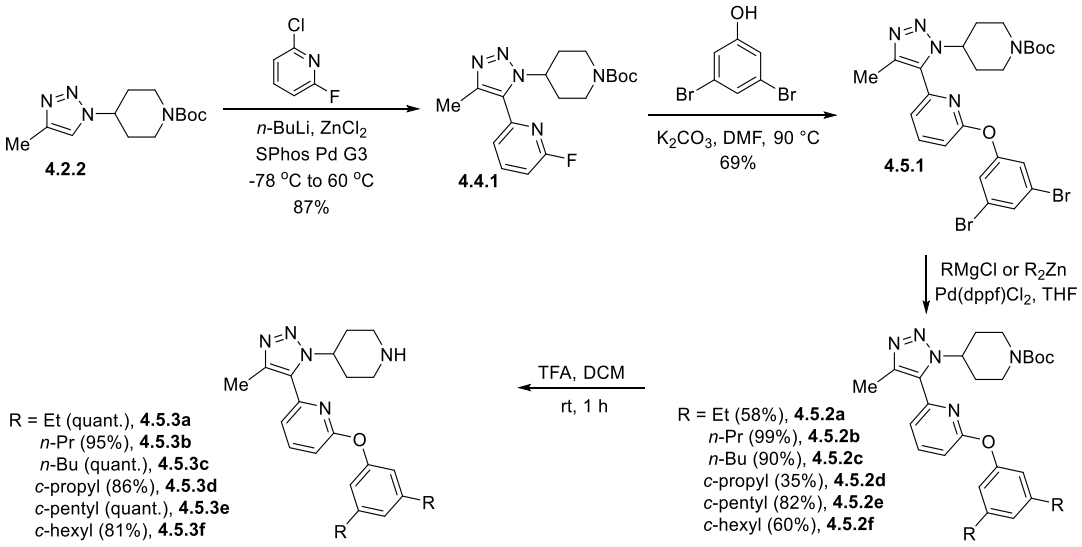


The affinity of these compounds for BRD4-D1 was examined (Table 4.8). Replacing the methyl groups (**4.7b**) with ethyl or cyclopropyl groups (**4.5.3a** and **4.5.3d**) provided a modest improvement in the affinity. Larger alkyl groups (**4.5.3c**, **4.5.3e**, and **4.5.3f**) likely hindered the inhibitor from binding effectively. Since altering the alkyl substituents did not provide the desired improvement in affinity, hydrogen bonding and halogen bonding interactions were targeted. Adding a hydroxymethyl significantly weakened the BRD4-D1 affinity likely due the hydrophobic nature of that region (**4.8a**). Incorporating bromines provided another small improvement (**4.8c**).

**Table 4.8.** Affinity for triazole analogs with different phenol substituents.

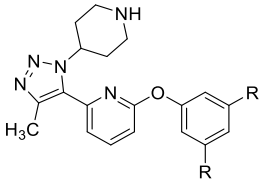

| Compound | R | $IC_{50}$ BRD4-D1 (μM) |
|---|---|---|
| **4.7b** | Me | 2.88 ± 0.3 |
| **4.5.3a** | Et | 1.50 ± 0.2 |
| **4.5.3b** | *n*-Pr | 2.60 ± 0.1 |
| **4.5.3c** | *n*-butyl | 12.5 ± 1.0 |

| | | |
|---|---|---|
| **4.5.3d** | cyclopropyl | 1.42 ± 0.09 |
| **4.5.3e** | cyclopentyl | 21.8 ± 3.0 |
| **4.5.3f** | cyclohexyl | 75.8 ± 13 |
| **4.8a** | $CH_2OH$ | 40.9 ± 6.0 |
| **4.8b** | Cl | 2.40 ± 0.20 |
| **4.8c** | Br | 0.980 ± 0.10 |

[a]$IC_{50}$ values were determined by fluorescence anisotropy. Data represents the mean and standard deviation of three independent trials.

Given the improvement observed with the 3,5-dibromophenol analog, the 2,5-dibromophenol analog (Figure 4.7, **4.7.1**) was also examined which provided another small improvement in the BRD4-D1 affinity. In a separate project, Huarui Cui found that adding a *N,N*-dimethylethyleneamine group onto the piperidine on the imidazole scaffold provided a 2-fold improvement in the potency.[40] This same modification provided a 7-fold improvement in the BRD4-D1 affinity with the 2,5-dibromo analog (compound **4.7.1** vs **4.7.2**) and a 20-fold improvement with the 3,5-dimethyl- analog (compound **4.7b** vs **4.7.3**). This could be due to an interaction between the dimethylamine and D144 in the BRD4-D1 binding site (Figure 4.7). In the co-crystal structure of compound **4.7.1** and BRD4-D1, the piperidine nitrogen is 6.3 Å from D144. The *N,N*-dimethylamino group in compound **4.7.2** may reach towards that residue and interact via bridging water molecules.

**Figure 4.7.** Functionalizing the piperidine ring.

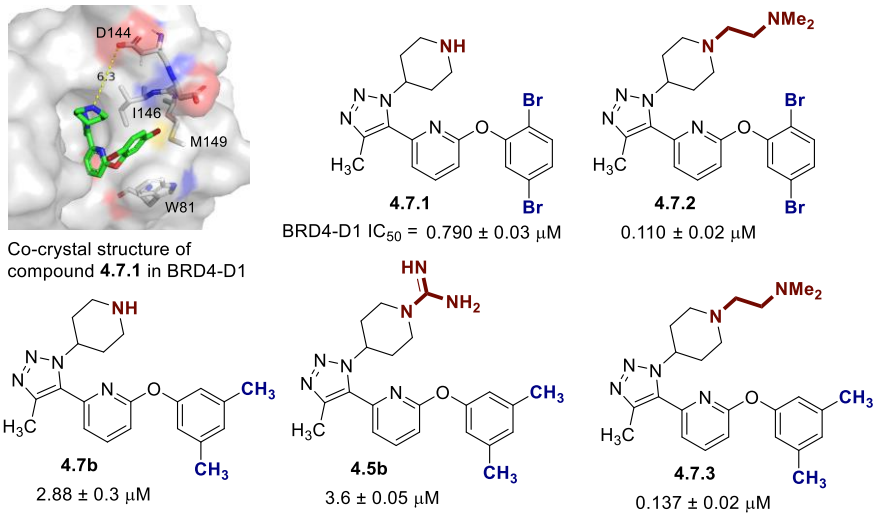


[a]$IC_{50}$ values were determined by fluorescence anisotropy. Data represents the mean and standard deviation of three independent trials.

In conclusion, the synthetic route for these inhibitors was significantly shortened by switching from an imidazole to a triazole scaffold (Figure 4.8, **V** to **4.2.8a**). Using this synthetic route, many analogs were synthesized which allowed invesitigation of three other goals. It was determined that the 4-fluorophenyl group in compound **V** is responsible for part of the unqiue BRD4-D1 selectivity. By removing the hydrogen bonding nitrogens and the 4-fluorophenyl group in compound **4.2.8a**, the off-target p38α activity was reduced by >90,000 fold. Lastly, the potency was improved 10-fold by switching the 3,5-dimethylphenyl ring (**4.5b**) to a 2,5-dibromophenyl ring (**4.7.2**) and adding a *N,N*-dimethylethyleneamine group onto the piperidine ring.

**Figure 4.8.** Summary of Results.

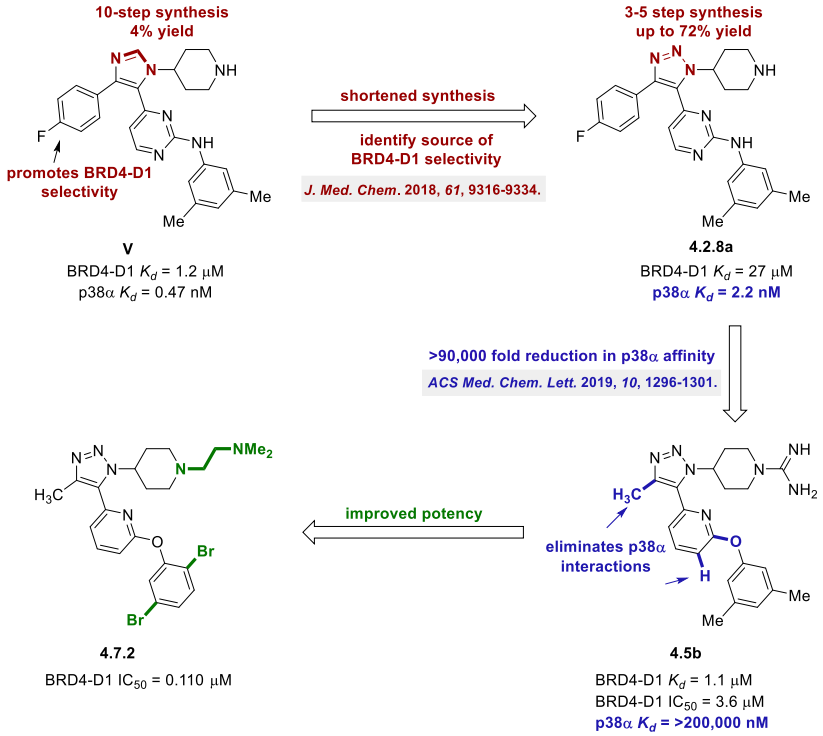


## 4.5 Experimental

Most of the experimental details and characterization data for this chapter can be found in *J. Med. Chem.* **2018**, *61*, 9316-9334 and *ACS Med. Chem. Lett.* **2019**, *10*, 1296-1301. The remaining experimental data is included below.

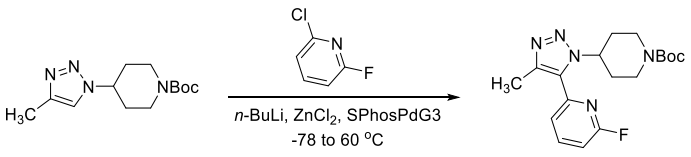

**Compound 4.4.1**

To a solution of triazole **4.2.2** (77.6 mg, 0.292 mmol) in DME (2 mL) cooled in a dry ice/acetone bath was added *n*-BuLi (0.13 mL, 2.5 M in hexanes, 0.32 mmol). After 15 min, a freshly prepared solution of $ZnCl_2$ (67.1 mg, 0.493 mmol) in THF (2 mL) was added and the reaction was warmed to rt. After 10 min, a solution of 2-chloro-6-fluoropyridine (77.5 mg, 0.589 mmol) and SPhosPdG3 (9.3 mg, 12 µmol) in DME (2 mL) was added and the reaction was heated to 60 °C. After 4 h, the reaction was cooled to rt and quenched by the addition of saturated aqueous $NH_4Cl$. The reaction mixture was extracted with EtOAc. The combined organic phases were washed with brine, dried ($Na_2SO_4$), filtered, and concentrated under reduced pressure. Final purification by column chromatography (40-80% EtOAc in Hexanes) afforded compound **4.4.1** (91.8 mg, 87%).

**$^1$H NMR (500 MHz, $CDCl_3$)** δ 7.98 (apparent q, *J* = 7.9 Hz, 1H), 7.37 (d, *J* = 7.4 Hz, 1H), 7.01 (dd, *J* = 8.4, 2.8 Hz, 1H), 4.98 (tt, *J* = 11.3, 4.1 Hz, 1H), 4.26 (br, 2H), 2.89 (br, 2H), 2.47 (s, 3H), 2.24 (br, 2H), 2.11 (apparent d, *J* = 12.1 Hz, 2H), 1.48 (s, 9H).
**$^{13}$C{$^1$H} NMR (126 MHz, $CDCl_3$)** δ 163.1 (d, $J_{C\text{-}F}$ = 241.9 Hz), 154.6, 146.1 (d, $J_{C\text{-}F}$ = 14.4 Hz), 142.3, 142.1 (d, $J_{C\text{-}F}$ = 8.0 Hz), 130.7, 121.5 (d, $J_{C\text{-}F}$ = 4.2 Hz), 109.2 (d, $J_{C\text{-}F}$ = 36.7 Hz), 79.8, 57.3, 43.5 (br), 32.1, 28.4, 11.8.
**$^{19}$F NMR (471 MHz, $CDCl_3$)** δ -64.83 (d, *J* = 8.1 Hz).
**IR (NaCl, thin film, cm$^{-1}$)**: 2976, 2932, 2864, 1692, 1601, 1575, 1474, 1425, 1366, 1332, 1246, 1166.
**HRMS (ESI-TOF)** *m/z* $[M + Na]^+$ calcd for $C_{18}H_{24}FN_5NaO_2^+$ 384.1806, found 384.1819.

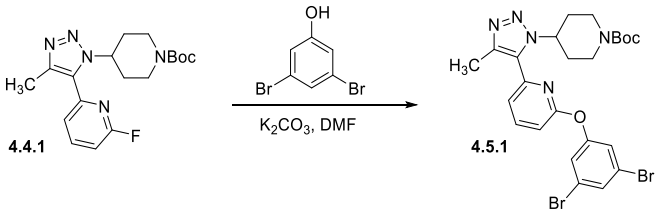


**Compound 4.5.1**

**General procedure I**: To a solution of pyridine **4.4.1** (1.07 g, 2.97 mmol) and 3,5-dibromophenol (1.07 g, 4.23 mmol) in DMF (5 mL) was added solid $K_2CO_3$ (637 mg, 4.62 mmol) at rt. The reaction was sealed under air and heated to 90 °C. After 48 h, the reaction was cooled to rt, quenched by addition of $H_2O$, and extracted with DCM. The combined organic phases were dried ($Na_2SO_4$), filtered, and concentrated under reduced pressure. Initial purification by column chromatography (5-30% IPA in hexanes followed by 30% IPA in DCM). Final purification by recrystallization (DCM/hexanes, ca. 1:10) afforded bromide **4.5.1** (1.22 g, 69%) as a white solid.
**$^1$H NMR (500 MHz, $CDCl_3$)** δ 7.91 (apparent t, *J* = 7.9 Hz, 1H), 7.55 (s, 1H), 7.29 (s, 2H), 7.24 (d, *J* = 7.4 Hz, 1H), 7.04 (d, *J* = 8.3 Hz, 1H), 4.63 (tt, *J* = 10.8, 4.0 Hz, 1H), 4.09 (br, 2H), 2.63 – 2.49 (m, 2H), 2.47 (s, 3H), 2.10 (apparent qd, *J* = 12.0, 4.3 Hz, 2H), 1.83 – 1.74 (m, 2H), 1.48 (s, 9H).
**$^{13}$C{$^1$H} NMR (126 MHz, $CDCl_3$)** δ 162.6, 154.6, 154.6, 145.5, 142.1, 140.9, 131.2, 130.8, 124.1, 123.1, 119.6, 111.5, 79.8, 56.9, 43.0 (br), 31.9, 28.5, 11.9.

**IR (NaCl, thin film, cm$^{-1}$)**: 3073, 2929, 2862, 1691, 1566, 1566, 1418, 1298, 1244, 1165.
**HRMS (ESI-TOF)** *m/z* [M + Na]$^+$ calcd for $C_{24}H_{27}Br_2N_5NaO_3^+$ 614.0373, found 614.0357.

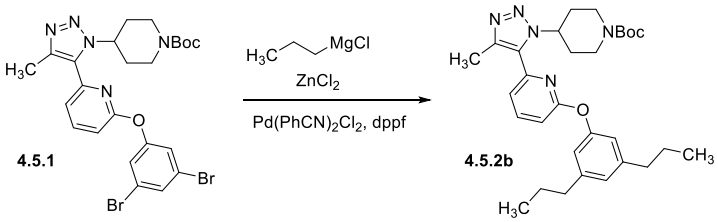


**Compound 4.5.2b**

**General procedure II** - To a solution of $ZnCl_2$ (54.3 mg, 0.399 mmol) in THF (3 mL) at rt was added *n*-propylmagnesium chloride (0.10 mL, 2.0 M in $Et_2O$, 0.20 mmol). After 10 min, a solution of $Pd(PhCN)_2Cl_2$ (1.6 mg, 4.1 µmol), dppf (3.3 mg, 6.0 µmol), and bromide **4.5.1** (52.3 mg, 88.2 µmol) in THF (4 mL) was added. The reaction was heated to 50 °C. After 20 h, the reaction was cooled to rt and quenched by addition of saturated aqueous $NH_4Cl$. The reaction mixture was extracted with EtOAc. The combined organic phases were washed with brine, dried ($Na_2SO_4$), filtered, and concentrated under reduced pressure. Final purification by column chromatography (40% EtOAc in hexanes) afforded product **4.5.2b** (45.5 mg, 99%) as a white solid.

**$^1$H NMR (500 MHz, $CDCl_3$)** δ 7.84 (dd, *J* = 8.3, 7.4 Hz, 1H), 7.17 (d, *J* = 7.4 Hz, 1H), 6.98 (d, *J* = 8.2 Hz, 1H), 6.88 (t, *J* = 1.5 Hz, 1H), 6.79 (d, *J* = 1.5 Hz, 2H), 4.73 (tt, *J* = 11.2, 4.0 Hz, 1H), 3.99 (br, 2H), 2.56 (t, 4H), 2.49 (s, 3H), 2.40 (br, 2H), 2.02 (apparent qd, *J* = 12.3, 4.2 Hz, 2H), 1.77 – 1.70 (m, 2H), 1.62 (hex, *J* = 7.4 Hz, 4H), 1.48 (s, 9H), 0.94 (t, *J* = 7.3 Hz, 6H).

**$^{13}$C{$^1$H} NMR (126 MHz, $CDCl_3$)** δ 163.6, 154.5, 153.5, 145.4, 144.4, 141.9, 140.2, 131.3, 125.5, 118.9, 118.3, 111.1, 79.6, 56.8, 43.1 (br), 37.9, 31.9, 28.4, 24.4, 13.9, 12.1.

**IR (NaCl, thin film, cm$^{-1}$)**: 2960, 2931, 2870, 1695, 1589, 1572, 1468, 1452, 1427, 1302, 1246, 1166, 1152.

**HRMS (ESI-TOF)** *m/z* [M + Na]$^+$ calcd for $C_{30}H_{41}N_5NaO_3^+$ 542.3102, found 542.3114

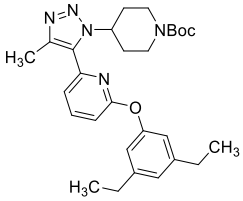


**Compound 4.5.2a**

General procedure II was used and product **4.5.2a** (13.1 mg, 58%) was isolated as a white solid.

**$^1$H NMR (500 MHz, $CDCl_3$)** δ 7.85 (dd, *J* = 8.3, 7.4 Hz, 1H), 7.18 (d, *J* = 7.4 Hz, 1H), 6.99 (d, *J* = 8.4 Hz, 1H), 6.93 (s, 1H), 6.81 (s, 2H), 4.74 (tt, *J* = 11.2, 4.0 Hz, 1H), 3.98 (br, 2H), 2.64 (q, *J* = 7.6 Hz, 4H), 2.49 (s, 3H), 2.38 (br, 2H), 2.02 (apparent qd, *J* = 12.3, 4.1 Hz, 2H), 1.77 – 1.69 (m, 2H), 1.48 (s, 9H), 1.23 (t, *J* = 7.6 Hz, 6H).

**$^{13}$C{$^1$H} NMR (126 MHz, $CDCl_3$)** δ 163.5, 154.6, 153.6, 146.0, 145.4, 141.9, 140.2, 131.3, 124.4, 118.4, 118.3, 111.1, 79.6, 56.8, 43.0 (br), 31.9, 28.7, 28.4, 15.4, 12.2.

**IR (NaCl, thin film, cm$^{-1}$)**: 2966, 2931, 2862, 1693, 1589, 1572, 1452, 1426, 1365, 1331, 1302, 1276, 1246, 1166, 1152.
**HRMS (ESI-TOF)** *m/z* $[M + Na]^+$ calcd for $C_{28}H_{37}N_5NaO_3^+$ 514.2789, found 514.2798.

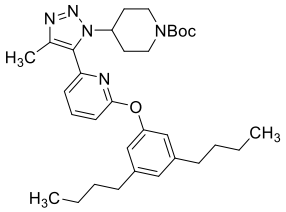


**Compound 4.5.2c**
**General procedure III** - To a solution of $ZnCl_2$ (74.6 mg, 0.549 mmol) in THF (2 mL) was added *n*-butylmagnesium chloride (0.10 mL, 2.0 M in THF, 0.20 mmol) at rt. After 5 min, the reaction was cooled in an ice bath. A solution of bromide **4.5.1** (48.6 mg, 82.0 µmol) in THF (2 mL) was added followed by $Pd(dppf)Cl_2$ (10.4 mg, 12.7 µmol). The reaction was removed from the ice bath and heated to 50 °C. After 18 h, the reaction was cooled to rt and quenched by addition of saturated aqueous $NH_4Cl$. The reaction mixture was extracted with EtOAc. The combined organic phases were washed with brine, dried ($Na_2SO_4$), filtered, and concentrated under reduced pressure. Final purification by column chromatography (30% EtOAc in hexanes) afforded product **4.5.2c** (40.3 mg, 90%) as a white solid.
**$^1$H NMR (500 MHz, $CDCl_3$)** δ 7.84 (dd, *J* = 8.3, 7.4 Hz, 1H), 7.17 (dd, *J* = 7.4, 0.7 Hz, 1H), 6.98 (dd, *J* = 8.3, 0.7 Hz, 1H), 6.88 (t, *J* = 1.6 Hz, 1H), 6.79 (d, *J* = 1.5 Hz, 2H), 4.73 (tt, *J* = 11.3, 4.0 Hz, 1H), 4.01 (br, 2H), 2.58 (t, *J* = 7.8 Hz, 4H), 2.49 (s, 3H), 2.40 (br, 2H), 2.03 (apparent qd, *J* = 12.3, 11.7, 3.3 Hz, 2H), 1.77 – 1.70 (m, 2H), 1.58 (p, *J* = 7.6 Hz, 4H), 1.48 (s, 9H), 1.35 (hex, *J* = 7.4 Hz, 4H), 0.92 (t, *J* = 7.4 Hz, 6H).
**$^{13}$C{$^1$H} NMR (126 MHz, $CDCl_3$)** δ 163.6, 154.5, 153.5, 145.4, 144.6, 141.9, 140.2, 131.3, 125.5, 118.8, 118.3, 111.1, 79.6, 56.8, 43.2 (br), 35.5, 33.5, 31.9, 28.4, 22.4, 13.9, 12.1.
**IR (NaCl, thin film, cm$^{-1}$)**: 2957, 2930, 2859, 1695, 1589, 1572, 1468, 1453, 1426, 1302, 1247, 1166, 1152.
**HRMS (ESI-TOF)** *m/z* $[M + Na]^+$ calcd for $C_{32}H_{45}N_5NaO_3^+$ 570.3415, found 570.3410.

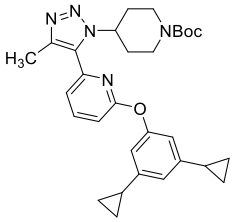


**Compound 4.5.2d**
General procedure III was used and product **4.5.2d** (16.3 mg, 35%) was isolated as a white solid.
**$^1$H NMR (500 MHz, $CDCl_3$)** δ 7.85 (dd, *J* = 8.3, 7.4 Hz, 1H), 7.18 (d, *J* = 7.4 Hz, 1H), 6.99 (d, *J* = 8.3 Hz, 1H), 6.65 – 6.61 (m, 3H), 4.77 (tt, *J* = 11.2, 4.0 Hz, 1H), 4.02 (br, 2H), 2.52 (s, 3H), 2.47 – 2.34 (m, 2H), 2.09 – 1.96 (m, 2H), 1.88 – 1.81 (m, 2H), 1.77 – 1.70 (m, 2H), 1.49 (s, 9H), 0.99 – 0.94 (m, 4H), 0.68 – 0.63 (m, 4H).
**$^{13}$C{$^1$H} NMR (126 MHz, $CDCl_3$)** δ 163.6, 154.5, 153.8, 146.0, 145.0, 141.6, 140.23, 131.5, 119.6, 118.3, 116.1, 111.4, 79.6, 57.1, 42.2 (br), 31.9, 28.5, 15.4, 12.0, 9.45.

**IR (NaCl, thin film, cm$^{-1}$)**: 3081, 2973, 2866, 1691, 1589, 1571, 1467, 1452, 1427, 1366, 1301, 1276, 1246, 1167.
**HRMS (ESI-TOF)** *m/z* [M + Na]$^+$ calcd for $C_{30}H_{37}N_5NaO_3^+$ 538.2789, found 538.2773.

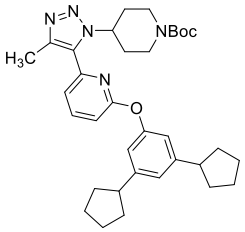

**Compound 4.5.2e**
General procedure III was used and product **4.5.2e** (35.3 mg, 82%) was isolated as a white solid.
**$^1$H NMR (500 MHz, $CDCl_3$)** δ 7.85 (dd, *J* = 8.3, 7.4 Hz, 1H), 7.18 (dd, *J* = 7.5, 0.7 Hz, 1H), 7.01 (t, *J* = 1.6 Hz, 1H), 6.98 (dd, *J* = 8.4, 0.7 Hz, 1H), 6.85 (d, *J* = 1.6 Hz, 2H), 4.76 (tt, *J* = 11.2, 4.0 Hz, 1H), 4.18 – 3.75 (m, 2H), 2.96 (tt, *J* = 10.0, 7.4 Hz, 2H), 2.51 (s, 3H), 2.36 – 2.24 (m, 2H), 2.10 – 1.91 (m, 6H), 1.84 – 1.75 (m, 4H), 1.74 – 1.62 (m, 6H), 1.61 – 1.51 (m, 4H), 1.47 (s, 9H).
**$^{13}$C{$^1$H} NMR (126 MHz, $CDCl_3$)** δ 163.5, 154.5, 153.4, 148.2, 145.3, 142.0, 140.2, 131.1, 123.0, 118.2, 117.7, 111.1, 79.5, 56.8, 46.0, 42.9 (br), 34.6, 31.9, 28.4, 25.4, 12.3.
**IR (NaCl, thin film, cm$^{-1}$)**: 2954, 2867, 1694, 1589, 1572, 1469, 1452, 1426, 1303, 1246, 1166, 1152.
**HRMS (ESI-TOF)** *m/z* [M + Na]$^+$ calcd for $C_{34}H_{45}N_5NaO_3^+$ 594.3415, found 594.3405.

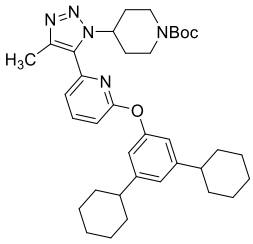

**Compound 4.5.2f**
General procedure III was used and product **4.5.2f** (30.2 mg, 60%) was isolated as a white solid.
**$^1$H NMR (500 MHz, $CDCl_3$)** δ 7.84 (dd, *J* = 8.3, 7.5 Hz, 1H), 7.18 (d, *J* = 7.4 Hz, 1H), 6.97 (d, *J* = 8.3 Hz, 1H), 6.95 (t, *J* = 1.6 Hz, 1H), 6.82 (d, *J* = 1.5 Hz, 2H), 4.76 (tt, *J* = 11.2, 4.0 Hz, 1H), 4.11 – 3.81 (m, 2H), 2.51 (s, 3H), 2.49 – 2.45 (m, 2H), 2.33 – 2.24 (m, 2H), 2.00 (apparent qd, *J* = 12.2, 4.1 Hz, 2H), 1.88 – 1.81 (m, 8H), 1.74 (apparent d, *J* = 12.5 Hz, 4H), 1.47 (s, 9H), 1.44 – 1.32 (m, 8H), 1.30 – 1.17 (m, 2H).
**$^{13}$C{$^1$H} NMR (126 MHz, $CDCl_3$)** δ 163.4, 154.4, 153.4, 149.8, 145.4, 141.9, 140.2, 131.2, 122.4, 118.2, 117.4, 111.1, 79.5, 56.9, 44.6, 42.9 (br), 34.4, 31.9, 28.4, 26.8, 26.1, 12.3.
**IR (NaCl, thin film, cm$^{-1}$)**: 2926, 2851, 1694, 1589, 1572, 1449, 1426, 1304, 1246, 1166, 1152.
**HRMS (ESI-TOF)** *m/z* [M + Na]$^+$ calcd for $C_{36}H_{49}N_5NaO_3^+$ 622.3728, found 622.3719.

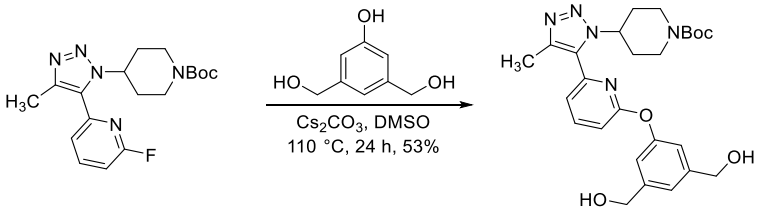


**Compound S1**

To a solution of pyridine **4.4.1** (45.1 mg, 0.125 mmol) and 3,5-Bis(hydroxymethyl)phenol (32.7 mg, 0.212 mmol) in DMSO (2.0 mL) was added $Cs_2CO_3$ (62.3 mg, 0.191 mmol) at rt. The reaction was sealed under air and heated to 110 °C. After 24 h, the reaction was cooled to rt and extract with EtOAc. The combined organic phases were washed with brine, dried ($Na_2SO_4$), filtered, and concentrated under reduced pressure. Final purification by column chromatography (40-75% EtOAc in DCM) afforded product **S1** (33.1 mg, 53%) as a white solid.

**$^1$H NMR (500 MHz, MeOD)** δ 8.01 (dd, *J* = 8.3, 7.4 Hz, 1H), 7.36 (dd, *J* = 7.4, 0.7 Hz, 1H), 7.21 (s, 1H), 7.14 (dd, *J* = 8.3, 0.7 Hz, 1H), 7.09 (s, 2H), 4.73 (tt, *J* = 11.2, 4.1 Hz, 1H), 4.64 (s, 4H), 3.94 (dt, *J* = 13.7, 2.8 Hz, 2H), 2.61 – 2.47 (m, 2H), 2.42 (s, 3H), 1.89 (apparent qd, *J* = 12.2, 4.3 Hz, 2H), 1.79 – 1.70 (m, 2H), 1.49 (s, 9H).

**$^{13}$C NMR (126 MHz, MeOD)** δ 163.7, 155.0, 154.2, 144.5, 143.8, 141.4, 140.9, 131.9, 121.0, 119.0, 118.2, 111.6, 79.9, 63.1, 56.7, 42.2 (br), 31.6, 27.3, 10.1.

**IR (NaCl, thin film, cm$^{-1}$)**: 3392, 2975, 2930, 2866, 1691, 1673, 1591, 1573, 1452, 1428, 1367, 1302, 1277, 1247, 1166.

**HRMS (ESI-TOF)** *m/z* $[M + Na]^+$ calcd for $C_{26}H_{33}N_5NaO_5^+$ 518.2374, found 518.2390.

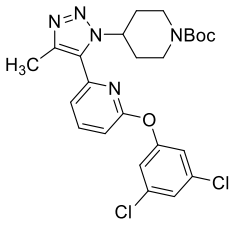


**Compound S2**

General procedure I was used and compound **S2** (32.3 mg, 79%) was isolated as a white solid.

**$^1$H NMR (500 MHz, $CDCl_3$)** δ 7.91 (dd, *J* = 8.2, 7.6 Hz, 1H), 7.25 (t, *J* = 1.8 Hz, 1H), 7.23 (dd, *J* = 7.5, 0.7 Hz, 1H), 7.09 (d, *J* = 1.8 Hz, 2H), 7.04 (dd, *J* = 8.4, 0.7 Hz, 1H), 4.62 (tt, *J* = 11.2, 4.0 Hz, 1H), 4.09 (br, 2H), 2.53 (br, 2H), 2.46 (s, 3H), 2.17 – 2.03 (m, 2H), 1.86 – 1.69 (m, 2H), 1.48 (s, 9H).

**$^{13}$C{$^1$H} NMR (126 MHz, $CDCl_3$)** δ 162.6, 154.5, 154.5, 145.5, 142.1, 140.9, 135.5, 131.2, 125.4, 120.8, 119.6, 111.6, 79.8, 56.9, 43.1 (br), 31.9, 28.4, 11.8.

**IR (NaCl, thin film, cm$^{-1}$)**: 3070, 2975, 2929, 2861, 1692, 1589, 1578, 1423, 1246, 1165.

**HRMS (ESI-TOF)** *m/z* $[M + Na]^+$ calcd for $C_{24}H_{27}Cl_2N_5NaO_3^+$ 526.1383, found 526.1387.

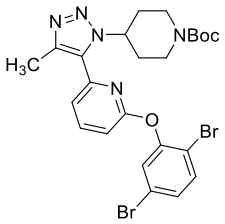

**Compound S3**

General procedure I was used and compound **S3** (31.0 mg, 63%) was isolated as a white solid.

**$^1$H NMR (500 MHz, $CDCl_3$)** δ 7.92 (dd, *J* = 8.3, 7.4 Hz, 1H), 7.53 (d, *J* = 8.5 Hz, 1H), 7.37 (d, *J* = 2.2 Hz, 1H), 7.30 (dd, *J* = 8.7, 2.2 Hz, 1H), 7.20 (d, *J* = 7.3 Hz, 1H), 7.12 (d, *J* = 8.3 Hz, 1H), 4.58 (tt, *J* = 11.2, 4.2 Hz, 1H), 4.08 (br, 2H), 2.63 (br, 2H), 2.43 (s, 3H), 2.08 (br, 2H), 1.72 – 1.60 (m, 2H), 1.49 (s, 9H).

**$^{13}$C{$^1$H} NMR (126 MHz, $CDCl_3$)** δ 162.4, 154.5, 151.4, 145.3, 142.0, 140.8, 134.4, 131.3, 129.9, 127.7, 121.4, 119.5, 115.7, 111.1, 79.8, 56.4, 43.2 (br), 31.9, 28.5, 11.7.

**IR (NaCl, thin film, cm$^{-1}$)**:2975, 2930, 2860, 1691, 1565, 1463, 1426, 1297, 1244, 1165.

**HRMS (ESI-TOF)** *m/z* $[M + Na]^+$ calcd for $C_{24}H_{27}Br_2N_5NaO_3^+$ 614.0373, found 614.0373.

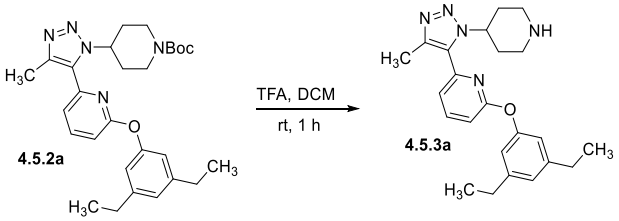


**Compound 4.5.3a**

**General procedure IV:** To a solution of compound **4.5.2a** (13.1 mg, 26.6 µmol) in DCM (0.5 mL) was added TFA (0.5 mL). After 1 h at rt, the reaction was concentrated under reduced pressure product, which afforded compound **4.5.3a** (17.9 mg, quant.) was isolated as a white solid. Analysis by $^{19}$F NMR with 2,2,2-trifluoroethanol as the internal standard indicated formation of a *bis*-TFA salt.

**$^1$H NMR (500 MHz, MeOD)** δ 8.02 (dd, *J* = 8.3, 7.4 Hz, 1H), 7.39 (dd, *J* = 7.5, 0.7 Hz, 1H), 7.12 (dd, *J* = 8.3, 0.7 Hz, 1H), 6.98 (t, *J* = 1.5 Hz, 1H), 6.86 (d, *J* = 1.5 Hz, 2H), 4.93 – 4.83 (m, 1H), 3.37 – 3.33 (m, 2H), 2.71 (apparent dd, *J* = 12.7, 3.1 Hz, 2H), 2.66 (q, *J* = 7.6 Hz, 4H), 2.46 (s, 3H), 2.32 – 2.20 (m, 2H), 2.04 (apparent dd, *J* = 14.1, 3.3 Hz, 2H), 1.24 (t, *J* = 7.6 Hz, 6H).

**$^{13}$C{$^1$H} NMR (126 MHz, MeOD)** δ 163.7, 154.1, 146.2, 144.2, 141.5, 140.9, 132.1, 123.9, 118.9, 118.0, 111.6, 53.5, 42.7, 28.6, 28.3, 14.7, 10.2.

**IR (NaCl, thin film, cm$^{-1}$)**: 2966, 2930, 2854, 1683, 1590, 1573, 1456, 1431, 1298, 1248, 1202, 1178, 1135.

**HRMS (ESI-TOF)** *m/z* $[M + H]^+$ calcd for $C_{23}H_{30}N_5O^+$ 392.2445, found 392.2432.

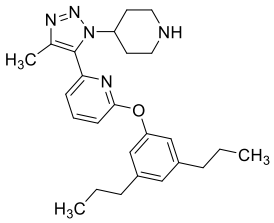

**Compound 4.5.3b**

General procedure **IV** was used and product **4.5.3b** (35.4 mg, 95%) was isolated as a white solid. Analysis by $^{19}$F NMR with 2,2,2-trifluoroethanol as the internal standard indicated formation of a *bis*-TFA salt.

**$^{1}$H NMR (500 MHz, MeOD)** δ 8.02 (dd, *J* = 8.4, 7.4 Hz, 1H), 7.38 (dd, *J* = 7.5, 0.7 Hz, 1H), 7.11 (dd, *J* = 8.4, 0.7 Hz, 1H), 6.94 (t, *J* = 1.5 Hz, 1H), 6.84 (d, *J* = 1.5 Hz, 2H), 4.87 (tt, *J* = 10.7, 4.1 Hz, 1H), 3.38 – 3.33 (m, 2H), 2.74 (apparent td, *J* = 12.7, 3.2 Hz, 2H), 2.60 (t, *J* = 7.4 Hz, 4H), 2.45 (s, 3H), 2.31 – 2.20 (m, 2H), 2.03 (apparent dd, *J* = 14.1, 3.6 Hz, 2H), 1.63 (hex, *J* = 7.4 Hz, 4H), 0.94 (t, *J* = 7.4 Hz, 6H).

**$^{13}$C{$^{1}$H} NMR (126 MHz, MeOD)** δ 163.8, 153.9, 144.5, 144.2, 141.5, 140.9, 132.2, 125.2, 118.9, 118.7, 111.6, 53.6, 42.7, 37.4, 28.6, 24.3, 12.7, 10.1.

**IR (NaCl, thin film, cm$^{-1}$)**: 2961, 2931, 2871, 1677, 1591, 1573, 1453, 1431, 1298, 1248, 1202, 1177, 1136.

**HRMS (ESI-TOF)** *m/z* [M + H]$^{+}$ calcd for $C_{25}H_{34}N_5O^{+}$ 420.2758, found 420.2767.

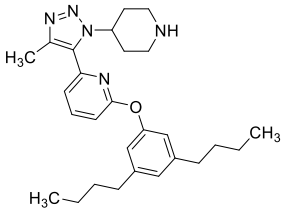

**Compound 4.5.3c**

General procedure **IV** was used and product **4.5.3c** (44.0 mg, quant.) was isolated as a white solid. Analysis by $^{19}$F NMR with 2,2,2-trifluoroethanol as the internal standard indicated formation of a *bis*-TFA salt.

**$^{1}$H NMR (400 MHz, MeOD)** δ 8.02 (apparent t, *J* = 7.9 Hz, 1H), 7.38 (d, *J* = 7.4 Hz, 1H), 7.11 (d, *J* = 8.3 Hz, 1H), 6.93 (s, 1H), 6.82 (s, 2H), 4.85 (tt, *J* = 10.6, 4.1 Hz, 1H), 3.40 – 3.33 (m, 2H), 2.75 (apparent td, *J* = 12.6, 3.1 Hz, 2H), 2.62 (t, *J* = 7.6 Hz, 4H), 2.45 (s, 3H), 2.33 – 2.18 (m, 2H), 2.08 – 1.97 (m, 2H), 1.59 (pent, *J* = 7.5 Hz, 4H), 1.34 (hex, *J* = 7.3 Hz, 4H), 0.91 (t, *J* = 7.3 Hz, 6H).

**$^{13}$C{$^{1}$H} NMR (126 MHz, MeOD)** δ 163.8, 154.0, 144.7, 144.1, 141.4, 140.9, 132.2, 125.1, 118.9, 118.6, 111.6, 53.6, 42.7, 35.0, 33.4, 28.6, 21.9, 12.8, 10.1.

**IR (NaCl, thin film, cm$^{-1}$)**: 2958, 2931, 2859, 2741, 1677, 1591, 1573, 1455, 1431, 1298, 1249, 1202, 1177, 1136.

**HRMS (ESI-TOF)** *m/z* [M + H]$^{+}$ calcd for $C_{27}H_{38}N_5O^{+}$ 448.3071, found 448.3081.

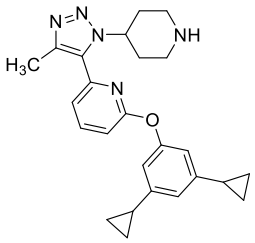

**Compound 4.5.3d**

General procedure **IV** was used and compound **4.5.3d** (14.4 mg, 86%) was isolated as a white solid. Analysis by $^{19}$F NMR with 2,2,2-trifluoroethanol as the internal standard indicated formation of a *mono*-TFA salt.

**$^{1}$H NMR (500 MHz, MeOD)** δ 8.02 (dd, *J* = 8.3, 7.5 Hz, 1H), 7.39 (d, *J* = 7.4 Hz, 1H), 7.11 (d, *J* = 8.2 Hz, 1H), 6.72 (t, *J* = 1.7 Hz, 1H), 6.65 (d, *J* = 1.6 Hz, 2H), 4.94 – 4.90 (m, 1H), 3.42 – 3.35 (m, 2H), 2.72 (td, *J* = 12.8, 3.2 Hz, 2H), 2.47 (s, 3H), 2.32 – 2.23 (m, 2H), 2.08 – 2.01 (m, 2H), 1.90 (tt, *J* = 8.4, 5.1 Hz, 2H), 1.02 – 0.97 (m, 4H), 0.71 – 0.65 (m, 4H).

**$^{13}$C{$^{1}$H} NMR (126 MHz, MeOD)** δ 163.6, 154.3, 146.3, 144.2, 141.6, 140.9, 132.1, 119.1, 118.8, 115.3, 111.7, 53.6, 42.8, 28.6, 14.7, 10.3, 8.7.

**IR (NaCl, thin film, cm$^{-1}$)**: 2999, 2726, 1678, 1589, 1572, 1470, 1456, 1430, 1297, 1247, 1202, 1136.

**HRMS (ESI-TOF)** *m/z* [M + H]$^{+}$ calcd for $C_{25}H_{30}N_5O^{+}$ 416.2445, found 416.2456.

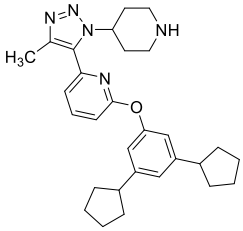

**Compound 4.5.3e**

General procedure **IV** was used and product **4.5.3e** (17.6 mg, quant.) was isolated as a white solid. Analysis by $^{19}$F NMR with 2,2,2-trifluoroethanol as the internal standard indicated formation of a *tris*-TFA salt.

**$^{1}$H NMR (500 MHz, MeOD)** δ 8.02 (dd, *J* = 8.3, 7.4 Hz, 1H), 7.39 (dd, *J* = 7.4, 0.7 Hz, 1H), 7.10 (dd, *J* = 8.2, 0.7 Hz, 1H), 7.06 (t, *J* = 1.7 Hz, 1H), 6.89 (d, *J* = 1.5 Hz, 2H), 4.90 – 4.83 (m, 1H), 3.37 – 3.33 (m, 2H), 3.02 (tt, *J* = 9.9, 7.5 Hz, 2H), 2.70 (apparent td, *J* = 12.7, 3.2 Hz, 2H), 2.46 (s, 3H), 2.32 – 2.21 (m, 2H), 2.12 – 2.02 (m, 6H), 1.87 – 1.77 (m, 4H), 1.76 – 1.66 (m, 4H), 1.62 – 1.53 (m, 4H).

**$^{13}$C{$^{1}$H} NMR (126 MHz, MeOD)** δ 163.7, 153.8, 148.3, 144.1, 141.5, 140.9, 132.2, 122.5, 118.9, 117.2, 111.6, 53.6, 45.8, 42.7, 34.3, 28.7, 25.0, 10.1.

**IR (NaCl, thin film, cm$^{-1}$)**: 2953, 2866, 1677, 1590, 1572, 1455, 1430, 1298, 1248, 1201, 1176, 1137.

**HRMS (ESI-TOF)** *m/z* [M + H]$^{+}$ calcd for $C_{29}H_{38}N_5O^{+}$ 472.3071, found 472.3059.

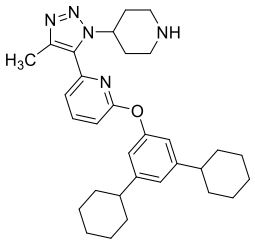

**Compound 4.5.3f**

General procedure **IV** was used and product **4.5.3f** (28.1 mg, 81%) was isolated as a white solid. Analysis by $^{19}F$ NMR with 2,2,2-trifluoroethanol as the internal standard indicated formation of a *tris*-TFA salt.

**$^{1}$H NMR (500 MHz, MeOD)** δ 8.01 (dd, *J* = 8.3, 7.4 Hz, 1H), 7.39 (d, *J* = 7.1 Hz, 1H), 7.08 (d, *J* = 8.3 Hz, 1H), 6.99 (t, *J* = 1.6 Hz, 1H), 6.86 (d, *J* = 1.5 Hz, 2H), 4.87 (tt, *J* = 10.6, 4.2 Hz, 1H), 3.36 – 3.30 (m, 2H), 2.72 (apparent td, *J* = 12.8, 3.0 Hz, 2H), 2.58 – 2.50 (m, 2H), 2.46 (s, 3H), 2.32 – 2.22 (m, 2H), 2.10 (apparent dd, *J* = 14.1, 3.2 Hz, 2H), 1.85 (apparent d, *J* = 8.8 Hz, 8H), 1.75 (d, *J* = 12.8 Hz, 2H), 1.51 – 1.37 (m, 8H), 1.36 – 1.25 (m, 2H).

**$^{13}$C{$^{1}$H} NMR (126 MHz, MeOD)** δ 163.6, 153.8, 149.9, 144.2, 141.5, 140.9, 132.3, 121.8, 119.0, 116.9, 111.6, 53.6, 44.4, 42.6, 34.3, 28.7, 26.5, 25.7, 10.1.

**IR (NaCl, thin film, cm$^{-1}$)**: 2926, 2852, 1677, 1590, 1572, 1449, 1430, 1310, 1248, 1201, 1180, 1139.

**HRMS (ESI-TOF)** *m/z* [M + H]$^{+}$ calcd for $C_{31}H_{42}N_5O^{+}$ 500.3384, found 500.3393.

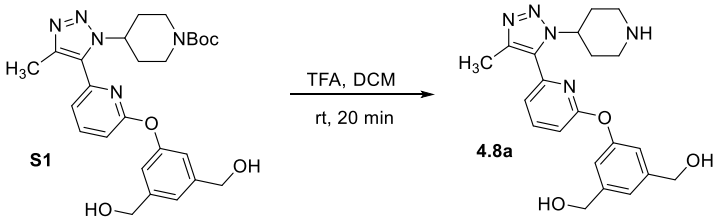


**Compound 4.8a**

To a solution of alcohol **S1** in DCM (1.0 mL) was added TFA (0.2 mL). The reaction was sealed under air at rt. After 20 min, the reaction was concentrated under reduced pressure. Final purification by column chromatography (5-50% MeOH in EtOAc with 1% TEA) afforded product **4.8a** (9.9 mg, 54%) as a white solid.

**$^{1}$H NMR (500 MHz, MeOD)** δ 8.01 (dd, *J* = 8.3, 7.4 Hz, 1H), 7.35 (d, *J* = 7.3 Hz, 1H), 7.22 (s, 1H), 7.14 (d, *J* = 8.3 Hz, 1H), 7.09 (s, 2H), 4.71 (tt, *J* = 11.4, 4.0 Hz, 1H), 4.65 (s, 4H), 2.96 (dt, *J* = 13.5, 3.6 Hz, 2H), 2.42 (s, 3H), 2.29 (td, *J* = 12.7, 2.7 Hz, 2H), 1.98 (apparent qd, *J* = 12.4, 4.2 Hz, 2H), 1.81 – 1.74 (m, 2H).

**$^{13}$C{$^{1}$H} NMR (126 MHz, MeOD)** δ 163.6, 154.2, 144.6, 143.8, 141.3, 140.8, 131.7, 121.0, 119.0, 118.2, 111.5, 63.1, 56.6, 44.3, 32.1, 10.1.

**IR (NaCl, thin film, cm$^{-1}$)**: 3294, 2923, 2852, 1641, 1590, 1572, 1451, 1429, 1298, 1246, 1191.

**HRMS (ESI-TOF)** *m/z* [M + H]$^{+}$ calcd for $C_{25}H_{30}N_5O^{+}$ 416.2445, found 416.2456.

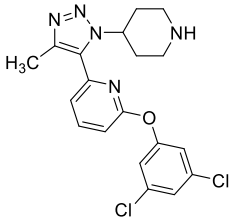

**Compound 4.8b**

General procedure **IV** was used and compound **4.8b** (15.7 mg, 76%) was isolated as a white solid. Analysis by $^{19}$F NMR with 2,2,2-trifluoroethanol as the internal standard indicated formation of a *mono*-TFA salt.

**$^{1}$H NMR (500 MHz, MeOD)** δ 8.09 (dd, *J* = 8.3, 7.4 Hz, 1H), 7.46 (d, *J* = 7.2 Hz, 1H), 7.40 (t, *J* = 1.8 Hz, 1H), 7.31 (d, *J* = 1.9 Hz, 2H), 7.23 (d, *J* = 8.1 Hz, 1H), 4.89 – 4.83 (m, 1H), 3.46 (dt, *J* = 13.1, 3.7 Hz, 2H), 2.95 – 2.84 (m, 2H), 2.44 (s, 3H), 2.39 – 2.27 (m, 2H), 2.11 – 2.02 (m, 2H).

**$^{13}$C{$^{1}$H} NMR (126 MHz, MeOD)** δ 162.8, 155.1, 144.2, 141.7, 141.5, 135.3, 132.1, 124.9, 120.9, 120.2, 112.0, 53.3, 42.6, 28.6, 9.9.

**IR (NaCl, thin film, cm$^{-1}$)**: 2968, 2730, 1680, 1577, 1425, 1247, 1202, 1134.

**HRMS (ESI-TOF)** *m/z* [M + Na]$^{+}$ calcd for $C_{19}H_{20}Cl_2N_5O^{+}$ 404.1039, found 404.1046.

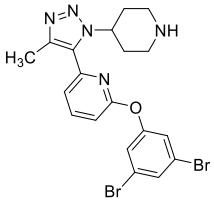

**Compound 4.8c**

General procedure **IV** was used and product **4.8c** (33.0 mg, quant.) was isolated as a white solid. Analysis by $^{19}$F NMR with 2,2,2-trifluoroethanol as the internal standard indicated formation of a *bis*-TFA salt.

**$^{1}$H NMR (500 MHz, MeOD)** δ 8.09 (dd, *J* = 8.3, 7.4 Hz, 1H), 7.68 (t, *J* = 1.7 Hz, 1H), 7.48 (d, *J* = 1.7 Hz, 2H), 7.46 (dd, *J* = 7.5, 0.7 Hz, 1H), 7.22 (dd, *J* = 8.4, 0.7 Hz, 1H), 4.89 – 4.83 (m, 1H), 3.47 (apparent dt, *J* = 13.1, 3.6 Hz, 2H), 2.90 (apparent td, *J* = 12.8, 3.0 Hz, 2H), 2.44 (s, 3H), 2.40 – 2.28 (m, 2H), 2.08 (apparent dd, *J* = 14.5, 4.0 Hz, 2H).

**$^{13}$C{$^{1}$H} NMR (126 MHz, MeOD)** δ 162.8, 155.1, 144.2, 141.8, 141.5, 132.1, 130.4, 124.2, 122.7, 120.2, 112.0, 53.3, 42.6, 28.6, 10.0.

**IR (NaCl, thin film, cm$^{-1}$)**: 2923, 2851, 1676, 1568, 1419, 1246, 1203, 1135.

**HRMS (ESI-TOF)** *m/z* [M + Na]$^{+}$ calcd for $C_{19}H_{19}Br_2N_5NaO^{+}$ 513.9849, found 513.9851.

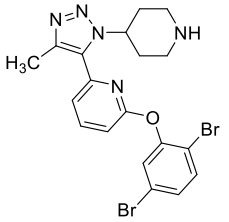

**Compound 4.7.1**

General procedure **IV** was used and compound **4.7.1** (24.1 mg, 80%) was isolated as a white solid. Analysis by $^{19}F$ NMR with 2,2,2-trifluoroethanol as the internal standard indicated formation of a *mono*-TFA salt.

**$^{1}$H NMR (500 MHz, MeOD)** δ 8.10 (dd, *J* = 8.3, 7.4 Hz, 1H), 7.67 (d, *J* = 8.6 Hz, 1H), 7.60 (d, *J* = 2.3 Hz, 1H), 7.45 – 7.41 (m, 2H), 7.26 (dd, *J* = 8.4, 0.7 Hz, 1H), 4.86 – 4.80 (m, 1H), 3.50 (dt, *J* = 13.5, 4.0 Hz, 2H), 3.01 – 2.91 (m, 2H), 2.41 (s, 3H), 2.35 – 2.25 (m, 2H), 2.03 – 1.97 (m, 2H).

**$^{13}$C{$^{1}$H} NMR (126 MHz, MeOD)** δ 162.6, 151.7, 144.0, 141.8, 141.5, 134.6, 132.1, 130.0, 127.5, 121.1, 119.9, 115.7, 111.6, 52.9, 42.6, 28.4, 9.8.

**IR (NaCl, thin film, cm$^{-1}$)**: 2985, 2848, 2740, 1676, 1567, 1466, 1428, 1388, 1203.

**HRMS (ESI-TOF)** *m/z* $[M + Na]^+$ calcd for $C_{19}H_{20}Br_2N_5O^+$ 492.0029, found 492.0019.

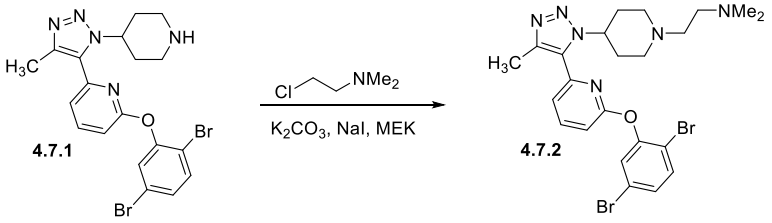


**Compound 4.7.2**

To a solution of compound **4.7.1** (183 mg, 0.302 mmol) in methyl ethyl ketone (6.0 mL) was added 2-chloro-*N*,*N*-dimethylethylamine (52.6 mg, 0.365 mmol), $K_2CO_3$ (136 mg, 0.986 mmol), and NaI (50.2 mg, 0.335 mmol). The reaction was sealed under air and heated to 40 °C. After 18 h, the reaction was cooled to rt and quenched by the addition of saturated aqueous $K_2CO_3$. The reaction mixture was extracted with EtOAc. The combined organic phases were washed with brine, dried ($Na_2SO_4$), and concentrated under reduced pressure. Final purification by column chromatography (10-50% MeOH in DCM) afforded compound **4.7.2** (11.8 mg, 7%) as a white solid.

**$^{1}$H NMR (500 MHz, MeOD)** δ 8.07 (apparent t, *J* = 7.9 Hz, 1H), 7.65 (d, *J* = 8.5 Hz, 1H), 7.54 (d, *J* = 2.3 Hz, 1H), 7.41 (dd, *J* = 8.6, 2.3 Hz, 1H), 7.38 (d, *J* = 7.4 Hz, 1H), 7.23 (d, *J* = 8.3 Hz, 1H), 4.49 (tt, *J* = 11.5, 4.2 Hz, 1H), 3.00 – 2.90 (m, 2H), 2.60 – 2.53 (m, 4H), 2.39 (s, 3H), 2.34 (s, 6H), 2.16 (apparent qd, *J* = 12.2, 3.6 Hz, 2H), 1.96 (td, *J* = 12.2, 2.4 Hz, 2H), 1.74 – 1.67 (m, 2H).

**$^{13}$C{$^{1}$H} NMR (126 MHz, MeOD)** δ 162.5, 151.6, 144.4, 141.5, 141.2, 134.7, 131.8, 129.9, 127.5, 121.1, 119.8, 115.7, 111.3, 56.5, 56.0, 55.2, 52.6, 44.4, 31.4, 9.8.

**IR (NaCl, thin film, cm$^{-1}$)**: 2922, 2850, 2816, 1596, 1581, 1565, 1463, 1427, 1384, 1296, 1241.

**HRMS (ESI-TOF)** *m/z* $[M + H]^+$ calcd for $C_{23}H_{29}Br_2N_6O^+$ 563.0764, found 563.0756.

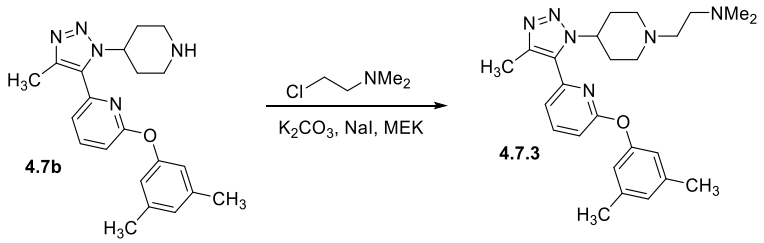


**Compound 4.7.3**

To a solution of compound **4.7b** (352 mg, 0.738 mmol) in methyl ethyl ketone (3.0 mL) was added 2-chloro-*N*,*N*-dimethylethylamine hydrochloride (117 mg, 0.815 mmol), $K_2CO_3$ (310 mg, 2.25 mmol), and NaI (125 mg, 0.834 mmol). The reaction was sealed under air and heated to 40 °C. After 18 h, the reaction was cooled to rt and quenched by the addition of saturated aqueous $K_2CO_3$. The reaction mixture was extracted with EtOAc. The combined organic phases were washed with brine, dried ($Na_2SO_4$), and concentrated under reduced pressure. Final purification by column chromatography (5-30% MeOH in DCM) afforded compound **4.7.3** (22.7 mg, 7%) as a white solid.

**$^1$H NMR (500 MHz, MeOD)** δ 7.99 (dd, *J* = 8.3, 7.4 Hz, 1H), 7.34 (d, *J* = 7.4 Hz, 1H), 7.09 (d, *J* = 8.3 Hz, 1H), 6.91 (s, 1H), 6.79 (s, 2H), 4.61 (tt, *J* = 11.7, 4.1 Hz, 1H), 2.85 (apparent d, *J* = 12.6 Hz, 2H), 2.56 – 2.46 (m, 4H), 2.43 (s, 3H), 2.34 (s, 6H), 2.33 (s, 6H), 2.13 (apparent qd, *J* = 12.3, 3.8 Hz, 2H), 1.78 – 1.70 (m, 4H).

**$^{13}$C{$^1$H} NMR (126 MHz, MeOD)** δ 163.6, 153.9, 144.6, 141.3, 140.7, 139.3, 131.9, 126.4, 119.1, 118.7, 111.5, 56.8, 56.1, 55.2, 52.5, 44.4, 31.4, 20.1, 10.1.

**IR (NaCl, thin film, cm$^{-1}$)**: 3428, 2954, 2829, 1682, 1589, 1573, 1432, 1301, 1210, 1181, 1135.

**HRMS (ESI-TOF)** *m/z* $[M + H]^+$ calcd for $C_{25}H_{35}N_6O^+$ 435.2867, found 435.2884.

## 4.6 References


(1) Filippakopoulos, P.; Knapp, S. The Bromodomain Interaction Module. *FEBS Lett.* **2012**, *586*, 2692–2704.

(2) Pervaiz, M.; Mishra, P.; Günther, S. Bromodomain Drug Discovery - the Past, the Present, and the Future. *Chem. Rec.* **2018**, *18*, 1808–1817.

(3) Gallinari, P.; Di Marco, S.; Jones, P.; Pallaoro, M.; Steinkühler, C. HDACs, Histone Deacetylation and Gene Transcription: From Molecular Biology to Cancer Therapeutics. *Cell Res.* **2007**, *17*, 195–211.

(4) Andrieu, G.; Belkina, A. C.; Denis, G. V. Clinical Trials for BET Inhibitors Run Ahead of the Science. *Drug Discov. Today Technol.* **2016**, *19*, 45–50.

(5) Bhattacharya, S.; Piya, S.; Borthakur, G. Bromodomain Inhibitors: What Does the Future Hold? *Clin. Adv. Hematol. Oncol.* **2018**, *16*, 504–515.

(6) Delmore, J. E.; Issa, G. C.; Lemieux, M. E.; Rahl, P. B.; Shi, J.-W.; Jacobs, H. M.; Kastritis, E.; Gilpatrick, T.; Paranal, R. M.; Qi, J.; Chesi, M.; Schinzel, A. C.; Mckeown, M. R.; Heffernan, T. P.; Vakoc, C. R.; Bergsagel, P. L.; Ghobrial, I. M.; Richardson, P. G.; Young, R. A.; Hahn, W. C.; Anderson, K. C.; Kung, A. L.; Bradner, J. E.; Mitsiades, C. S. BET Bromodomain Inhibition as a Therapeutic Strategy to Target C-Myc. *Cell* **2011**, *146*, 904–917.

(7) Andrieu, G.; Belkina, A. C.; Denis, G. V. Clinical Trials for BET Inhibitors Run Ahead of the Science. *Drug Discov. Today Technol.* **2016**, *19*, 45–50.

(8) Ember, S. W. J.; Zhu, J.-Y.; Olesen, S. H.; Martin, M. P.; Becker, A.; Berndt, N.; Georg, G. I.; Schonbrunn, E. Acetyl-Lysine Binding Site of Bromodomain-Containing Protein 4 (BRD4) Interacts with Diverse Kinase Inhibitors. *ACS Chem. Biol.* **2014**, *9*, 1160–1171.

(9) Carlino, L.; Rastelli, G. Dual Kinase-Bromodomain Inhibitors in Anticancer Drug Discovery: A Structural and Pharmacological Perspective. *J. Med. Chem.* **2016**, *59*, 9305–9320.

(10) Boehm, J. C.; Bower, M. J.; Gallagher, T. F.; Kassis, S.; Johnson, S. R.; Adams, J. L. Phenoxypyrimidine Inhibitors of P38α Kinase Synthesis and Statistical Evaluation of the P38 Inhibitory Potencies of a Series of 1-(Piperidin-4-Yl)-4-(4-Fluorophenyl)-5-(2-Phenoxypyrimidine-4-Yl) Imidazoles. *Bioorg. Med. Chem. Lett.* **2001**, *11*, 1123–1126.

(11) Ciceri, P.; Müller, S.; O'Mahony, A.; Fedorov, O.; Filippakopoulos, P.; Hunt, J. P.; Lasater, E. A.; Pallares, G.; Picaud, S.; Wells, C.; Martin, S.; Wodicka, L. M.; Shah, N. P.; Treiber, D. K.; Knapp, S. Dual Kinase-Bromodomain Inhibitors for Rationally Designed Polypharmacology. *Nat. Chem. Biol.* **2014**, *10*, 305–312.

(12) Martin, M. P.; Olesen, S. H.; Georg, G. I.; Schönbrunn, E. The Cyclin-Dependent Kinase Inhibitor Dinaciclib Interacts with the Acetyl-Lysine Recognition Site of Bromodomains. *ACS Chem. Biol.* **2013**, *8*, 2360–2365.

(13) Urick, A. K.; Hawk, L. M. L.; Cassel, M. K.; Mishra, N. K.; Liu, S.; Adhikari, N.; Zhang, W.; Dos Santos, C. O.; Hall, J. L.; Pomerantz, W. C. K. Dual Screening of BPTF and Brd4 Using Protein-Observed Fluorine NMR Uncovers New Bromodomain Probe Molecules. *ACS Chem. Biol.* **2015**, *10*, 2246–2256.

(14) Ember, S. W.; Lambert, Q. T.; Berndt, N.; Gunawan, S.; Ayaz, M.; Tauro, M.; Zhu, J.-Y.; Cranfill, P. J.; Greninger, P.; Lynch, C. C.; Benes, C. H.; Lawrence, H. R.; Reuther, G. W.; Lawrence, N. J.; Schönbrunn, E. Potent Dual BET Bromodomain-Kinase Inhibitors as Value-Added Multitargeted Chemical Probes and Cancer Therapeutics. *Mol. Cancer Ther.* **2017**, *16*, 1054–1067.

(15) Divakaran, A.; Talluri, S. K.; Ayoub, A. M.; Mishra, N.; Cui, H.; Widen, J. C.; Berndt, N.; Zhu, J.-Y.; Carlson, A. S.; Topczewski, J. J.; Schönbrunn, E.; Harki, D. A.; Pomerantz, W. C. K. Molecular Basis for the N-Terminal Bromodomain and Extra Terminal (BET) Family Selectivity of a Dual Kinase-Bromodomain Inhibitor. *J. Med. Chem.* **2018**, *61*, 9316–9334.

(16) Watts, E.; Heidenreich, D.; Tucker, E.; Raab, M.; Strebhardt, K.; Chesler, L.; Knapp, S.; Bellenie, B.; Hoelder, S. Designing Dual Inhibitors of Anaplastic Lymphoma Kinase (ALK) and Bromodomain-4 (BRD4) by Tuning Kinase Selectivity. *J. Med. Chem.* **2019**, *62*, 2618–2637.

(17) Chen, L.; Yap, J. L.; Yoshioka, M.; Lanning, M. E.; Fountain, R. N.; Raje, M.; Scheenstra, J. A.; Strovel, J. W.; Fletcher, S. BRD4 Structure-Activity Relationships of Dual PLK1 Kinase/BRD4 Bromodomain Inhibitor BI-2536. *ACS Med. Chem. Lett.* **2015**, *6*, 764–769.

(18) Filippakopoulos, P.; Picaud, S.; Mangos, M.; Keates, T.; Lambert, J. P.; Barsyte-Lovejoy, D.; Felletar, I.; Volkmer, R.; Müller, S.; Pawson, T.; Gingras, A. C.; Arrowsmith, C. H.; Knapp, S. Histone Recognition and Large-Scale Structural Analysis of the Human Bromodomain Family. *Cell* **2012**, *149*, 214–231.

(19) Matzuk, M. M.; McKeown, M. R.; Filippakopoulos, P.; Li, Q.; Ma, L.; Agno, J. E.; Lemieux, M. E.; Picaud, S.; Yu, R. N.; Qi, J.; Knapp, S.; Bradner, J. E. Small-Molecule Inhibition of BRDT for Male Contraception. *Cell* **2012**, *150*, 673–684.

(20) Ouyang, L.; Zhang, L.; Liu, J.; Fu, L.; Yao, D.; Zhao, Y.; Zhang, S.; Wang, G.; He, G.; Liu, B. Discovery of a Small-Molecule Bromodomain-Containing Protein 4 (BRD4) Inhibitor That Induces AMP-Activated Protein Kinase-Modulated Autophagy-Associated Cell Death in Breast Cancer. *J. Med. Chem.* **2017**, *60*, 9990–10012.

(21) Brand, M.; Measures, A. M.; Wilson, B. G.; Cortopassi, W. A.; Alexander, R.; Höss, M.; Hewings, D. S.; Rooney, T. P. C.; Paton, R. S.; Conway, S. J. Small Molecule Inhibitors of Bromodomain–Acetyl-Lysine Interactions. *ACS Chem. Biol.* **2015**, *10*, 22–39.

(22) Amorim, S.; Stathis, A.; Gleeson, M.; Iyengar, S.; Magarotto, V.; Leleu, X.; Morschhauser, F.; Karlin, L.; Broussais, F.; Rezai, K.; Herait, P.; Kahatt, C.; Lokiec, F.; Salles, G.; Facon, T.; Palumbo, A.; Cunningham, D.; Zucca, E.;

Thieblemont, C. Bromodomain Inhibitor OTX015 in Patients with Lymphoma or Multiple Myeloma: A Dose-Escalation, Open-Label, Pharmacokinetic, Phase 1 Study. *Lancet Haematol.* **2016**, *3*, 196–204.

(23) Aldeghi, M.; Ross, G. A.; Bodkin, M. J.; Essex, J. W.; Knapp, S.; Biggin, P. C. Large-Scale Analysis of Water Stability in Bromodomain Binding Pockets with Grand Canonical Monte Carlo. *Commun. Chem.* **2018**, *1*, 19.

(24) Bharatham, N.; Slavish, P. J.; Young, B. M.; Shelat, A. A. The Role of ZA Channel Water-Mediated Interactions in the Design of Bromodomain-Selective BET Inhibitors. *J. Mol. Graph. Model.* **2018**, *81*, 197–210.

(25) Baran, R. Essentials of Heterocyclic Chemistry - I. Heterocyclic Chemistry.

(26) Abboud, J. L. M.; Foces-Foces, C.; Notario, R.; Trifonov, R. E.; Volovodenko, A. P.; Ostrovskii, V. A.; Alkorta, I.; Elguero, J. Basicity of N-H- and N-Methyl-1,2,3-Triazoles in the Gas Phase, in Solution, and in the Solid State - An Experimental and Theoretical Study. *Eur. J. Org. Chem.* **2001**, *2001*, 3013–3024.

(27) Zhai, W.; Chapin, B. M.; Yoshizawa, A.; Wang, H.-C.; Hodge, S. A.; James, T. D.; Anslyn, E. V.; Fossey, J. S. "Click-Fluors": Triazole-Linked Saccharide Sensors. *Org. Chem. Front.* **2016**, *3*, 918–928.

(28) Sabat, M.; VanRens, J. C.; Clark, M. P.; Brugel, T. A.; Maier, J.; Bookland, R. G.; Laufersweiler, M. J.; Laughlin, S. K.; Golebiowski, A.; De, B.; Hsieh, L. C.; Walter, R. L.; Mekel, M. J.; Janusz, M. J. The Development of Novel C-2, C-8, and N-9 Trisubstituted Purines as Inhibitors of TNF-α Production. *Bioorganic Med. Chem. Lett.* **2006**, *16*, 4360–4365.

(29) Simard, J. R.; Getlik, M.; Grutter, C.; Pawar, V.; Wulfert, S.; Rabiller, M.; Rauh, D. Development of a Fluorescent-Tagged Kinase Assay System for the Detection and Characterization of Allosteric Kinase Inhibitors. *J. Am. Chem. Soc.* **2009**, *131*, 13286–13296.

(30) Townes, J. A.; Golebiowski, A.; Clark, M. P.; Laufersweiler, M. J.; Brugel, T. A.; Sabat, M.; Bookland, R. G.; Laughlin, S. K.; VanRens, J. C.; De, B.; Hsieh, L. C.; Xu, S. C.; Janusz, M. J.; Walter, R. L. The Development of New Bicyclic Pyrazole-Based Cytokine Synthesis Inhibitors. *Bioorganic Med. Chem. Lett.* **2004**, *14*, 4945–4948.

(31) Wang, Z.; Canagarajah, B. J.; Boehm, J. C.; Kassisa, S.; Cobb, M. H.; Young, P. R.; Abdel-Meguid, S.; Adams, J. L.; Goldsmith, E. J. Structural Basis of Inhibitor Selectivity in MAP Kinases. *Structure* **1998**, *6*, 1117–1128.

(32) Gallagher, T. F.; Seibel, G. L.; Kassis, S.; Laydon, J. T.; Blumenthal, M. J.; Lee, J. C.; Lee, D.; Boehm, J. C.; Fier-Thompson, S. M.; Abt, J. W.; Soreson, M. E.; Smietana, J. M.; Hall, R. F.; Garigipati, R. S.; Bender, P. E.; Erhard, K. F.; Krog, A. J.; Hofman, G. A.; Sheldrake, P. L.; McDonnell, P. C.; Kumar, S. K.; Young, P. R.; Adams, J. L. Regulation of Stress-Induced Cytokine Production by Pyridinylimidazoles; Inhibition of CSBP Kinase. *Bioorganic Med. Chem.* **1997**, *5*, 49–64.

(33) Meldal, M.; Tornøe, C. W. Cu-Catalyzed Azide−Alkyne Cycloaddition Cu-Catalyzed Azide-Alkyne Cycloaddition. *Chem. Rev.* **2008**, *108*, 2952–3015.

(34) Wu, Q.; Heidenreich, D.; Ackloo, S.; Krämer, A.; Nakka, K.; Lima-Fernandes, E.; Deblois, G.; Duan, S.; Vellanki, R. N.; Li, F.; Vedadi, M.; Dilworth, J.; Lupien, M.; Brennan, P. E.; Arrowsmith, C. H.; Muller, S.; Fedorov, O.; Filippakopoulos, P.; Knapp, S. A Chemical Toolbox for the Study of Bromodomains and Epigenetic Signaling. *Nat. Commun.* **2019**, *10*, 1915–1929.

(35) Brand, M.; Measures, A. R.; Wilson, B. G.; Cortopassi, W. A.; Alexander, R.; Höss, M.; Hewings, D. S.; Rooney, T. P. C.; Paton, R. S.; Conway, S. J. Small Molecule Inhibitors of Bromodomain-Acetyl-Lysine Interactions. *ACS Chem. Biol.* **2015**, *10*, 22–39.

(36) Dinér, P.; Andersson, T.; Kjellén, J.; Elbing, K.; Hohmann, S.; Grøtli, M. Short Cut to 1,2,3-Triazole-Based P38 MAP Kinase Inhibitors via [3+2]-Cycloaddition Chemistry. *New J. Chem.* **2009**, *33*, 1010–1016.

(37) Albrecht, B. K.; Gehling, V. S.; Hewitt, M. C.; Vaswani, R. G.; Côté, A.; Leblanc, Y.; Nasveschuk, C. G.; Bellon, S.; Bergeron, L.; Campbell, R.; Cantone, N.; Cooper, M. R.; Cummings, R. T.; Jayaram, H.; Joshi, S.; Mertz, J. A.; Neiss, A.; Normant, E.; O'Meara, M.; Pardo, E.; Poy, F.; Sandy, P.; Supko, J.; Sims, R. J.; Harmange, J. C.; Taylor, A. M.; Audia, J. E. Identification of a Benzoisoxazoloazepine Inhibitor (CPI-0610) of the Bromodomain and Extra-Terminal (BET) Family as a Candidate for Human Clinical Trials. *J. Med. Chem.* **2016**, *59*, 1330–1339.

(38) Gehling, V. S.; Hewitt, M. C.; Vaswani, R. G.; Leblanc, Y.; Côté, A.; Nasveschuk, C. G.; Taylor, A. M.; Harmange, J.-C.; Audia, J. E.; Pardo, E.; Joshi, S.; Sandy, P.; Mertz, J. A.; Robert J. Sims, I.; Bergeron, L.; Bryant, B. M.; Bellon, S.; Poy, F.; Jayaram, H.; Sankaranarayanan, R.; Yellapantula, S.; Srinivasamurthy, N. B.; Birudukota, S.; Albrecht, B. K. Discovery, Design, and Optimization of Isoxazole Azepine BET Inhibitors. *ACS Med. Chem. Lett.* **2013**, *4*, 835–840.

(39) Ayoub, A. M.; Hawk, L. M. L.; Herzig, R. J.; Jiang, J.; Wisniewski, A. J.; Gee, C. T.; Zhao, P.; Zhu, J.-Y.; Berndt, N.; Offei-Addo, N. K.; Scott, T. G.; Qi, J.; Bradner, J. E.; Ward, T. R.; Schönbrunn, E.; Georg, G. I.; Pomerantz, W. C. K. BET Bromodomain Inhibitors with One-Step Synthesis Discovered from Virtual Screen. *J. Med. Chem.* **2017**, *60*, 4805–4817.

(40) Pomerantz, W. C. K.; Cui, H.; Divakaran, A.; Pandey, A. K.; Johnson, J. A.; Zahid, H.; Hoell, Z. J.; Ellingson, M. O.; Shi, K.; Aihara, H.; Harki, D. A. Selective N-Terminal BET Bromodomain Inhibitors by Targeting Non-Conserved Residues and Structured Water Displacement. *Angew. Chem. Int. Ed.* **2020**, *Accepted*.

## Bibliography

### Chapter 1 References


(1) Vitaku, E.; Smith, D. T.; Njardarson, J. T. Analysis of the Structural Diversity, Substitution Patterns, and Frequency of Nitrogen Heterocycles among U.S. FDA Approved Pharmaceuticals. *J. Med. Chem.* **2014**, *57*, 10257–10274.

(2) Kwon, Y.; Jeon, M.; Park, J. Y.; Rhee, Y. H.; Park, J. Y. Synthesis of 1H-Azadienes and Application to One-Pot Organic Transformations. *RSC Adv.* **2016**, *6*, 661–668.

(3) Sá, M. M. Allylic Azides as Potential Building Blocks for the Synthesis of Nitrogenated Compounds. *J. Braz. Chem. Soc.* **2003**, *14*, 1005–1010.

(4) Wang, W. X.; Zhang, Q. Z.; Zhang, T. Q.; Li, Z. S.; Zhang, W.; Yu, W. N-Bromosuccinimide-Mediated Radical Cyclization of 3-Arylallyl Azides: Synthesis of 3-Substituted Quinolines. *Adv. Synth. Catal.* **2015**, *357*, 221–226.

(5) Zanatta, N.; Schneider, J. M. F. M.; Schneider, P. H.; Wouters, A. D.; Bonacorso, H. G.; Martins, M. A. P.; Wessjohann, L. A. Regiospecific Synthesis of 4-Alkoxy and 4-Amino Substituted 2-Trifluoromethyl Pyrroles. *J. Org. Chem.* **2006**, *71*, 6996–6998.

(6) Chandrasekhar, S.; Narsihmulu, C. Direct Conversion of Azides to Carbamates and Sulfonamides Using Fe/NH4Cl: Effect of Sonication. *Tetrahedron Lett.* **2000**, *41*, 7969–7972.

(7) Paraskar, A. S.; Sudalai, A. Co-Catalyzed Reductive Cyclization of Azido and Cyano Substituted α,β-Unsaturated Esters with NaBH4: Enantioselective Synthesis of (R)-Baclofen and (R)-Rolipram. *Tetrahedron* **2006**, *62*, 4907–4916.

(8) Ueda, M.; Uenoyama, Y.; Terasoma, N.; Doi, S.; Kobayashi, S.; Ryu, I.; Murphy, J. A. A Construction of 4,4-Spirocyclic γ-Lactams by Tandem Radical Cyclization with Carbon Monoxide. *Beilstein J. Org. Chem.* **2013**, *9*, 1340–1345.

(9) Fringuelli, F.; Pizzo, F.; Vaccaro, L. Cobalt(II) Chloride-Catalyzed Chemoselective Sodium Borohydride Reduction of Azides in Water. *Synthesis* **2000**, 646–650.

(10) Satyanarayana, N.; Periasamy, M. Hydroboration or Hydrogenation of Alkenes with CoCl2-NaBH4. *Tetrahedron Lett.* **1984**, *25*, 2501–2504.

(11) Tjeng, A. A. Stereoselective Synthesis of Nitrogen Containing Compounds from Hydroxy Allylic Azides. *Ph.D Diss. Univ. Toronto* **2011**.

(12) Yang, C.; Shen, H. One Pot Multiple-Steps Reactions of Allyl Azide and Alkenes

Carrying Electron-Withdrawing Groups. *Tetrahedron Lett.* **1993**, *34*, 4051–4054.

(13) Yang, C. H.; Lee, L. T.; Yang, J. H.; Wang, Y.; Lee, G. H. Spiropyrazolines from Tandem Reaction of Azides and Alkyl Vinyl Ketones. *Tetrahedron* **1994**, *50*, 12133–12142.

(14) Yang, C.-H.; Shen, H.-J.; Wang, R.-H.; Wang, J.-C. 2,3,7-Triazabicyclo[3.3.0]Octenes Prepared by Tandem Cascade Reaction of Allyl Azides and Olefinic Dipolarophiles. *J. Chinese Chem. Soc.* **2002**, *49*, 95–102.

(15) Tornøe, C. W.; Christensen, C.; Meldal, M. Peptidotriazoles on Solid Phase: [1,2,3]-Triazoles by Regiospecific Copper(I)-Catalyzed 1,3-Dipolar Cycloadditions of Terminal Alkynes to Azides. *J. Org. Chem.* **2002**, *67*, 3057–3064.

(16) Rostovtsev, V. V.; Green, L. G.; Fokin, V. V.; Sharpless, K. B. A Stepwise Huisgen Cycloaddition Process: Copper(I)-Catalyzed Regioselective "Ligation" of Azides and Terminal Alkynes. *Angew. Chem. Int. Ed.* **2002**, *41*, 2596–2599.

(17) Bonandi, E.; Christodoulou, M. S.; Fumagalli, G.; Perdicchia, D.; Rastelli, G.; Passarella, D. The 1,2,3-Triazole Ring as a Bioisostere in Medicinal Chemistry. *Drug Discov. Today* **2017**, *22*, 1572–1581.

(18) Sun, S.; Jia, Q.; Zhang, Z. Applications of Amide Isosteres in Medicinal Chemistry. *Bioorganic Med. Chem. Lett.* **2019**, *29*, 2535–2550.

(19) Filippakopoulos, P.; Picaud, S.; Mangos, M.; Keates, T.; Lambert, J. P.; Barsyte-Lovejoy, D.; Felletar, I.; Volkmer, R.; Müller, S.; Pawson, T.; Gingras, A. C.; Arrowsmith, C. H.; Knapp, S. Histone Recognition and Large-Scale Structural Analysis of the Human Bromodomain Family. *Cell* **2012**, *149*, 214–231.

(20) Filippakopoulos, P.; Qi, J.; Picaud, S.; Shen, Y.; Smith, W. B.; Fedorov, O.; Morse, E. M.; Keates, T.; Hickman, T. T.; Felletar, I.; Philpott, M.; Munro, S.; McKeown, M. R.; Wang, Y.; Christie, A. L.; West, N.; Cameron, M. J.; Schwartz, B.; Heightman, T. D.; La Thangue, N.; French, C. a; Wiest, O.; Kung, A. L.; Knapp, S.; Bradner, J. E. Selective Inhibition of BET Bromodomains. *Nature* **2010**, *468*, 1067–1073.

(21) Urick, A. K.; Hawk, L. M. L.; Cassel, M. K.; Mishra, N. K.; Liu, S.; Adhikari, N.; Zhang, W.; Dos Santos, C. O.; Hall, J. L.; Pomerantz, W. C. K. Dual Screening of BPTF and Brd4 Using Protein-Observed Fluorine NMR Uncovers New Bromodomain Probe Molecules. *ACS Chem. Biol.* **2015**, *10*, 2246–2256.

(22) Divakaran, A.; Talluri, S. K.; Ayoub, A. M.; Mishra, N.; Cui, H.; Widen, J. C.; Berndt, N.; Zhu, J.-Y.; Carlson, A. S.; Topczewski, J. J.; Schönbrunn, E.; Harki, D. A.; Pomerantz, W. C. K. Molecular Basis for the N-Terminal Bromodomain and

Extra Terminal (BET) Family Selectivity of a Dual Kinase-Bromodomain Inhibitor. *J. Med. Chem.* **2018**, *61*, 9316–9334.

**Chapter 2 References**

(1) Phillips, F. C. Researches upon the Phenomena of Oxidation and Chemical Properties of Gases. *Am. Chem. J.* **1894**, *16*, 255–277.

(2) Jira, R. Acetaldehyde from Ethylene - A Retrospective on the Discovery of the Wacker Process. *Angew. Chem. Int. Ed.* **2009**, *48*, 9034–9037.

(3) Smidt, J.; Hafner, W.; Jira, R.; Sedlmeier, F.; Sieber, R.; Kojer, H.; Juttinger, R. Catalytic Reactions of Olefins on Compounds of the Platinum Group. *Angew. Chem.* **1959**, *71*, 176.

(4) Eckert, M.; Fleischmann, G.; Jira, R.; Bolt, H.; Golka, K. Acetaldehyde. *Ullman's Encycl. Ind. Chem.* **2012**, *1*, 191–205.

(5) Keith, J. A.; Henry, P. M. The Mechanism of the Wacker Reaction: A Tale of Two Hydroxypalladations. *Angew. Chem. Int. Ed.* **2009**, *48*, 9038–9049.

(6) Kurti, L.; Czako, B. *Strategic Applications of Named Reactions in Organic Synthesis*; 2005.

(7) Makabe, H.; Kong, L. K.; Hirota, M. Total Synthesis of (-)-Cassine. *Org. Lett.* **2003**, *5*, 27–29.

(8) Wickens, Z. K.; Morandi, B.; Grubbs, R. H. Aldehyde-Selective Wacker-Type Oxidation of Unbiased Alkenes Enabled by a Nitrite Co-Catalyst. *Angew. Chem. Int. Ed.* **2013**, *52*, 11257–11260.

(9) Morandi, B.; Wickens, Z. K.; Grubbs, R. H. Regioselective Wacker Oxidation of Internal Alkenes: Rapid Access to Functionalized Ketones Facilitated by Cross-Metathesis. *Angew. Chem. Int. Ed.* **2013**, *52*, 9751–9754.

(10) Choi, P. J.; Sperry, J.; Brimble, M. A. Heteroatom-Directed Reverse Wacker Oxidations. Synthesis of the Reported Structure of (-)-Herbaric Acid. *J. Org. Chem.* **2010**, *75*, 7388–7392.

(11) Deluca, R. J.; Edwards, J. L.; Steffens, L. D.; Michel, B. W.; Qiao, X.; Zhu, C.; Cook, S. P.; Sigman, M. S. Wacker-Type Oxidation of Internal Alkenes Using Pd(Quinox) and TBHP. *J. Org. Chem.* **2013**, *78*, 1682–1686.

(12) Lerch, M. M.; Morandi, B.; Wickens, Z. K.; Grubbs, R. H. Rapid Access to β-Trifluoromethyl-Substituted Ketones: Harnessing Inductive Effects in Wacker-Type Oxidations of Internal Alkenes. *Angew. Chem. Int. Ed.* **2014**, *53*, 8654–8658.

(13) Carlson, A. S.; Calcanas, C.; Brunner, R. M.; Topczewski, J. J. Regiocontrolled Wacker Oxidation of Cinnamyl Azides. *Org. Lett.* **2018**, *20*, 1604–1607.

(14) Bräse, S.; Gil, C.; Knepper, K.; Zimmermann, V. Organic Azides: An Exploding Diversity of a Unique Class of Compounds. *Angew. Chem. Int. Ed.* **2005**, *44*,

5188–5240.

(15) Gagneux, A.; Winstein, S.; Young, W. G. Rearrangement of Allyl Azides. *J. Am. Chem. Soc.* **1960**, *82*, 5956–5957.

(16) Carlson, A. S.; Topczewski, J. J. Allylic Azides: Synthesis, Reactivity, and the Winstein Rearrangement. *Org. Biomol. Chem.* **2019**, *17*, 4406–4429.

(17) Goswami, P. P.; Suding, V. P.; Carlson, A. S.; Topczewski, J. J. Direct Conversion of Aldehydes and Ketones into Azides by Sequential Nucleophilic Addition and Substitution. *Eur. J. Org. Chem.* **2016**, 4805–4809.

(18) Giovani, S.; Singh, R.; Fasan, R. Efficient Conversion of Primary Azides to Aldehydes Catalyzed by Active Site Variants of Myoglobin. *Chem. Sci.* **2016**, *7*, 234–239.

(19) Barragan, E.; Bugarin, A. π-Conjugated Triazenes: Intermediates That Undergo Oxidation and Substitution Reactions. *J. Org. Chem.* **2017**, *82*, 1499–1506.

(20) Collins, K. D.; Glorius, F. A Robustness Screen for the Rapid Assessment of Chemical Reactions. *Nat. Chem.* **2013**, *5*, 597–601.

(21) Gensch, T.; Teders, M.; Glorius, F. Approach to Comparing the Functional Group Tolerance of Reactions. *J. Org. Chem.* **2017**, *82*, 9154–9159.

(22) Packard, M. H.; Cox, J. H.; Suding, V. P.; Topczewski, J. J. The Effect of Proximal Functionality on the Allylic Azide Equilibrium. *Eur. J. Org. Chem.* **2017**, *2017*, 6365–6368.

**Chapter 3 References**

(1) Vitaku, E.; Smith, D. T.; Njardarson, J. T. Analysis of the Structural Diversity, Substitution Patterns, and Frequency of Nitrogen Heterocycles among U.S. FDA Approved Pharmaceuticals. *J. Med. Chem.* **2014**, *57*, 10257–10274.

(2) Wang, Y.-Y.; Bode, J. W. Olefin Amine (OLA) Reagents for the Synthesis of Bridged Bicyclic and Spirocyclic Saturated N-Heterocycles by Catalytic Hydrogen Atom Transfer (HAT) Reactions. *J. Am. Chem. Soc.* **2019**, *141*, 9739–9745.

(3) Lovering, F.; Bikker, J.; Humblet, C. Escape from Flatland: Increasing Saturation as an Approach to Improving Clinical Success. *J. Med. Chem.* **2009**, *52*, 6752–6756.

(4) Lovering, F. Escape from Flatland 2: Complexity and Promiscuity. *Med. Chem. Commun.* **2013**, *4*, 515–519.

(5) Meanwell, N. A. Improving Drug Design: An Update on Recent Applications of Efficiency Metrics, Strategies for Replacing Problematic Elements, and Compounds in Nontraditional Drug Space. *Chem. Res. Toxicol.* **2016**, *29*, 564–

616.

(6) Ritchie, T. J.; MacDonald, S. J. F.; Young, R. J.; Pickett, S. D. The Impact of Aromatic Ring Count on Compound Developability: Further Insights by Examining Carbo- and Hetero-Aromatic and -Aliphatic Ring Types. *Drug Discov. Today* **2011**, *16*, 164–171.

(7) Orr, S. T. M.; Ripp, S. L.; Ballard, T. E.; Henderson, J. L.; Scott, D. O.; Obach, R. S.; Sun, H.; Kalgutkar, A. S. Mechanism-Based Inactivation (MBI) of Cytochrome P450 Enzymes: Structure–Activity Relationships and Discovery Strategies To Mitigate Drug–Drug Interaction Risks. *J. Med. Chem.* **2012**, *55*, 4896–4933.

(8) Campos, K. R.; Coleman, P. J.; Alvarez, J. C.; Dreher, S. D.; Garbaccio, R. M.; Terrett, N. K.; Tillyer, R. D.; Truppo, M. D.; Parmee, E. R. The Importance of Synthetic Chemistry in the Pharmaceutical Industry. *Science* **2019**, *363*, 244–252.

(9) Levin, J. I.; Venkatesan, A. M.; Chan, P. S.; Bailey, T. K.; Vice, G.; Coupet, J. 6-Substituted Quinazolinone Angiotensin II Receptor Antagonists. *Bioorg. Med. Chem. Lett.* **1994**, *4*, 1819–1824.

(10) Møllerud, S.; Pinto, A.; Marconi, L.; Frydenvang, K.; Thorsen, T. S.; Laulumaa, S.; Venskutonyte, R.; Winther, S.; Moral, A. M. C.; Tamborini, L.; Conti, P.; Pickering, D. S.; Kastrup, J. S. Structure and Affinity of Two Bicyclic Glutamate Analogues at AMPA and Kainate Receptors. *ACS Chem. Neurosci.* **2017**, *8*, 2056–2064.

(11) Liu, G.-N.; Luo, R.-H.; Zhou, Y.; Zhang, X.-J.; Li, J.; Yang, L.-M.; Zheng, Y.-T.; Liu, H. Synthesis and Anti-HIV-1 Activity Evaluation for Novel 3a,6a-Dihydro-1H-Pyrrolo[3,4-c]Pyrazole-4,6-Dione Derivatives. *Molecules* **2016**, *21*, 1198.

(12) Chen, P.; Feng, D.; Qian, X.; Apgar, J.; Wilkening, R.; Kuethe, J. T.; Gao, Y. D.; Scapin, G.; Cox, J.; Doss, G.; Eiermann, G.; He, H.; Li, X.; Lyons, K. A.; Metzger, J.; Petrov, A.; Wu, J. K.; Xu, S.; Weber, A. E.; Yan, Y.; Roy, R. S.; Biftu, T. Structure-Activity-Relationship of Amide and Sulfonamide Analogs of Omarigliptin. *Bioorganic Med. Chem. Lett.* **2015**, *25*, 5767–5771.

(13) Deaton, D. N.; Haffner, C. D.; Henke, B. R.; Jeune, M. R.; Shearer, B. G.; Stewart, E. L.; Stuart, J. D.; Ulrich, J. C. 2,4-Diamino-8-Quinazoline Carboxamides as Novel, Potent Inhibitors of the NAD Hydrolyzing Enzyme CD38: Exploration of the 2-Position Structure-Activity Relationships. *Bioorganic Med. Chem.* **2018**, *26*, 2107–2150.

(14) Quiclet-Sire, B.; Zard, S. Z. Observations on the Reaction of Hydrazones with Iodine: Interception of the Diazo Intermediates. *Chem. Commun.* **2006**, 1831–1832.

(15) Kapras, V.; Pohl, R.; Císařová, I.; Jahn, U. Asymmetric Domino Aza-Michael Addition/[3+2] Cycloaddition Reactions as a Versatile Approach to α,β,γ-Triamino Acid Derivatives. *Org. Lett.* **2014**, *16*, 1088–1091.

(16) Just, D.; Hernandez-Guerra, D.; Kritsch, S.; Pohl, R.; Císařová, I.; Jones, P. G.; Mackman, R.; Bahador, G.; Jahn, U. Lithium Chloride Catalyzed Asymmetric Domino Aza-Michael Addition/[3+2] Cycloaddition Reactions for the Synthesis of Spiro- and Bicyclic α,β,γ-Triamino Acid Derivatives. *Eur. J. Org. Chem.* **2018**, 5213–5221.

(17) Yang, C.-H.; Sherf, H.-J.; Wang, R.-H.; Wang, J.-C. 2,3,7-Triazabicyclo[3.3.0]Octenes Prepared by Tandem Cascade Reaction of Allyl Azides and Olefinic Dipolarophiles. *J. Chin. Chem. Soc.* **2002**, *49*, 95–102.

(18) Yang, C.; Shen, H. One Pot Multiple-Steps Reactions of Allyl Azide and Alkenes Carrying Electron-Withdrawing Groups. *Tetrahedron Lett.* **1993**, *34*, 4051–4054.

(19) Herdeis, C.; Schiffer, T. Synthesis of Nonracemic 2,3,6-Trisubstituted Piperidine Derivatives from Sugar Lactones via Tandem Wittig [2+3] Cycloaddition Reaction. A Novel Entry to Prosopis and Cassia Alkaloids. *Tetrahedron* **1999**, *55*, 1043–1056.

(20) Broeckx, W.; Overbergh, N.; Samyn, C.; Smets, G.; L'abbé, G. Cycloaddition Reactions of Azides with Electron-Poor Olefins. *Tetrahedron* **1971**, *27*, 3527–3534.

(21) L'abbé, G. Decomposition and Addition Reactions of Organic Azides. *Chem. Rev.* **1969**, *69*, 345–363.

(22) Yang, C.-H.; Shen, H.-J.; Wang, R.-H.; Wang, J.-C. 2,3,7-Triazabicyclo[3.3.0]Octenes Prepared by Tandem Cascade Reaction of Allyl Azides and Olefinic Dipolarophiles. *J. Chinese Chem. Soc.* **2002**, *49*, 95–102.

(23) Huisgen, R. Proceedings of the Chemical Society. October 1961. *Proc. Chem. Soc.* **1961**, 357–396.

(24) Huisgen, R.; Szeimies, G.; Möbius, L. 1.3-Dipolar Cycloadditions. XXXII. Kinetics of the Addition of Organic Azides to Carbon-Carbon Multiple Bonds. *Chem. Ber.* **1967**, *100*, 2494–2507.

(25) Liddon, J. T. R.; Lindsay-Scott, P. J.; Robertson, J. Secondary Products from Intramolecular Cycloadditions of Azidoalkyl Enol Ethers and Azidoalkyl Vinyl Bromides: 1-Azadienes, Their Reactions with Diphenylketene, and Radical Cyclizations To Form Bi- and Tricyclic Lactams. *J. Org. Chem.* **2019**, *84*, 13780–13793.

(26) Xie, S.; Lopez, S. A.; Ramström, O.; Yan, M.; Houk, K. N. 1,3-Dipolar Cycloaddition Reactivities of Perfluorinated Aryl Azides with Enamines and Strained Dipolarophiles. *J. Am. Chem. Soc.* **2015**, *137*, 2958–2966.

(27) Krivopalov, V. P.; Shkurko, O. P. 1,2,3-Triazole and Its Derivatives. Development of Methods for the Formation of the Triazole Ring. *Russ. Chem. Rev.* **2005**, *74*, 339–379.

(28) Yang, C. H.; Lee, L. T.; Yang, J. H.; Wang, Y.; Lee, G. H. Spiropyrazolines from Tandem Reaction of Azides and Alkyl Vinyl Ketones. *Tetrahedron* **1994**, *50*, 12133–12142.

(29) Teng, J.-T.; Yang, C.-H. A Stereoselective Preparation of 1,2,7-Triazabicyclo[3.3.0]Oct-2-Enes. *J. Chinese Chem. Soc.* **1998**, *45*, 375–380.

(30) Hamadi, N. Ben; Louhichi, N.; Msaddek, M. Synthesis and Photolysis of Hexahydropyrrolo [3,4-c] Pyrazole Derivatives. *J. Chem. Res.* **2007**, *10*, 569–571.

(31) Gagneux, A.; Winstein, S.; Young, W. G. Rearrangement of Allyl Azides. *J. Am. Chem. Soc.* **1960**, *82*, 5956–5957.

(32) Carlson, A. S.; Topczewski, J. J. Allylic Azides: Synthesis, Reactivity, and the Winstein Rearrangement. *Org. Biomol. Chem.* **2019**, *17*, 4406–4429.

(33) Ott, A. A.; Packard, M. H.; Ortuño, M. A.; Johnson, A.; Suding, V. P.; Cramer, C. J.; Topczewski, J. J. Evidence for a Sigmatropic and an Ionic Pathway in the Winstein Rearrangement. *J. Org. Chem.* **2018**, *83*, 8214–8224.

(34) Nugent, T. C. *Chiral Amine Synthesis: Methods, Developments and Applications*, 1st ed.; Wiley, 2010.

(35) Carlson, A. S.; Liu, E.-C.; Topczewski, J. J. A Cascade Reaction of Cinnamyl Azides with Acrylates Directly Generates Tetrahydro-Pyrrolo-Pyrazole Heterocycles. *J. Org. Chem.* **2020**, 85, 6044-6059.

(36) Carlson, A. S.; Petre, A. M.; Topczewski, J. J. A Cascade Reaction of Cinnamyl Azides with Vinyl Sulfones Directly Generates Dihydro-Pyrrolo-Pyrazole Heterocycles. *Submitted*.

**Chapter 4 References**

(1) Filippakopoulos, P.; Knapp, S. The Bromodomain Interaction Module. *FEBS Lett.* **2012**, *586*, 2692–2704.

(2) Pervaiz, M.; Mishra, P.; Günther, S. Bromodomain Drug Discovery - the Past, the Present, and the Future. *Chem. Rec.* **2018**, *18*, 1808–1817.

(3) Gallinari, P.; Di Marco, S.; Jones, P.; Pallaoro, M.; Steinkühler, C. HDACs, Histone Deacetylation and Gene Transcription: From Molecular Biology to Cancer Therapeutics. *Cell Res.* **2007**, *17*, 195–211.

(4) Andrieu, G.; Belkina, A. C.; Denis, G. V. Clinical Trials for BET Inhibitors Run Ahead of the Science. *Drug Discov. Today Technol.* **2016**, *19*, 45–50.

(5) Bhattacharya, S.; Piya, S.; Borthakur, G. Bromodomain Inhibitors: What Does the Future Hold? *Clin. Adv. Hematol. Oncol.* **2018**, *16*, 504–515.

(6) Delmore, J. E.; Issa, G. C.; Lemieux, M. E.; Rahl, P. B.; Shi, J.-W.; Jacobs, H. M.; Kastritis, E.; Gilpatrick, T.; Paranal, R. M.; Qi, J.; Chesi, M.; Schinzel, A. C.; Mckeown, M. R.; Heffernan, T. P.; Vakoc, C. R.; Bergsagel, P. L.; Ghobrial, I. M.; Richardson, P. G.; Young, R. A.; Hahn, W. C.; Anderson, K. C.; Kung, A. L.; Bradner, J. E.; Mitsiades, C. S. BET Bromodomain Inhibition as a Therapeutic Strategy to Target C-Myc. *Cell* **2011**, *146*, 904–917.

(7) Andrieu, G.; Belkina, A. C.; Denis, G. V. Clinical Trials for BET Inhibitors Run Ahead of the Science. *Drug Discov. Today Technol.* **2016**, *19*, 45–50.

(8) Ember, S. W. J.; Zhu, J.-Y.; Olesen, S. H.; Martin, M. P.; Becker, A.; Berndt, N.; Georg, G. I.; Schonbrunn, E. Acetyl-Lysine Binding Site of Bromodomain-Containing Protein 4 (BRD4) Interacts with Diverse Kinase Inhibitors. *ACS Chem. Biol.* **2014**, *9*, 1160–1171.

(9) Carlino, L.; Rastelli, G. Dual Kinase-Bromodomain Inhibitors in Anticancer Drug Discovery: A Structural and Pharmacological Perspective. *J. Med. Chem.* **2016**, *59*, 9305–9320.

(10) Boehm, J. C.; Bower, M. J.; Gallagher, T. F.; Kassis, S.; Johnson, S. R.; Adams, J. L. Phenoxypyrimidine Inhibitors of P38α Kinase Synthesis and Statistical Evaluation of the P38 Inhibitory Potencies of a Series of 1-(Piperidin-4-Yl)-4-(4-Fluorophenyl)-5-(2-Phenoxypyrimidine-4-Yl) Imidazoles. *Bioorg. Med. Chem. Lett.* **2001**, *11*, 1123–1126.

(11) Ciceri, P.; Müller, S.; O'Mahony, A.; Fedorov, O.; Filippakopoulos, P.; Hunt, J. P.; Lasater, E. A.; Pallares, G.; Picaud, S.; Wells, C.; Martin, S.; Wodicka, L. M.; Shah, N. P.; Treiber, D. K.; Knapp, S. Dual Kinase-Bromodomain Inhibitors for Rationally Designed Polypharmacology. *Nat. Chem. Biol.* **2014**, *10*, 305–312.

(12) Martin, M. P.; Olesen, S. H.; Georg, G. I.; Schönbrunn, E. The Cyclin-Dependent Kinase Inhibitor Dinaciclib Interacts with the Acetyl-Lysine Recognition Site of Bromodomains. *ACS Chem. Biol.* **2013**, *8*, 2360–2365.

(13) Urick, A. K.; Hawk, L. M. L.; Cassel, M. K.; Mishra, N. K.; Liu, S.; Adhikari, N.; Zhang, W.; Dos Santos, C. O.; Hall, J. L.; Pomerantz, W. C. K. Dual Screening of BPTF and Brd4 Using Protein-Observed Fluorine NMR Uncovers New Bromodomain Probe Molecules. *ACS Chem. Biol.* **2015**, *10*, 2246–2256.

(14) Ember, S. W.; Lambert, Q. T.; Berndt, N.; Gunawan, S.; Ayaz, M.; Tauro, M.; Zhu, J.-Y.; Cranfill, P. J.; Greninger, P.; Lynch, C. C.; Benes, C. H.; Lawrence, H.

R.; Reuther, G. W.; Lawrence, N. J.; Schönbrunn, E. Potent Dual BET Bromodomain-Kinase Inhibitors as Value-Added Multitargeted Chemical Probes and Cancer Therapeutics. *Mol. Cancer Ther.* **2017**, *16*, 1054–1067.

(15) Divakaran, A.; Talluri, S. K.; Ayoub, A. M.; Mishra, N.; Cui, H.; Widen, J. C.; Berndt, N.; Zhu, J.-Y.; Carlson, A. S.; Topczewski, J. J.; Schönbrunn, E.; Harki, D. A.; Pomerantz, W. C. K. Molecular Basis for the N-Terminal Bromodomain and Extra Terminal (BET) Family Selectivity of a Dual Kinase-Bromodomain Inhibitor. *J. Med. Chem.* **2018**, *61*, 9316–9334.

(16) Watts, E.; Heidenreich, D.; Tucker, E.; Raab, M.; Strebhardt, K.; Chesler, L.; Knapp, S.; Bellenie, B.; Hoelder, S. Designing Dual Inhibitors of Anaplastic Lymphoma Kinase (ALK) and Bromodomain-4 (BRD4) by Tuning Kinase Selectivity. *J. Med. Chem.* **2019**, *62*, 2618–2637.

(17) Chen, L.; Yap, J. L.; Yoshioka, M.; Lanning, M. E.; Fountain, R. N.; Raje, M.; Scheenstra, J. A.; Strovel, J. W.; Fletcher, S. BRD4 Structure-Activity Relationships of Dual PLK1 Kinase/BRD4 Bromodomain Inhibitor BI-2536. *ACS Med. Chem. Lett.* **2015**, *6*, 764–769.

(18) Filippakopoulos, P.; Picaud, S.; Mangos, M.; Keates, T.; Lambert, J. P.; Barsyte-Lovejoy, D.; Felletar, I.; Volkmer, R.; Müller, S.; Pawson, T.; Gingras, A. C.; Arrowsmith, C. H.; Knapp, S. Histone Recognition and Large-Scale Structural Analysis of the Human Bromodomain Family. *Cell* **2012**, *149*, 214–231.

(19) Matzuk, M. M.; McKeown, M. R.; Filippakopoulos, P.; Li, Q.; Ma, L.; Agno, J. E.; Lemieux, M. E.; Picaud, S.; Yu, R. N.; Qi, J.; Knapp, S.; Bradner, J. E. Small-Molecule Inhibition of BRDT for Male Contraception. *Cell* **2012**, *150*, 673–684.

(20) Ouyang, L.; Zhang, L.; Liu, J.; Fu, L.; Yao, D.; Zhao, Y.; Zhang, S.; Wang, G.; He, G.; Liu, B. Discovery of a Small-Molecule Bromodomain-Containing Protein 4 (BRD4) Inhibitor That Induces AMP-Activated Protein Kinase-Modulated Autophagy-Associated Cell Death in Breast Cancer. *J. Med. Chem.* **2017**, *60*, 9990–10012.

(21) Brand, M.; Measures, A. M.; Wilson, B. G.; Cortopassi, W. A.; Alexander, R.; Höss, M.; Hewings, D. S.; Rooney, T. P. C.; Paton, R. S.; Conway, S. J. Small Molecule Inhibitors of Bromodomain–Acetyl-Lysine Interactions. *ACS Chem. Biol.* **2015**, *10*, 22–39.

(22) Amorim, S.; Stathis, A.; Gleeson, M.; Iyengar, S.; Magarotto, V.; Leleu, X.; Morschhauser, F.; Karlin, L.; Broussais, F.; Rezai, K.; Herait, P.; Kahatt, C.; Lokiec, F.; Salles, G.; Facon, T.; Palumbo, A.; Cunningham, D.; Zucca, E.; Thieblemont, C. Bromodomain Inhibitor OTX015 in Patients with Lymphoma or Multiple Myeloma: A Dose-Escalation, Open-Label, Pharmacokinetic, Phase 1 Study. *Lancet Haematol.* **2016**, *3*, 196–204.

(23) Aldeghi, M.; Ross, G. A.; Bodkin, M. J.; Essex, J. W.; Knapp, S.; Biggin, P. C. Large-Scale Analysis of Water Stability in Bromodomain Binding Pockets with Grand Canonical Monte Carlo. *Commun. Chem.* **2018**, *1*, 19.

(24) Bharatham, N.; Slavish, P. J.; Young, B. M.; Shelat, A. A. The Role of ZA Channel Water-Mediated Interactions in the Design of Bromodomain-Selective BET Inhibitors. *J. Mol. Graph. Model.* **2018**, *81*, 197–210.

(25) Baran, R. Essentials of Heterocyclic Chemistry - I. Heterocyclic Chemistry.

(26) Abboud, J. L. M.; Foces-Foces, C.; Notario, R.; Trifonov, R. E.; Volovodenko, A. P.; Ostrovskii, V. A.; Alkorta, I.; Elguero, J. Basicity of N-H- and N-Methyl-1,2,3-Triazoles in the Gas Phase, in Solution, and in the Solid State - An Experimental and Theoretical Study. *Eur. J. Org. Chem.* **2001**, *2001*, 3013–3024.

(27) Zhai, W.; Chapin, B. M.; Yoshizawa, A.; Wang, H.-C.; Hodge, S. A.; James, T. D.; Anslyn, E. V.; Fossey, J. S. "Click-Fluors": Triazole-Linked Saccharide Sensors. *Org. Chem. Front.* **2016**, *3*, 918–928.

(28) Sabat, M.; VanRens, J. C.; Clark, M. P.; Brugel, T. A.; Maier, J.; Bookland, R. G.; Laufersweiler, M. J.; Laughlin, S. K.; Golebiowski, A.; De, B.; Hsieh, L. C.; Walter, R. L.; Mekel, M. J.; Janusz, M. J. The Development of Novel C-2, C-8, and N-9 Trisubstituted Purines as Inhibitors of TNF-α Production. *Bioorganic Med. Chem. Lett.* **2006**, *16*, 4360–4365.

(29) Simard, J. R.; Getlik, M.; Grutter, C.; Pawar, V.; Wulfert, S.; Rabiller, M.; Rauh, D. Development of a Fluorescent-Tagged Kinase Assay System for the Detection and Characterization of Allosteric Kinase Inhibitors. *J. Am. Chem. Soc.* **2009**, *131*, 13286–13296.

(30) Townes, J. A.; Golebiowski, A.; Clark, M. P.; Laufersweiler, M. J.; Brugel, T. A.; Sabat, M.; Bookland, R. G.; Laughlin, S. K.; VanRens, J. C.; De, B.; Hsieh, L. C.; Xu, S. C.; Janusz, M. J.; Walter, R. L. The Development of New Bicyclic Pyrazole-Based Cytokine Synthesis Inhibitors. *Bioorganic Med. Chem. Lett.* **2004**, *14*, 4945–4948.

(31) Wang, Z.; Canagarajah, B. J.; Boehm, J. C.; Kassisa, S.; Cobb, M. H.; Young, P. R.; Abdel-Meguid, S.; Adams, J. L.; Goldsmith, E. J. Structural Basis of Inhibitor Selectivity in MAP Kinases. *Structure* **1998**, *6*, 1117–1128.

(32) Gallagher, T. F.; Seibel, G. L.; Kassis, S.; Laydon, J. T.; Blumenthal, M. J.; Lee, J. C.; Lee, D.; Boehm, J. C.; Fier-Thompson, S. M.; Abt, J. W.; Soreson, M. E.; Smietana, J. M.; Hall, R. F.; Garigipati, R. S.; Bender, P. E.; Erhard, K. F.; Krog, A. J.; Hofman, G. A.; Sheldrake, P. L.; McDonnell, P. C.; Kumar, S. K.; Young, P. R.; Adams, J. L. Regulation of Stress-Induced Cytokine Production by Pyridinylimidazoles; Inhibition of CSBP Kinase. *Bioorganic Med. Chem.* **1997**, *5*, 49–64.

(33) Meldal, M.; Tornøe, C. W. Cu-Catalyzed Azide−Alkyne Cycloaddition Cu-Catalyzed Azide-Alkyne Cycloaddition. *Chem. Rev.* **2008**, *108*, 2952–3015.

(34) Wu, Q.; Heidenreich, D.; Ackloo, S.; Krämer, A.; Nakka, K.; Lima-Fernandes, E.; Deblois, G.; Duan, S.; Vellanki, R. N.; Li, F.; Vedadi, M.; Dilworth, J.; Lupien, M.; Brennan, P. E.; Arrowsmith, C. H.; Muller, S.; Fedorov, O.; Filippakopoulos, P.; Knapp, S. A Chemical Toolbox for the Study of Bromodomains and Epigenetic

Signaling. *Nat. Commun.* **2019**, *10*, 1915–1929.

(35) Brand, M.; Measures, A. R.; Wilson, B. G.; Cortopassi, W. A.; Alexander, R.; Höss, M.; Hewings, D. S.; Rooney, T. P. C.; Paton, R. S.; Conway, S. J. Small Molecule Inhibitors of Bromodomain-Acetyl-Lysine Interactions. *ACS Chem. Biol.* **2015**, *10*, 22–39.

(36) Dinér, P.; Andersson, T.; Kjellén, J.; Elbing, K.; Hohmann, S.; Grøtli, M. Short Cut to 1,2,3-Triazole-Based P38 MAP Kinase Inhibitors via [3+2]-Cycloaddition Chemistry. *New J. Chem.* **2009**, *33*, 1010–1016.

(37) Albrecht, B. K.; Gehling, V. S.; Hewitt, M. C.; Vaswani, R. G.; Côté, A.; Leblanc, Y.; Nasveschuk, C. G.; Bellon, S.; Bergeron, L.; Campbell, R.; Cantone, N.; Cooper, M. R.; Cummings, R. T.; Jayaram, H.; Joshi, S.; Mertz, J. A.; Neiss, A.; Normant, E.; O'Meara, M.; Pardo, E.; Poy, F.; Sandy, P.; Supko, J.; Sims, R. J.; Harmange, J. C.; Taylor, A. M.; Audia, J. E. Identification of a Benzoisoxazoloazepine Inhibitor (CPI-0610) of the Bromodomain and Extra-Terminal (BET) Family as a Candidate for Human Clinical Trials. *J. Med. Chem.* **2016**, *59*, 1330–1339.

(38) Gehling, V. S.; Hewitt, M. C.; Vaswani, R. G.; Leblanc, Y.; Côté, A.; Nasveschuk, C. G.; Taylor, A. M.; Harmange, J.-C.; Audia, J. E.; Pardo, E.; Joshi, S.; Sandy, P.; Mertz, J. A.; Robert J. Sims, I.; Bergeron, L.; Bryant, B. M.; Bellon, S.; Poy, F.; Jayaram, H.; Sankaranarayanan, R.; Yellapantula, S.; Srinivasamurthy, N. B.; Birudukota, S.; Albrecht, B. K. Discovery, Design, and Optimization of Isoxazole Azepine BET Inhibitors. *ACS Med. Chem. Lett.* **2013**, *4*, 835–840.

(39) Ayoub, A. M.; Hawk, L. M. L.; Herzig, R. J.; Jiang, J.; Wisniewski, A. J.; Gee, C. T.; Zhao, P.; Zhu, J.-Y.; Berndt, N.; Offei-Addo, N. K.; Scott, T. G.; Qi, J.; Bradner, J. E.; Ward, T. R.; Schönbrunn, E.; Georg, G. I.; Pomerantz, W. C. K. BET Bromodomain Inhibitors with One-Step Synthesis Discovered from Virtual Screen. *J. Med. Chem.* **2017**, *60*, 4805–4817.

(40) Pomerantz, W. C. K.; Cui, H.; Divakaran, A.; Pandey, A. K.; Johnson, J. A.; Zahid, H.; Hoell, Z. J.; Ellingson, M. O.; Shi, K.; Aihara, H.; Harki, D. A. Selective N-Terminal BET Bromodomain Inhibitors by Targeting Non-Conserved Residues and Structured Water Displacement. *Angew. Chem. Int. Ed.* **2020**, *Accepted.*